Structure-Function analysis of zebrafish germ plasm components

Dissertation

Zur Erlangung des Grades

Doktor der Naturwissenschaften

Am Fachbereich Biologie

Der Johannes Gutenberg-Universität Mainz

Alessandro Consorte

Geb. am 28 August 1992 in Pescara, Italien

Mainz, 2023

Dekan:

1. Berichterstatter:

2. Berichterstatter:

Tag der mündlichen Prüfung:

Table of Contents

Abstract

Germline specification relies, in many species, on phase-separation properties of cytoplasmic condensates, generally refer to as germ plasm, which collect crucial determinants for germ cell identity. In zebrafish these structures start to assemble during oogenesis, when they form a network of proteins and RNAs which together trigger interesting dynamics throughout egg maturation and early embryogenesis. In this Thesis I explore the role of two multi-Tudor containing proteins, Tdrd6a and Tdrd6c, revealing that their maternal contribution is essential for the fertility of the offspring in zebrafish. This is due to the fact that Tdrd6a and Tdrd6c are crucial for the stability of the germ plasm during its segregation in the early embryo and for enrichment of primordial germ cells in the larval stages. Tdrd6a and Tdrd6c are likely carrying out their function via interaction with Bucky ball, the organizer of zebrafish germ plasm, affecting Bucky ball intrinsic phase-separation properties. In particular, in this work, I collect evidence that the predicted Prion-like domain of Tdrd6c has influence on Bucky ball dynamics, which may be relevant during germ plasm segregation. The understanding of this interaction could lead to new views applicable to studies of germline specification but could also be extended to other phase-separation processes driven by Prion-like domain containing proteins.

Zusammenfassung

Die Keimbahnspezifikation beruht bei vielen Arten auf den Phasentrennungseigenschaften von Zytoplasmakondensaten, die im Allgemeinen als Keimplasma bezeichnet werden und entscheidende Determinanten für die Keimzellidentität sammeln. Bei Zebrafischen beginnen sich diese Strukturen während der Oogenese zusammenzusetzen, wenn sie ein Netzwerk aus Proteinen und RNAs bilden, die zusammen während der Eireifung und der frühen Embryogenese interessante Dynamiken auslösen. In dieser Arbeit untersuche ich die Rolle von zwei Multi-Tudor-enthaltenden Proteinen, Tdrd6a und Tdrd6c, und zeige, dass ihr maternaler Beitrag für die Fruchtbarkeit der Nachkommen im Zebrafisch wesentlich ist. Dies liegt daran, dass Tdrd6a und Tdrd6c für die Stabilität des Keimplasmas während seiner Segregation im frühen Embryo und für die Anreicherung der Urkeimzellen im Larvenstadium von entscheidender Bedeutung sind. Tdrd6a und Tdrd6c erfüllen ihre Funktion wahrscheinlich durch Interaktion mit Bucky Ball, dem Organisator des Zebrafisch-Keimplasmas, und beeinflussen die intrinsischen Phasentrennungseigenschaften von Bucky Ball. Insbesondere sammle ich in dieser Arbeit Beweise dafür, dass die vorhergesagte Prion-ähnliche Domäne von Tdrd6c Einfluss auf die Bucky-Ball-Dynamik hat, was während der Keimplasmasegregation relevant sein könnte. Das Verständnis dieser Wechselwirkung könnte zu neuen Ansichten führen, die auf Studien zur Keimbahnspezifikation anwendbar sind, könnte aber auch auf andere Phasentrennungsprozesse ausgeweitet werden, die durch Proteine, die Prion-ähnliche Domänen enthalten, gesteuert werden.

1 – List of abbreviations, Tables and Figures

1.1 – List of abbreviations

3D	Three-dimensional
°C	Degree Celsius
aa	Amino-acids
AF	Alpha Fold
ATP	Adenosine Tri-Phosphate
Bb	Balbiani body
bp	Base pairs
Cas9	CRISPR Associated protein 9
Cat#	Catalog number
cDNA	Complementary DNA
CRISPR	Clustered Regularly Interspaced Short Palindromic Repeats
Da	Dalton
DAPI	4',6-diamidino-2-phenylindole
DNA	Deoxyribonucleic Acid
e.g.	*Exempli gratia*
ENU	N-Ethyl-N-Nitrosourea
et al.	*et alii*
etc.	*et cetera*
Fig.	Figure
g	Gravity of Earth
GFP	Green Fluorescent Protein
GMO	Genetically Modified Organism

hpf	Hours Post-Fertilization
IDP	Intrinsically Disordered Protein
IDR	Intrinsically Disordered Region
IP	Immunoprecipitation
LCR	Low Complexity Region
LLPS	Liquid-Liquid Phase Separation
MBP	Maltose Binding Protein
min.	Minutes
MLO	Membrane-less Organelle
mmut	Maternal mutant
MO	Morpholino
mRNA	Messenger RNA
MS	Mass Spectrometry
N/A	Not Applicable
NMD	Nonsense-Mediated Decay
o/n	Over night
ORF	Open Reading Frame
PCR	Polymerase Chain Reaction
PGC	Primordial Germ Cell
piRNA	Piwi-Interacting RNA
PrLD	Prion-like Domain
PIWI	P-element Induced Whimpy Testes
PRMT	Protein Arginine Methyltransferase
PTM	Post-Translational Modification
RBP	RNA-binding protein
RNA	Ribonucleic Acid
rpm	Revolutions per minute
RT	Room temperature
SG	Stress Granule
smFISH	single molecule fluorescent *in situ* hybridization
TE	Transposable Element

tRNA	Transfer RNA
TSE	Transmissible Spongiform Encephalopathy
utr	Untranslated region
wpf	Weeks Post-Fertilization
wt	Wild type
w/v	Weight over volume
ZGA	Zygotic Genome Activation

1.2 – List of Tables and Figures

1.2.1 – Tables

1.2.2 - Figures

3 – Introduction

3.1 – Overview of phase-separation features in nature

3.1.1 – Definition of Membrane-less Organelles

The cell is the fundamental unit of life. In its relatively small volume, the cell encloses an environment where metabolic processes can occur efficiently and where important information can be stored safely in the form of macro-molecules, ensuring the viability of unicellular and multicellular species. This requires a tight control over the cellular bio-chemistry, preventing harmful errors and favoring the accurate and punctual generation of products in need for the organism. This regulation is achieved by the use of compartmentalized logistics that allows cells to enrich for specific molecules at precise time and space within their volumes. In fact, inside the cell we can identify several distinct environments that concentrate specific molecules and exhibit determined functions. These definite spaces are generally called organelles (Nelson and Cox, 2017). These are usually characterized by lipid-membranes which delimit their volumes and allow them to isolate their *lumen* from the rest of the cellular cytoplasm. Membranes of distinct organelles have different compositions in order to permit selective diffusion of molecules and promote only specific reactions in each compartment. This way, each organelle can exhibit certain functions and contribute to the cellular self-sustainability. Examples of these specializations are mitochondria, where energy is converted in the form of ATP, or lysosomes, where bio-molecules are digested (Friedman and Nunnari, 2014; Luzio et al., 2007).

Overall, membrane-bound organelles have been well described, as many studies have unveiled their molecular composition, functions and relevance in different aspects of biology. In contrast to membrane-bound organelles, another type of cellular compartmentalization relies solely on the interaction of proteins and RNAs to build up distinct volumes within the cytoplasm or nucleoplasm. This implies that certain proteins and RNAs, without the assistance of lipidic barriers, can together de-mix from the surrounding environment, forming condensates that can be referred to as membrane-less

organelles (MLOs) (Banani et al., 2017; Hyman et al., 2014). In fact, MLOs are also able to have a selective molecular composition and exhibit distinct functions for the cell, playing crucial roles for different biochemical pathways. However, MLO composition, structure and dynamics have been only superficially understood and described compared to the knowledge collected for the membrane-bound organelles. This is true despite the fact that some examples of MLOs have been observed already since more than a century, as for example the nucleolus or the Cajal bodies inside the nucleus, or the cytoplasmic Balbiani body (Balbiani, 1864; von Wittich, 1845; Cajal, 1903; Wagner, 1835). Moreover, in the last few decades, more and different specialized MLOs have been found and linked to different biological processes, increasing the interest and excitement towards the understanding of their formation and function.

As mentioned, MLOs are predominantly assembled upon the interaction of proteins and RNAs that are able to create a molecular network and de-mix from the surrounding environment in the cell. This state is referred to as phase-separation as it describes the co-existence of different phases of the same molecules in the same solvent: typically the condensed phase and the dilute phase. Moreover, these biophysical states can variegate and differ in their appearances and features (Fig. 1). For example, certain MLOs have been shown to have liquid-like properties. In such cases, distinct condensates can fuse together, mixing their contents, in a process known as liquid-liquid phase-separation (LLPS). Examples of such MLOs are for instance P-granules in *C. elegans* or of the nucleoli in *Xenopus laevis* (Brangwynne et al., 2011, 2009). In other condensates, the phase-separated *status* appears more solid-like, as observed for instance in the Balbiani body of *Xenopus* oocytes, where proteins exhibit low mobility within the spherical volume of a large cytoplasmic granule (Boke et al., 2016). Furthermore, MLOs can appear in conditions between liquid- and solid-like, often referred to as gel-like, as it was firstly measured in a study of the nucleopore structure (Frey and Görlich, 2007). Importantly, such *material properties* of an MLO can change over time: for instance, a study in *Drosophila melanogaster* has suggested that liquid-to-solid phase transition of *oskar*-driven condensates is crucial for the correct expression of *oskar*, a crucial step to ensure the correct development of the fly (Bose et al., 2022; Ephrussi et al., 1991; Lehmann and Nüsslein-Volhard, 1986). Another example comes from Bucky ball-organized structures in

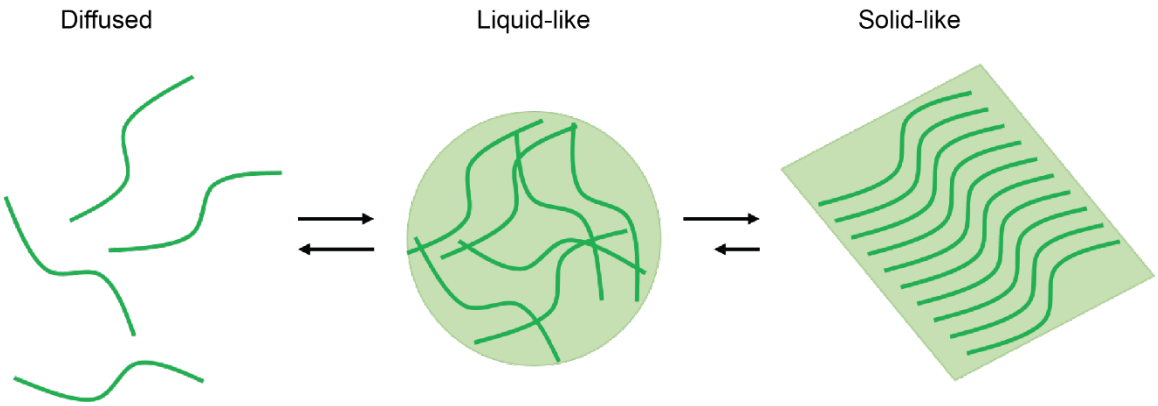

Fig. 1. Different states of phase-separation of proteins inside the cell. Upon a certain concentration and within specific environmental conditions (pH, salts concentration, temperature, *etc.*) a protein (green) is diffused within the solvent. Increasing the protein concentration or changes in the surrounding environment can trigger the protein to phase-separate and form liquid-like structures, which are likely reversible (as indicated by the similar size of the arrows). Upon further changes of the cellular conditions or increased concentrations, the protein can start aggregating and form solid-like fibril that are observed to be irreversible in most cases, often linked to severe diseases.

in zebrafish, where the formation of a large solid-like Balbiani body has to be followed by its disassembly into smaller granules in order to ensure the correct maturation of oocytes (Gupta et al., 2010; Riemer et al., 2015). Also, as displayed in the study of *Arabidopsis thaliana*'s protein ELF3, biological condensates can form and disassemble in a temperature-dependent fashion, regulating the growth of the plant at different conditions (Jung et al., 2020). Therefore, it is clear that biophysical properties and dynamics are relevant for the function of specific MLOs, regulating aspects such as molecular composition and fluctuations occurring within the condensates, their localization and structure, as well as governing the possible chemical reactions occurring within their volumes, this way contributing to the correct functioning of the cell.

The molecular control over these dynamics, however, is not only important for the correct function of the biological condensates, but also crucial to prevent degeneration of the phase-separated *status* of the molecules involved, as this can lead to harm and death of the cell. Indeed, several conditions, especially neurological disorders, have been linked to the mis-regulation of proteins interaction which results into the formation of large aggregates that interfere with the cell machinery (Shin and Brangwynne, 2017).

Because MLOs can differ in their composition of proteins and RNAs, one of the main interest of this area of research is to investigate the similarities and shared features of these molecules and their relevance in favoring phase-separation in the cell. Indeed, the research fields of physics, chemistry and biology have come together in the last decade with a shared effort in studying and understanding MLOs composition and dynamics. In particular, certain proteins have been recognized as organizers (scaffolds) of specific condensates, being necessary to form the fundamental molecular hub to recruit other components (clients) and together form MLOs (Banjade et al., 2015; Ditlev et al., 2018; Harmon et al., 2017). These features have stimulated the interest towards the intrinsic capabilities of individual proteins: what biophysical conditions (temperature, pH, solvent composition) do they require to manifest phase-separation? Which kind of physical state (liquid-, gel-, solid-like) are they able to form? What are the critical concentrations at which they can reach specific physical states? All of these questions are being addressed also with focus on amino-acidic sequences, analyzing which combination of residues and specific domains of proteins are relevant to control their phase-separating behavior. This way, the knowledge of the qualities of the proteins and their domains in relation to the regulation of processes dependent on phase-separation has significantly expanded in the last years. I will discuss these information in the next paragraphs, highlighting the current state and perspective of this area of research.

3.1.2 – Multi-valency of proteins

Proteins have been observed to be key components of MLOs inside cells, but how are they able to participate in or drive the process of phase-separation? Certainly, this would depend heavily on their interaction with surrounding molecules. Indeed, once expressed in the cellular environment, proteins are presented to a wide spectrum of molecules that they can potentially interact with, occupying the same cytoplasmic or nuclear space. However, in most cases proteins possess affinities for specific substrates which characterize their biological function. Often, the specificity of the interaction and function of a protein is carried out by its folded regions, also called protein domains. Over the years, many protein domains have been characterized to be responsible for the recognition of different

substrates. The specificity of each domain is dictated by its amino-acid composition, which determines its folded structure within the biological environment. However, also disordered unstructured regions of proteins can have interactions with various substrates and I will discuss these features in dedicated paragraphs (Introduction – 3.1.3 and 3.1.4).

What is important to highlight in this section is that proteins can exhibit one or multiple domains within their sequences and these domains can be similar or different relatively to their structure and function. Having multiple domains, even if belonging to the same family, confers to a protein the ability to interact simultaneously with multiple substrates. This characteristic is called multi-valency and it is known to favor and regulate phase-separation processes (Banani et al., 2017, 2016; Shin and Brangwynne, 2017). In fact, one multi-valent protein can function as a hub for multiple substrates, which themselves can display multiple domains, eventually escalating into the quick growth of a large molecular network (Harmon et al., 2017; Li et al., 2012; Lin et al., 2015; Mohanty et al., 2022). Prominent examples of multi-valent proteins involved in phase-separation are displayed by proteins containing Tudor domains (TDs), SH3 domains or the Sterile Alpha Motif (SAM) (Amaya et al., 2018; Beutel et al., 2019; Courchaine et al., 2021; Hirakata et al., 2019; Kim and Bowie, 2003; Mittag and Pappu, 2022; Siomi et al., 2010, Lasko, 2010). These domains are often present in multiple copies or in combination with other interacting domains within the protein sequence, hence manifesting multi-valency targeting simultaneously multiple substrates. A peculiar family of multi-valent proteins is the multi-Tudor domain containing proteins (Tdrds), to which I will dedicate a specific paragraph to discuss their structures and functions in detail (Introduction – 3.2.5).

What is also important to highlight in regard of multi-valency-favored networks, is that these do not necessarily only include proteins but can also feature nucleic acids, as certain multi-valent proteins have been identified as RNA-binding proteins (RBPs). Hence, some multi-valent proteins possess one or multiple RNA-binding domains that confer them the capability of recruiting RNAs, which interestingly has also been reported to contribute in the formation and regulation of biological condensates (Banerjee et al., 2017; Han et al., 2012; Sanders et al., 2020; Schwartz et al., 2013). Consequently, proteins with multiple interacting domains are key catalyzers of processes that gather different molecules within

a concise volume, generating a complex network and eventually favoring the formation of biological condensates.

3.1.3 – Intrinsically Disordered Proteins

Besides structured domains, proteins are also often composed of unstructured regions. While short linkers and loops between secondary structures have always been recognized as important features of globular formations of proteins, the relevance of larger unstructured stretches has only emerged in the last 30 years, as the phase-separation field of research has enhanced the general attention for such features (Alberti, 2017; Banani et al., 2017; Banjade et al., 2015). These unstructured domains are also called Intrinsically Disordered Regions (IDRs) and it is estimated that 44% of known proteins contain at least one IDR of 30 residues or longer (Romero et al., 2001). Accordingly, proteins that are largely disordered are also named Intrinsically Disordered Proteins (IDPs). IDPs and IDRs are enriched in hydrophilic and charged residues often arranged in a pattern of repeats within the peptide (Wang et al., 2018). These sequences confer flexible structural features to IDRs, allowing for transient interaction with substrates, rearranging themselves and presenting different residues to the environment at different conformational states. In particular, IDRs seem to favor interaction through cation-π affinity between the phenyl ring of Tyrosine residues and the charged amino-acids Arginine and Lysine, but also through π-π interactions between aromatic residues (Tyrosines, Phenylalanines, Tryptophanes) (Banani et al., 2016; Das et al., 2020; Pak et al., 2016; Qamar et al., 2018; Vernon et al., 2018). The studies of these non-covalent interactions have highlighted their relevance in the regulation of phase-separation via transient and dynamic protein-protein affinities which are key features of biological condensates. Interestingly, interaction of IDRs with RNA molecules, in particular via Arginine residues, has also been highlighted as critical for the composition and functioning of MLOs, further validating the relevance of nucleic acids in phase-separation events (Kroschwald et al., 2015; Protter et al., 2018; Wang et al., 2018).

Altogether, the studies of the last decade over IDPs clearly show their importance for the correct assembly of MLOs, thanks to their transient interaction with different substrates

and the flexibility of their 3D structures. These features, especially in the dynamic environment of the cellular context, make IDPs an interesting and challenging category of proteins to study. Furthermore, many IDPs have not been analyzed in their mechanics and functions, with most of the current knowledge deriving from detailed research of only few "model" proteins. For this reason, it is important to investigate the dynamics and interaction of different IDPs belonging to different MLOs in order to achieve a better and more complete understanding of the biochemistry that governs phase-separation processes and their relevance in living organisms.

3.1.4 – Low Complexity Regions and Prion-like domains

When looking at the amino-acidic sequence of a structured or unstructured peptide, it is possible to detect regions peculiarly enriched in only one or few residues, which for this reason are distinguished and named Low Complexity Regions (LCRs). These can manifest themselves both as unstructured IDRs as well as globular domains of a protein, being subject of conformational changes upon variations of the conditions of the environment. Within the classification of LCRs we find also Prion-like Domains (PrLDs), which are regions particularly enriched in uncharged polar amino-acids like Asparagine, Glutamine and Threonine (King et al., 2012).

PrLDs are structurally similar to the Prion protein that was discovered the study of Scrapie, a degenerative disease known since the 18th century but molecularly characterized in the second half of the 20th century (Plummer, 1946; Griffith, 1967; Prusiner, 1982). This condition is described to affect the nervous system of sheep and goats, where mis-folding and accumulation of the Prion protein inside cells result in the deterioration of the brain, causing severe behavioral symptoms and ultimately the death of the animal. More in detail, upon mis-folding, the Prion protein not only alters its own structure, but also forces the same conformational changes to other interacting Prion molecules, eventually forming fibrils in the cell. These formations are protein aggregate that can grow into amyloid assemblies, which ultimately interfere with the correct functioning of the cell, thus triggering cell death (Prusiner, 1991). Interestingly, also other diseases have been reported, in different species, to be caused by Prion proteins that behave (or rather mis-behave)

similarly and form harmful amyloid structures, leading to the development of comparable symptoms in the animals (including humans) (Aguzzi and De Cecco, 2020; Liemann and Glockshuber, 1998; Sprunger and Jackrel, 2021). Accordingly, these conditions are known as Prion-diseases but are formally classified as Transmissible Spongiform Encephalopathies (TSEs). In fact, they can be transmitted genetically, with mutations in the *prion* gene, but also by the infective action of the mis-folded Prion protein that, as mentioned, is able to drastically alter the cellular environment in which is present. In other words, transfer of one mis-folded Prion to cells that express correctly-folded Prion proteins, even to cells belonging to a completely new host, is sufficient to trigger a chain of reactions that leads to cell death and severe tissue damages, hence making the disease transmissible. Similarly to the Prion protein, PrLDs identified in different proteins are supposed to possess the ability of switching their conformation in the cell, transitioning from a globular to a disordered state (Alberti et al., 2009; Shorter and Lindquist, 2005). Furthermore, PrLDs often can interact with other proteins, eventually influencing their 3D conformation, similarly to what is observed in TSEs (Malinovska et al., 2013; Sprunger and Jackrel, 2021). Indeed, the elasticity of PrLDs can result in the formation of large amyloid structures, which can cause cellular malfunctioning, also in tissues other than the nervous system (Malinovska et al., 2013; Sprunger and Jackrel, 2021). On the other hand, PrLDs have been also shown to be crucial for the correct regulation and biological functioning of MLOs (Boke et al., 2016; Gilks et al., 2004; Han et al., 2012; Lin et al., 2015; Molliex et al., 2015). For example, it was highlighted that the PrLD of the protein TIA-1, in mammalian cells, plays an essential role in the formation of stress granules (SGs), which are phase-separated structures controlling RNA expression during harmful conditions (Gilks et al., 2004)**.** In *Arabidopsis*, the PrLD of the ELF3 protein was shown to function as a crucial thermo-sensor, triggering cellular speckles formation in response to high temperatures, thereby sequestering molecules and favor the growth of the plant (Jung et al., 2020). Another interesting example appears in oocytes of *Xenopus*, where the PrLD of Xvelo has been revealed to confer the essential amyloid features to a large granule, named Balbiani body, playing an essential role for germline development (Boke et al., 2016). Interestingly, in all described scenarios, it was reported that MLOs formed by PrLDs can modify (or even completely reverse) their phase-separated state, in coordination with the

cellular needs. More importantly, these proteins expressing PrLDs can escape uncontrolled aggregation that would harm the cells, in contrast to the example of the already discussed TSEs. These observations contributed to the raise of interest towards PrLDs, their amino-acid sequences and their modes of interaction with different substrates, as their understanding can unveil more features of both healthy and unhealthy cellular condition and phase-separation processes.

Another interesting feature of PrLDs is their ability to bind not only proteins but also RNA molecules. This interaction has been well described in the studies of the proteins FUS and TDP43, in which RNA interaction was highlighted as a requirement for the formation of phase-separated structures and their features (Burke et al., 2015; Ishiguro et al., 2017; Kitamura et al., 2016; Shelkovnikova et al., 2014). In these scenarios, Arginine residues may be important amino-acids, as they are often drivers of interactions with nucleic acids and indeed seem to play a role in the context of stress-granule (Burke et al., 2015; Calnan et al., 1991). Additionally, poly-Q stretches (which are found more generally in LCDs) have been shown to confer RNA-affinity, as it was described in the study of the protein Whi3 of *Saccharomices cerevisiae* (Langdon et al., 2018). However, the understanding of PrLD-RNA affinities remains elusive, probably due to the flexible conformation of both molecules, which makes their study rather challenging on the structural level. Therefore, these features should be further investigated and described, especially considering that the interactions between proteins and RNAs can have crucial influences over the modulation of LLPS dynamics, stressing the importance of comprehending the role of these molecules and domains in relation to MLOs (Banerjee et al., 2017; Han et al., 2012; Maharana et al., 2018).

Because of their conformational flexibility and dynamic interactions with other macro-molecules, PrLDs have been in the spotlight of LLPS studies in biology. Although different studies have unveiled the relevance of specific amino-acid composition of PrLDs, many questions regarding their regulation and stability remain unanswered. Which conditions alter their conformation? What kind of chemistry lays behind their interaction with other molecules? What key differences are between PrLDs that contribute to functioning of MLOs and the ones that cause degenerative diseases? The discoveries of more and different PrLD-containing proteins and MLOs depending on them, in the last few decades, are

providing a solid ground to investigate these features, which are important to be understood in relation to both healthy and unhealthy biological processes.

3.2 – Specification and maintenance of the animal germline

3.2.1 – Epigenesis and Pre-formation

A crucial feature of living organisms is their strategy of reproduction, which can be incredibly variegate in nature, especially in the behavioral aspects that I will unfortunately not cover in this introduction. Instead, I will focus on describing the molecular processes which ensure the fertility of organisms, in particular the zebrafish *Danio rerio*, as this has been the *focus* of my research interest and of the work for this Thesis.

In order to be fertile, multicellular organisms need to specify and maintain a particular cellular lineage: the germline. The germline consists in a set of cells (the germ cells) which possess the qualities to mature into gametes, the only cells capable of forming the zygote, *ergo* a new whole individual. In fact, the zygote is a totipotent cell that carries all the necessary information to develop into a full-grown organism. In species that reproduce sexually, the formation of the zygote happens via the event of fertilization: the fusion of two parental gametes, which in animals are named oocyte and sperm. Therefore, a crucial moment in the development of any multicellular individual is the establishment of its germline, as that is the first fundamental step to ensure fertility.

Germline specification in animal development can occur via diverse molecular processes, which fall in one of two main strategies: epigenesis or pre-formation (Extavour, 2003). These strategies are fundamentally different, with epigenesis only initiating after fertilization with the occurrence of signaling pathways (from surrounding cells or from the environment) that trigger few cells to differentiate as primordial germ cells (PGCs), which are the precursor of the adult germline (Fig. 2A). The first evidences of this mechanism was exhibited in studies of urodele amphibians (salamanders), where transplantation-based

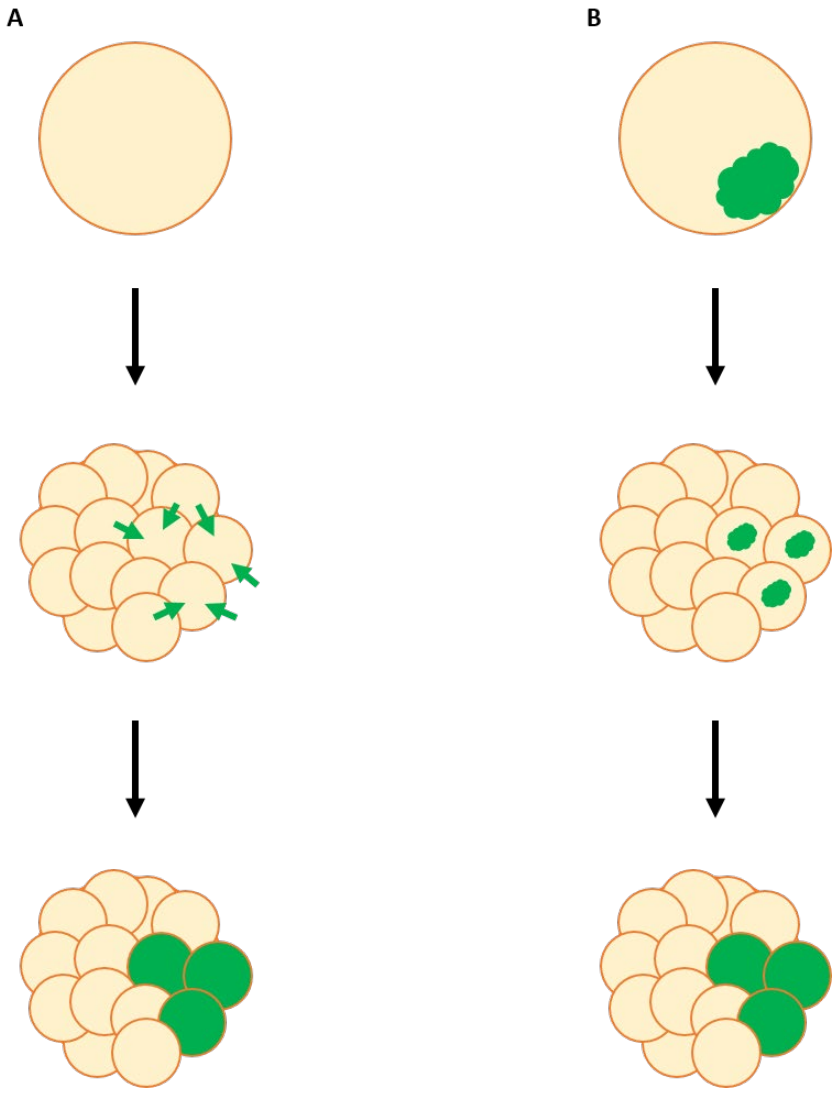

Fig. 2. Germline specification strategies: Epigenesis vs Pre-formation. (A) Epigenesis: in the egg (on top of the scheme) determinants relevant for germline specification are not expressed; after fertilization, cell division initiate and, at a certain time of development, few cells receive signals (green arrows) from surrounding environment and/or other cells. These signals suffice to induce differentiation of PGCs (green). (B) Pre-formation: in the egg there is accumulation of expressed determinants relevant for germline specification, which phase-separate into cytoplasmic condensates (green cloud); these determinants, after fertilization, distribute in the embryo and enrich in only few cells which are driven to differentiate into PGCs (green).

experiments showed that the presence of the ventral endoderm suffice to induce PGCs specification of adjacent cells, independently of their previous cytological identity (Niewkoop, 1976; Boterenbrood, 1973). Similar approaches revealed that also mouse

embryos rely on the positioning of cells within the proximal epiblast in order to differentiate as germ cells (Tam and Zhou, 1996; Tsang et al., 2001). Furthermore, the signaling pathway leading to PGC specification has been shown to involve molecules of the bone morphogenetic protein (BMP) family (Tam and Zhou, 1996; Hogan, 1996). Although detailed studies of most animal *phyla* are lacking, epigenesis is currently argued to be the most ancient and conserved mechanism in animals, as it is proposed to be widely spread from sponges to mammalian species (Extavour, 2003).

Pre-formation, on the other hand, is less prevalent in nature, as it was characterized neither in mammalian nor in non-Bilateria systems, thus seemingly evolved more recently and maintained only in few branches of the phylogenetic tree (Extavour, 2003). Germline specification via pre-formation, in contrast to epigenesis, starts already in the parental lineage and relies on the storage of determinants in the gametes, more specifically in oocytes (maternal lineage) (Fig. 2B). Determinants are most commonly proteins and RNAs that are expressed in the gametes and are inherited by the zygote, being essential regulators of developmental processes before the zygotic genome activation (ZGA) (Jukam et al., 2017). In the case of pre-formation, storage of determinants in the oocyte, as well as their specific distribution in the developing embryo, has appeared to be linked with phase-separation phenomena, making this strategy quite fascinating to observe in its bio-chemical and bio-physical dynamics (Boke et al., 2016; Bose et al., 2022; Brangwynne et al., 2009; Roovers et al., 2018). In the next paragraph, I will report interesting findings collected in different model organisms that specify their germline via pre-formation mechanisms, highlighting similarities and differences of their phase-separation related features.

3.2.2 – Pre-formation processes and phase-separation dynamics

As stated in the previous paragraph, pre-formation mechanisms are less spread within the animal taxonomy when compared to epigenesis-based germline specification. However, it is perhaps curious to notice that the pre-formation strategy has been characterized in most classic model organisms of developmental biology studies. In fact, these processes are objects of study in *Caenorhabditis elegans*, *Drosophila melanogaster*, *Danio rerio* and *Xenopus*. In this section I will summarize and discuss the observations collected on these

species only, although pre-formation has also been found to guide germline specification in other species (Extavour, 2003). Studies on these model organisms have described different germline condensates, collectively referred to as germ plasm, highlighting essential properties of phase-separation that drive their functionality in relation to PGCs specification, contributing to the understanding of phase-separation-driven processes in biology.

In *C. elegans* the germ plasm appears in the oocytes in the form of small droplets distributed homogenously in the cytoplasm (Strome and Wood, 1983). These droplets have been named P-granules as they give raise to the 'P lineage' of cells, from which the germline of the worm is derived (Wang and Seydoux, 2013). In a ground breaking study, P-granules have been shown to possess liquid-like properties, as droplets were observed to fuse into one condensate within a matter of seconds (Brangwynne et al., 2009). This was the first observation that linked germ plasm structures to the field of LLPS. After fertilization, P-granules are inherited by the embryo and are dispersed homogenously within the cytoplasmic space (Fig. 3A). However, before the first cellular division, P-granules start to enrich particularly in the presumptive posterior pole of the embryo, in a process seemingly driven by a molecular gradient that forces P-granule to distribute asymmetrically (Smith et al., 2016). This gradient is established following a chain of events that starts with the penetration of the sperm pronucleus in the egg, marking the posterior pole with its associated centrosome. This cue sets up the cytoskeleton to distribute asymmetrically certain interacting molecules, such as the PAR proteins that concentrate at the cortex of the newly formed zygote, defining the anterior-posterior polarity (Hoege and Hyman, 2013; Kemphues et al., 1988). Following this patterning of the embryo, the MEX-5 protein enriches at the anterior pole, where it competes with the formation of P-granules, which consequently localize at the posterior pole of the zygote (Saha et al., 2016; Smith et al., 2016). This specific localization of P-granules, by the 24-cells stage of embryogenesis, ends up being restricted to only one cell (named P4, from the P-lineage) from which the germline of the worm is derived (Gallo et al., 2010; Strome and Wood, 1983; Wang and Seydoux, 2013). If these dynamics were not fascinating enough, in recent years it was described how P-granules at the zygotic stage possess two different phases: a core liquid phase, containing the PGL-3 protein, and an outer phase, that forms a more solid-shell-like

structure formed by the proteins MEG-3 and MEG-4 (Folkmann et al., 2021). The equilibrium between the two phases appears to be important for P-granule enrichment and regulation of RNA expression, making this composition a fascinating model to study to unveil more phase-separation dynamics in biology.

In *Drosophila* the germ plasm journey and distribution differ from the ones observed in worms. In fact, germ plasm components are not initially expressed in the maturing egg but in the adjacent nurse cells (Mahowald, 1972). From these cells, germline determinants are transported into the maturing oocyte, crossing the cytoplasm until reaching the membrane at the distal pole relatively to the nurse cells. Once there, one of the transported determinants, the *oskar* mRNA, starts to be translated and the produced protein can initiate the assembly of the germ plasm, which in this system is named pole plasm (Ephrussi et al., 1991; Lehmann and Nüsslein-Volhard, 1986). Thus, Oskar protein has been referred to as the pole plasm organizer in *Drosophila*, because it initiates the gathering of other proteins and RNAs and organize them into small condensates during oocyte maturation. After fertilization the pole plasm remains localized at the same pole in proximity of the cytoplasmic membrane, marking now the posterior pole of the embryo (Fig. 3B). In the fly, the first thirteen nuclear divisions occur without cytokinesis, thus forming a syncytium. Interestingly, the first cells gaining independence from the syncytium, *ergo* forming a membrane and enclosing their cytoplasmic environment, are the cells at the posterior side of the embryo, corresponding to the cells enriching for Oskar and for germline determinants (Ephrussi et al., 1991; Lehmann and Nüsslein-Volhard, 1986). Consequently, these cells, also called pole cells, will be determined as PGCs in the larva, contributing to the fertility of the organism. Interestingly, also in the fly the bio-physical state of the pole plasm has been shown to be crucial for the correct expression of proteins and RNAs, specifically in the regulation of a transition between a solid-like state to a liquid-like state (Bose et al., 2022). These observations further increased the interest towards the understanding of germ plasm LLPS and the molecules that govern it.

Germ plasm related structures have been found also in vertebrate systems, where they have been linked to a large dense granule found in oocytes, named Balbiani body (Bb) after the studies performed by Balbiani on eggs of spiders and myriapods, which followed up the first observations of von Wittich in 1845 (Balbiani, 1864; Kloc et al., 2004; von Wittich,

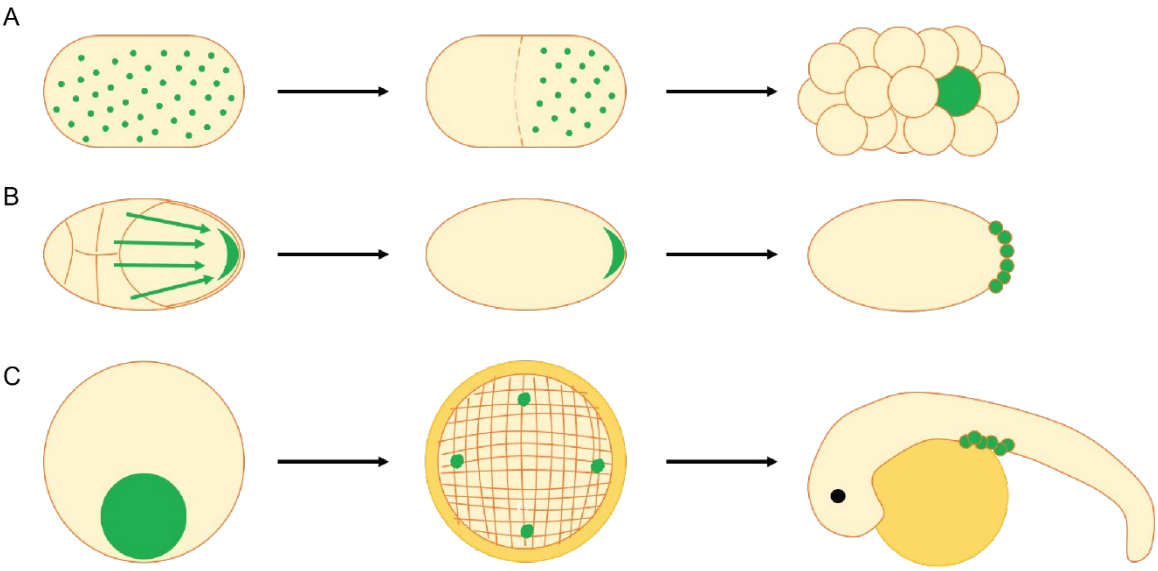

Fig. 3. Pre-formation germline specification in different model organisms. (A) In *C. elegans* the P-granules (green) are distributed homogenously in the cytoplasm of the egg (left); after fertilization, but before the first cell division, the P-granules enrich only at the posterior pole of the embryo, ending only in one of the two formed cells; after few cell divisions, P-granules are enriched only in the P cell lineage (green cell, on the right), establishing the germline of the worm. (B) In *D. Melanogaster* germ plasm components are first expressed in the nurse cells and then transferred and transported (green arrows) to the posterior pole of the egg (green half-moon); cells forming at posterior pole, acquiring the germ plasm, develop into PGCs (green circles, on the right). (C) In *D. rerio* the germ plasm is first assembled into an amyloid-like spherical granule in the oocyte (green circle, on the left); after fertilization, the germ plasm is distributed as smaller droplets, enriching particularly four *foci* on cleavage furrows at four poles of the embryo; enrichment in germ plasm drives a small population of cells to differentiate as PGCs (green circles, on the right).

1845). After its first observation, structures similar to the Bb were found in eggs of different animal species, although their role and function remains under debate (Kloc et al., 2004). In *Xenopus* and the zebrafish *Danio rerio*, however, the Bb has been characterized and it is now recognized to collect important determinants for germ cell development of the offspring, showing similar dynamics and homologies in the two organisms. In fact, both organisms produce rather large oocytes, in whose cytoplasm the Bb can form, marking the vegetal pole, opposite to the animal pole (Fig. 3C). Bb formation is driven by the protein Xvelo in the *Xenopus* and by Bucky ball (Buc) in zebrafish (Bontems et al., 2009). These two proteins are homologs and similar in their amino-acidic composition. Interestingly, both proteins are largely unstructured and can be categorized as IDPs. Furthermore, they

both possess a predicted Prion-like domain (PrLD), in their N-terminal sequence, which have been tested *in vivo* in *Xenopus*, revealing to be essential in conferring amyloid-like features to the Bb (Boke et al., 2016). However, more dynamics, components and regulators of the Bb have been only recently described, in the last 15 years of research, and I will discuss the knowledge collected in the zebrafish model in the next paragraph.

3.2.3 – Zebrafish germ plasm dynamics and regulators

Zebrafish germline specification is an example of pre-formation strategy and, as already mentioned, starts during oogenesis with the formation of the Bb, a large spherical cytoplasmic condensate where germ cell determinants are collected. In zebrafish, Bb assembly initiates in the perinuclear cytoplasmic environment, during the zygotene phase of oogenesis, when specific proteins and RNAs start to gather in the distinct proximity to the nuclear chromosomal bouquet formation (Elkouby et al., 2016) (Fig. 4A). At this specific location, the components of the Bb accumulate in a nuclear cleft, breaking the symmetry of the egg and marking the vegetal pole, opposite to the animal pole. In this site, the collected proteins and RNAs concentrate together into a granule that matures into the characteristic spherical Bb structure during the phase of diplotene. These initial dynamics rely on the expression of the protein Bucky ball (Buc), as *buc* knock out zebrafish mutants fail to form the Bb, making Buc the recognized organizer of the Bb in zebrafish (Bontems et al., 2009; Dosch et al., 2004.; Marlow and Mullins, 2008). It is important to notice that *buc* mutants exhibit severe egg polarity defects, not being able to establish the animal and vegetal poles correctly. This causes, after their fertilization, the early arrest of embryonic development within the first attempted cell divisions (Dosch et al., 2004). For this reason, the role of maternally provided Buc has not been fully unveiled. In particular, it is not known whether maternal inheritance of Buc is necessary for germ plasm segregation and PGC specification during embryogenesis.

According to studies carried out in the *Xenopus* system, the Bb seems to obtain amyloid-like characteristics from the N-terminal PrLD of Buc (Boke et al., 2016). These features usually correspond to a rather solid and compact structure often in an irreversible state in biology (Sprunger and Jackrel, 2021). However, with the maturation and growth of

zebrafish oocytes, the Bb begins to disperse into smaller non-spherical aggregates that distribute at vegetal cortex of the egg (vegetal granules), despite keeping its protein and RNA composition. This process of Bb dismantling has been shown to be also a key to the correct development of the egg in zebrafish, as inhibition of this process exhibited in *magellan* mutants resulted in a severe phenotype similar to the one observed in *buc* mutants where the Bb is absent (Gupta et al., 2010). Moreover, the analysis of the interaction between Buc and Tdrd6a, a multi-Tudor containing protein, provided evidence that the vegetal granules may be sufficient to confer the polarity to the zebrafish egg (Roovers et al., 2018). In this study, mutants expressing Buc with three Arginines mutated into Lysines (BucRtoK mutants), disrupting the Buc-Tdrd6a interaction, were shown to lack the formation of the large Bb while still displaying localization of vegetal granules (Roovers et al., 2018). Although the majority of these oocytes would fail development after fertilization, circa 15% of them were able to successfully reach the larval stages. Altogether, these observations hint at the possibility that the assembly of the vegetal granules suffice to ensure egg maturation in zebrafish, despite lack of Bb formation.

After fertilization of oocytes, the vegetally-localized germ plasm migrates to the animal pole, where the embryo develops, in the form of droplets that distribute homogenously in proximity of the plasma membrane (Fig. 4B, B'). During the first cycle of embryonic cell division, germ plasm droplets start to anchor at the forming cleavage furrows. The same process is observed during the second cycle of cell division, when reaching the 4-cells stage. This results in the formation of four clusters of germ plasm droplets, one at each distal part of the two formed furrows (four poles of the dividing embryo). From this moment on, throughout the cleavage phase of development, these four clusters of germ plasm droplets stably localize at the poles of the embryo, where they condense within smaller volumes of the furrows. Upon reaching the dome stage (~3 hpf), each one of the four germ plasm clusters is taken up by one cell, which will start segregating it symmetrically to the daughter cells during cell division, creating four sets of germ plasm-positive cells, which will all assume germ cell fate (D'Orazio et al., 2021; Jukam et al., 2017). Therefore, correct segregation and enrichment of the germ plasm during embryonic stages is also a crucial dynamic to induce PGCs specification. Indeed, it was shown that physical removal of germ plasm in zebrafish is sufficient to impair PGCs development

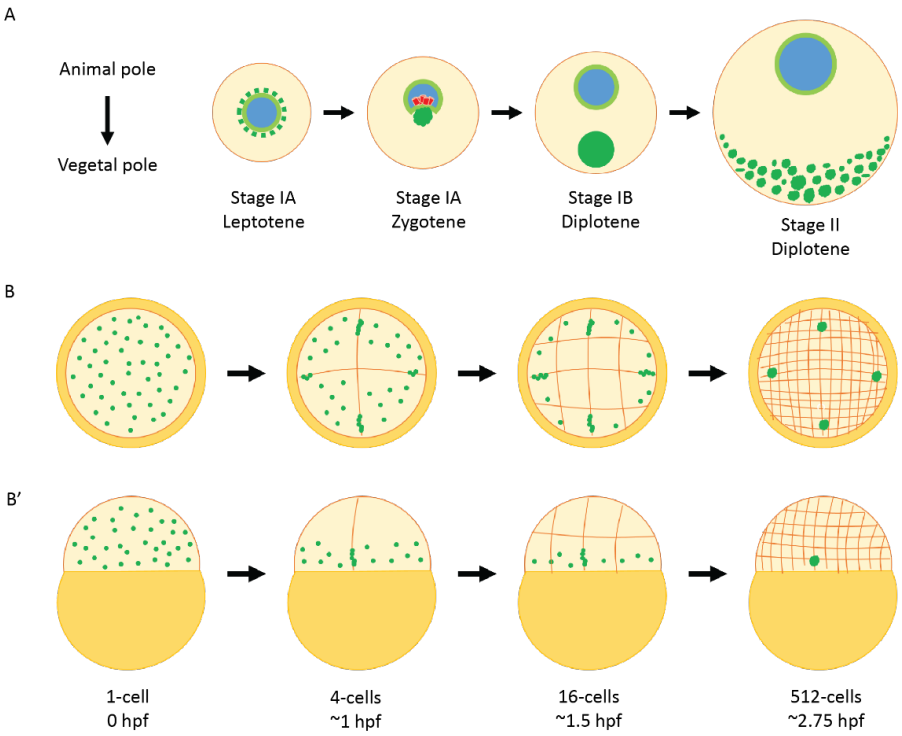

Fig. 4. Dynamics of germ plasm structures in zebrafish. (A) Highlights of Bb formation and disassembly during oogenesis (oocytes oriented with the animal pole on top and vegetal pole on the bottom). During the phase of Leptotene, Bb components (green) are surrounding the nucleus (blue). During Zygotene, Bb components gather in a nuclear cleft formed in proximity of the telomeres (red) of the chromosomal bouquet. In the beginning of the phase of Diplotene, the Bb matures into a spherical granule at the vegetal cortex, leaving the proximity of the nucleus, which is still surrounded by the *nuage* (light green). In a later stage of Diplotene, during the growth in size of the oocyte, the Bb disassembles into granules that spread on the vegetal cortex of the egg. (B and B') Highlights of germ plasm droplets (green) segregation during early embryogenesis (animal view in B, highlighting the embryo, lateral view in B', showing yolk at the bottom and embryo on top). In the zygote (1-cell stage), germ plasm droplets are distributed homogenously in proximity of the cellular membrane. With the formation of the first two cleavage furrows, at the 4-cell stage, germ plasm droplets start to enrich at the poles of the developing embryo. Upon reaching the 512-cell stage, the droplets of germ plasm restrict their localization to few cells that will be induced to become PGCs.

(Hashimoto et al., 2004). Furthermore, the already mentioned protein Tdrd6a was revealed to be required to regulate germ plasm stability, as its absence resulted in PGC abundancy defects (Roovers et al., 2018). In particular, Tdrd6a is important in the regulation of Buc mobility, thus playing a significant role in the phase-separation properties of the germ plasm and its distribution and enrichment during embryogenesis (Roovers et al., 2018).

To summarize the content of this paragraph, it is evident that zebrafish germline specification relies on the regulation of phase-separated structures, first during oogenesis, when the formation and disassembly of a large amyloid-like body are crucial for correct egg maturation, and then in the embryo, where small droplets need to be properly distributed to ensure PGCs abundancy in early development. Studies carried out in the last two decades have brought evidence of a few proteins involved in the regulation of the germ plasm in zebrafish, but many other candidates, as well as molecular features, remain largely unexplored, keeping many important questions unanswered. First, how are different phases of Bb formation (maturation into amyloid structure and disassembly into granules) regulated? Is the presence and local concentration of specific determinants driving these dynamics? Is the cytoskeleton involved and how? Are some post-translational modifications the key behind these transitions? Later in the embryo, how are the germ plasm droplet enriching only specific sites of the embryo and localizing at the cleavage furrows? What happens to the determinants that do not manage to reach these sites? Are they just diffusing in the space or being actively degraded? Once the germ plasm is accumulated in PGC, how are the determinants guiding the cell to the germ cell fate? Are they, or some of them, active only after exiting the phase-separated state? Which mechanisms and pathway are involved to trigger specific regulation of gene expression? These are just some of the questions, which would require several projects and studies, that could contribute in solving the puzzle of zebrafish germline specification. However, any advance in this model could also hopefully provide clues to follow in other systems (and *vice versa*) as there are similarities in the pre-formation strategies within species and within the molecules that regulate such processes. Furthermore, it is important to keep the cross-talk of this field with the studies of diseases caused by mis-regulation of phase-separating proteins, as both areas of research could help each other in the understanding of the molecular grammar governing phase-separation processes in healthy and unhealthy conditions.

3.2.4 – The *nuage* and the piRNA-mediated gene silencing

Another interesting condensate structure found specifically in germ cells is a perinuclear electron-dense environment, also called *nuage* (André and Rouiller, 1956, al-Mukhtar, 1971). This formation is not involved in the specification of the germline and, compared to the condensates described in previous paragraphs, offers less dynamics to observe (also implied by its other nomenclature of 'inter-mitochondrial cement'). However, the structure and composition of the *nuage* is crucial for germline maintenance, as it is residence for proteins and RNAs involved in a specific gene silencing machinery: the piRNA pathway (Cox et al., 1998; Lin and Spradling, 1997; Luteijn and Ketting, 2013). This pathway relies on the interaction of germline specific Argonaute proteins, the PIWI proteins, with small single-stranded RNAs, the piRNAs, in order to target and silence expression of 'non-self' genetic material (Malone and Hannon, 2009). These targeted sequences often correspond to transposable elements (TEs), as these have been observed to be potentially harmful for genomic stability, although eventually contributing to evolutionary processes (Kazazian, 2004). Because genomic instability and related mutations occurring in the germline would spread in following generations, organisms have urgently adopted an adequate surveillance system with the piRNA pathway. Indeed, the presence of piRNAs and PIWI proteins have been found in the germline of different species, both in animals and plants, although the molecular mechanism behind their functioning has been unveiled only to limited extents and in few organisms (Luteijn and Ketting, 2013). Interestingly, the piRNA pathway can operate on different levels of gene silencing: piRNAs can recognize directly mRNAs and induce their degradation, inhibit their translation or they can recruit chromatin remodelers and impede transcription of the targeted genes (Huang et al., 2013; Malone and Hannon, 2009). In order to guarantee the efficient functioning of this silencing mechanism, the *nuage* requires the assembling of a suitable environment, in composition and structural features, enabling the correct interactions between key molecules.

Besides the already mentioned Argonaute proteins, within the *nuage* can often be found multi-Tudor containing proteins (Tdrds), which I have already introduced when describing multi-valency and phase-separation (Introduction – 3.1.2). Indeed, several Tdrds have been highlighted to contribute in the organization of the perinuclear environment in the germline of different organisms, interacting with PIWI proteins and participating to the piRNA-

silencing machinery (Arkov et al., 2006; Chen et al., 2009; Handler et al., 2011; Hosokawa et al., 2007; Huang et al., 2011; Nishida et al., 2009; Reuter et al., 2009; Sato et al., 2015; Siomi et al., 2010; Vrettos et al., 2021; Wang et al., 2009). Interestingly, in zebrafish, the PIWI protein Ziwi and Tdrd6a have both been shown to be part of the *nuage* during oogenesis as well as enriching to embryonic germ plasm after fertilization (Houwing et al., 2007; Roovers et al., 2018). The inheritance of PIWI-pathway components, both proteins and RNAs, from the parental lineage to the zygote, could serve as a crucial process to ensure the protection of the embryo from the activity of TEs, as emerged from studies in *Drosophila* (Brennecke et al., 2008). Therefore, the molecules forming the *nuage* and their modes of interaction are interesting aspects to study in order to better understand gene silencing, inheritance of determinants and germline maintenance processes.

3.2.5 – Multi-Tudor containing proteins

Throughout this introduction I have mentioned multi-Tudor containing proteins (Tdrds) and their importance in relation to different processes. First, I highlighted how they are relevant in the promotion of phase-separation of MLOs, as they are capable of multi-valent interactions and regulation of molecular networks (Introduction – 3.1.2). Then, I mentioned how they participate to the formation and functioning of germline-specific condensates in different organisms (Introduction – 3.2.3 and 3.2.4). This is the case also in zebrafish where, for instance, Tdrd1 and Tdrd6a have been shown to be enriched in the perinuclear environment of zebrafish eggs where they interact with the two PIWI proteins of zebrafish: Ziwi and Zili (Huang et al., 2011; Roovers et al., 2018). In the study of Tdrd1, these interactions have been suggested to regulate the efficiency of the piRNA-mediated silencing machinery, as RNA population defects were measured in *tdrd1* knock-out mutant fish (Huang et al., 2011). Tdrd6a, on the other hand, was observed to play a role in the regulation of Buc during the formation of the Bb in oocytes and ensuring germ plasm enrichment during embryogenesis (Roovers et al., 2018). Indeed, Tdrd6a does not localize only to the *nuage* but also in the Bb of oocytes and it is then maternally inherited by the embryo, where it is found within the germ plasm assemblies (Roovers et al., 2018). Within these condensates, Tdrd6a is suggested to interact directly with Buc, affecting its mobility,

this way being an important regulator of Buc-induced condensates in zebrafish and influencing PGC specification (Roovers et al., 2018). Another example of Tdrd-contribution to germline-related condensates in zebrafish was reported in the study of Tdrd7 (D'Orazio et al., 2021). This protein has been shown to be an important component of perinuclear granules in zebrafish PGCs during larval stages, where its function seems to regulate the cross-talk between the cytoplasm and the nucleus, this way driving correct gene expression (D'Orazio et al., 2021). With these examples, it appears clear (and consistent with studies of other organisms) that Tdrds in zebrafish can impact germline condensate formations and functions in various ways. However, in zebrafish, 12 different Tdrds (Tdrd1-Tdrd12) have been identified, each possessing at least one Tudor Domain (TD), to a maximum of 7 TDs as displayed by Tdrd6 proteins. Therefore, it is important to dissect the structural features of these domains in order to propose more precise hypothesis over their interactions and functions in different Tdrds.

The Tudor domain (TD) has been characterized originally from the *tudor* gene of *Drosophila melanogaster*, which was discovered as one of the essential genes for germ plasm assembly in the fly (Boswell' and Mahowaldt, 1985). The gene *tudor* encodes for a protein with eleven TDs, which later have been structurally characterized and observed to be present in several expressed protein in animal species (Callebaut and Mornon, 1997; Ponting, 1997). In particular, similarly to the original *Drosophila tudor*, different proteins are recognized as multi-Tudor containing proteins, having more than one predicted TD within the translated peptide. The TD has been characterized to fold into a barrel formation consisting of four β-sheets with one additional α-helix (Selenko, 2001). Within this 3D structure, key amino-acids are responsible to control the TD target binding. In particular, aromatic residues often appear in a conserved pattern that forms a pocket where the ligand can find residues to interact with. However, the variability of the amino-acidic sequence of TDs have pointed at various types of interactions which reflect on the binding of different substrates (Kawale and Burmann, 2021; Liu et al., 2018). Furthermore, TD have been often found adjacent to additional β-sheets and α-helices in a folded structure resembling an SN domain (H. Liu et al., 2010; K. Liu et al., 2010). Altogether, the core TD barrel structure and the SN extension is referred to as extended Tudor domain (eTD). This composition further increases the spectrum of possible interaction of multi-Tudor containing proteins.

However, among protein-protein interaction, it has been unveiled that eTDs have a tendency to bind di-methylated Arginines of their substrates (Kim et al., 2006; H. Liu et al., 2010; K. Liu et al., 2010; Vagin et al., 2009). In particular, methylated Arginine residues interacting with eTDs have been found in RG repeats within protein sequences as a consequence of the specific action of methyl-transferases members of the PRMT family (Nishida et al., 2009; Siomi et al., 2010). Interestingly, these type of interactions have been revealed to often guide TD proteins to interact with Piwi proteins in different organisms (Chen et al., 2009; Reuter et al., 2009; Vagin et al., 2009; Vrettos et al., 2021; Wang et al., 2009). Indeed, TD proteins, consistently with the characterization of the first *tudor*, have been observed to be relevant to regulate germ cell features, in particular in the regards of the piRNA pathway, as stressed already in previous paragraphs (Hosokawa et al., 2007; Huang et al., 2011; Sato et al., 2015; Siomi et al., 2010). However, TDs have also been described to be involved in the interaction with non-methylated substrates, displaying plasticity and a broader spectrum of affinities (Kawale and Burmann, 2021; Liu et al., 2018; Zhang et al., 2017).

As most TD-containing proteins exhibit multi-valent capabilities, in particular when expressing multiple TDs, the structural features and biochemical dynamics of these domains are relevant to be studied in the context of LLPS and regulation of different MLOs. The understanding of these characteristics can contribute to different areas of research, as TDs are present in many expressed proteins involved in several mechanisms that rely on protein-protein interaction.

3.3 – Rational and Objectives of the Thesis

In recent years, more evidence for the relevance of phase-separation in biology have emerged, with the characterization of different MLOs and their components. However, the proteins responsible for the assembly and dynamics of condensates in the cells have been challenging to study, due to their flexible 3D structures and low sequence conservation during evolution. Studies carried out in *Xenopus* and zebrafish have highlighted important players of the regulation of a peculiar condensate, the germ plasm, showing that alteration

of its bio-physical properties can lead to severe phenotypes influencing important germline features in the organisms (Boke et al., 2016; Bontems et al., 2009; Gupta et al., 2010; Marlow and Mullins, 2008; Roovers et al., 2018). The protein Buc, in zebrafish, has been characterized to be the organizer of the amyloid-like Bb (Bontems et al., 2009). In a recent work, Tdrd6a has emerged as a regulator of Buc LLPS features, affecting germ plasm structure both during oogenesis and embryogenesis (Roovers et al., 2018). Interestingly, in the same study, Tdrd6a was found also in the *nuage* of zebrafish oocytes, although its absence in *tdrd6a* mutant did not result in a significant alteration of gene expression. However, the phenotypes scored in *tdrd6a* mutants could be compensated by the presence of Tdrd6a paralog Tdrd6c, which was found to interact with Buc and Tdrd6a in pull-downs experiments (Roovers et al., 2018).

With this knowledge, in my Thesis I addressed the role of Tdrd6c in zebrafish development and oogenesis. First, it is important to study Tdrd6c expression and localization in the fish, as this can provide solid evidence to plan further experiments. Then, a *tdrd6c* mutant line would need to be generated in order to observe and measure possible phenotypes and unveil the role of Tdrd6c in zebrafish. Furthermore, the role of Tdrd6c should be also analyzed in the context of *tdrd6a* mutant fish, in order to comprehend possible functional redundancy between the two proteins and if the absence of both could lead to severe phenotypes in the germline. Finally, as Tdrd6c is a rather large protein exhibiting different domains, the features of its structure and mode of interaction are crucial aspects to be analyzed, especially considering the impact that multi-TD proteins can have in regulating MLOs phase-separation features.

Overall, this Thesis aims to elucidate the role of Tdrd6c protein and the nature and relevance of its interaction with Buc, the germ plasm organizer in zebrafish. Furthermore, the molecular understanding of this process can potentially unveil important general characteristics of MLOs, possibly influencing other research areas of the phase-separation field, including the ones directly focusing on degenerative diseases.

4 – Methods

4.1 – Experimental Model and Subject Details

4.1.1 – Zebrafish lines

Zebrafish strains were housed at the Institute of Molecular Biology in Mainz and bred and maintained under standard conditions (26-28°C room and water temperature and lighting conditions in cycles of 14:10 hours light:dark) (Westerfield, 1995). Larvae < 5 days post fertilization were kept in E3 medium (5 mM NaCl, 0.17 mM KCl, 0.33 mM CaCl2, 0.33 mM MgSO4) at 28°C. The zebrafish strains used for this work are listed in the table below (Table 1). Each line was eventually crossed to another to combine them for different experimental set ups, as it will be explained in within other sections (Results – 5.1.3, Table 7). Periodic out-crossing of each line was done with mating to zebrafish *wild type (wt)* strains (AB or TU). All experiments were conducted according to the European animal welfare law and approved and licensed by the ministry of Rhineland-Palatinate.

Allele	Description	References
tdrd6c^{mz69}	CRISPR-induced knock out mutant allele	This thesis (Results – 5.1.2)
tdrd6a^{Q185X}	Knock out allele from ENU mutagenized library	(Roovers et al., 2018; Wienholds et al., 2002)
tdrd6c^{mz87tg}	Transgenic line expressing Tdrd6c – mKate2 protein	This thesis (Results – 5.1.3)
vasa-eGFP	Transgenic line expressing Vasa-eGFP protein	(Krøvel and Olsen, 2002)
buc-eGFP	Transgenic line expressing Buc-eGFP protein	(Riemer et al., 2015)
GFP-piRNA	Measuring transgene rescue effect in case of measurable phenotypes	Unpublished work from Edoardo Caspani

Table 1. List of zebrafish alleles. Names, descriptions and references of the zebrafish alleles used for the work of this Thesis.

4.1.2 – Cell culture

BmN4 cells were cultured at 27°C in IPL-41 (Gibco) medium supplemented with 10% Fetal Bovine Serum (Gibco) and 0.5% Pen-Strep. For imaging, cells were grown in 8-well µ-slides (Ibidi, Cat# 80826).

4.2 – Method Details

4.2.1 – Design and cloning of CRISPR-guide-RNAs

Crispr-guide RNAs (gRNAs) were designed using CRISPRscan in the UCSC genome browser (Moreno-Mateos et al., 2015) and corresponding oligonucleotides were produced by Integrated DNA Technology. Pairs of complementary oligonucleotides were annealed in a Thermocycler for 5 minutes at 95°C and gradual cool down to room temperature (RT). The pDR274 plasmid was linearized by digestion by BsaI restriction enzyme (NEB, Cat# R3733) and extracted from gel (QIAquick Gel Extraction Kit, Cat# 28704). Linearized backbones were then incubated with the inserts and T4 ligation mix (NEB, Cat#M0202) at RT for 30 min. to obtain plasmids for gRNAs expression.

4.2.2 – Transformation of bacterial cells and plasmid purification

Cells from different *E. coli* strains (Table 2) were transformed by incubation of 1-10 ng of plasmid within 50 µL of cells stock on ice for 25 minutes. Cells were then heat-shocked in water bath at 42°C for 40-50 seconds and then chilled on ice for 5-10 minutes. 250 µL of S.O.C. medium (NEB, Cat# B9020S) were added to the transformed cells that were then incubated at 37°C for at least 1 hour at 220 revolutions per minute (rpm). After incubation, 100 µL of medium containing cells was plated on Luria Broth (0.17 M NaCl, 1% w/v Bacto-Tryptone, 0.5% w/v Bacto-Yeast extract, pH 7.0) plates (1.5% w/v Agar) with appropriate antibiotics (100 µg/ml Ampicillin or 30 µg/ml Kanamycin). Colonies were selected after one night of incubation and grown in Luria Broth medium shaking at 220 rpm o/n at 37°C. Plasmids were purified with NucleoSpin DNA purification kit (Macherey-

Nagel, Cat# 740588.50), eluted in sterile water and sequenced by Sanger sequencing (Sanger et al., 1977) by StarSEQ (Table 5).

Name	Usage within this Thesis	Identifier
Subcloning Efficiency™ DH5α™ Competent Cells	General cloning strategies	Thermo Fisher (Cat# 18265017)
One Shot™ Top10 Chemically Competent Cells	Cloning of Tdrd6c-epitope (Methods – 4.2.10)	Thermo Fisher (Cat# C404003)
BL21(DE3) Competent Cells	For Tdrd6c-epitope expression (Methods – 4..12)	Thermo Fisher (Cat# EC0114)
One Shot™ *ccd*B Survival™ 2 $T1^R$ Competent Cells	Cloning of *tdrd6c-mKate2* final plasmid (Methods – 4.2.7, Results – 5.1.3)	Thermo Fisher (Cat# A10460)

Table 2. List of cellular bacterial strains used in this Thesis. Names, description of their usage and identifiers of bacterial strains used for different cloning strategies and purposes of this Thesis.

4.2.3 – Expression of CRISPR-guide-RNAs

Plasmids containing gRNAs encoding sequences (Methods 6.2.1) were linearized with DraI restriction enzyme (NEB, Cat# R0129L) and extracted from gel (QIAquick Gel Extraction Kit, Cat# 28704). Linearized sequences were used for RNA *in vitro* transcription (MEGAscript SP6 Transcription Kit, Cat# AM1330). Expressed gRNAs were treated with Turbo DNase (Invitrogen, Cat# AM2239) for 30 min. at 37°C and purified by precipitation in 100% EtOH and with 1 µL of GlycoBlue (Invitrogen, Cat# AM9516) o/n at -20°C. The following day the RNA-containing samples were spin at 17000 g for 30 min. at 4°C. Supernatant was removed and 1 mL of 80% EtOH was added to the samples. Samples were vortexed heavily and spin for 15 min. at 4°C at 17000 g. Pellet was re-suspended in 15 µL of RNase free water.

4.2.4 – Zebrafish ovary extraction

Adult zebrafish female (older than 3 months) were sacrificed in ice-cold water. Fish were decapitated and their belly was cut open by ventral dissection from the anterior side toward the posterior side until the anal fin. Ovaries were extracted with forceps and placed into tubes.

For whole mount fixation, 1 mL of PBS-Tw (0.5% Tween20 in PBS) with 4% Paraformaldehyde (PFA) was added to each tube containing one ovary. These were incubated for 3 hours, shaking, at RT and then washed twice in PBS-Tw and then gradually brought to 100% Methanol (MetOH) with MetOH/PBS dilutions (50%, 75%, 87.5% and 100%) and stored at -20°C for at least 72 hours.

Alternatively, ovaries were not fixed but used promptly for RNA extraction protocol (Methods – 4.2.10).

4.2.5 – Chemical fixation of zebrafish embryos and larvae

Embryos from mating of zebrafish were collected in petri dishes with E3 medium. At stages between 1 hour post fertilization (hpf) and 3 hpf, 30-50 zebrafish embryos were collected into tubes. At larval stages (~24 hpf), 20-30 zebrafish larvae were manually de-chorionated with forceps and collected into tubes.

From tubes containing embryos or larvae, water was sucked out and replaced with 1 mL of 4%PFA/PBS-Tw for fixation. Embryos were kept in 4%PFA/PBS-Tw for 3 hours at RT with mild shaking while zebrafish larvae were kept in 4%PFA/PBS-Tw o/n at 4°C rotating on a wheel. Embryos were washed twice in PBS-Tw and de-chorionated with forceps in PBS-containing petri dishes under a Stereomicroscope. Larvae samples were washed twice in PBS-Tw. Both zebrafish embryos and larvae were brought to 100% Methanol (MetOH) with series of MetOH/PBS dilutions (50%, 75%, 87.5% and 100%) and stored at -20°C o/n or longer.

4.2.6 – RNA extraction and cDNA preparation

Ovaries from fish were homogenized in TRIzol Reagent (Thermo Fisher, Cat# 15596018) using a sterile pestle in a 1.5 mL sterile tubes. Samples were centrifuged at 12000 g, at 4°C, for 5 min. and the clear supernatant was transferred to a new tube. To each tube, 0.2 mL of chloroform were added. Tubes were vortexed for 20-30 seconds and then incubated for 2-3 min. Samples were centrifuged for 15 min. at 4°C at 12000 g. The upper aqueous phase was transferred to new tubes and 0.5 mL of isopropanol were added. Samples were incubated 1 hour at -80°C and then centrifuged for 10 minutes at 4°C at 16000 g. Supernatant was discarded and pellet re-suspended in 1 mL of 75% Ethanol (EtOH). Samples were vortexed and centrifuged for 5 min. at 160000 g at 4°C. Supernatant was discarded and samples were let dry. Pellets were re-suspended in 20 µL of sterile water.

4.2.7 – Gateway Cloning of *tdrd6c-mKate2*

The plasmid containing the *tdrd6c-mKate2* sequence was generated with the Tol2kit for multisite-Gateway cloning (Kwan et al., 2007). The *tdrd6c* ORF and the *tdrd6c-3'utr* were amplified from zebrafish ovarian cDNA (Methods – 4.2.6). The *mKate2* sequence was amplified from existing plasmid in the lab and annealed to the *tdrd6c-3'utr* with incubation at 95°C for 5 min. in a Thermocycler and gradual cool down. The *tdrd6c* ORF sequence and the *mKate2-tdrd6c-3'utr* sequence were cloned respectively into the pDonr221 and the p2r-P3 vectors using BP clonase reactions (Thermo Fisher, Cat# 11789020). The LR reaction (Thermo Fisher, Cat# 12538120) was performed using the two obtained plasmids from the BP reaction and the p5E_pziwi (containing the *ziwi promoter*) together with the destination vector tol2CG2 (Kwan et al., 2007).

4.2.8 – Injection of zebrafish zygotes

CRISPR-gRNAs were diluted in 0.05% Phenol red (Sigma-Aldrich, Cat# 143-74-8) to a final concentration between 100-500 ng/µL, together with 2 µM of Cas9 protein (NEB, Cat# M0646T). Tol2-plasmids were diluted in 0.05% Phenol red to a final concentration

of 100 ng/µL, together with Transposase encoding mRNA (100 ng/µL). A volume between 2 and 5 nL (1 to 2.5 µg of each RNA or 200 ng to 500 ng of plasmid) was injected to wild type zebrafish zygotes via glass needles capillaries (Harvard Apparatus, Cat# EC1 30-0038).

4.2.9 – Genotyping of zebrafish strains

Fish were anesthetized in 4.2% Tricaine (0.4% w/v Ethyl 3-aminobenzoate methanesulfonate, 21 mM TRIS, pH 9) and DNA was extracted from caudal fin tissue with incubation in 20 µL of Lysis Buffer (50 mM KCl, 2.5 mM MgCl2, 10 mM Tris, 0.5% NP40, 0.5% Tween20, 0,01% w/v Gelatine and 0,1 mg/mL Proteinase K, pH 8) for 1 hour at 60°C. Proteinase K was then inactivated for 15 min. at 95°C and samples diluted with at least 50 µL of sterile water. The primers used to amplify and sequence the different alleles are listed in the Table 3.

4.2.10 – Gibson Assembly Cloning

Plasmids used for transfection of BmN4 cells and for protein expression were cloned using Gibson Assembly strategy (Gibson et al., 2009), using the reagents produced by the IMB Protein Production Core Facility (Gibson Assembly Reaction Mix) and following their provided protocols.

4.2.11 – Count of PGCs

At 24 hpf, Vasa-eGFP-positive zebrafish larvae were dechorionated and fixed in 4%PFA/PBS-Tw. Then, samples were washed twice in PBS and placed in 8-wells slides (Ibidi, Cat# 80826) and analyzed under the 10X objective of the Visitron VisiScope microscope.

Name	Sequence	Purpose
AC_seq_1F	TCCCAAATCGCACAGCCCTA	Amplification and sequencing of *tdrd6c*
AC_seq_1R	AAGAATGATCCGGGATGGCA	Amplification and sequencing of *tdrd6c*
AC_seq_2F	TGCGGTCTTGCTCCAAAAGT	Amplification and sequencing of *tdrd6c*
AC_seq_2R	GGATCCCCACACATCTTCTCGT	Amplification and sequencing of *tdrd6c*
AC_seq_3F	GACAAAGGTGTTGGATGGCGG	Amplification and sequencing of *tdrd6c*
AC_seq_3R	TTGGTCTTGCTCCACAGGTCTT	Amplification and sequencing of *tdrd6c*
AC_seq_4F	CGCCACAGACTGCATGTTCA	Amplification and sequencing of *tdrd6c*
AC_seq_4R	TGCAGTGTACTTGGGATTCGCT	Amplification and sequencing of *tdrd6c*
AC_seq_5F	AGGCAGCAGGTGAAAATGGT	Amplification and sequencing of *tdrd6c*
AC_seq_5R	CTGGTTGTATCACACGTTGGGG	Amplification and sequencing of *tdrd6c*
AC_seq_6F	AACCAATGCAGGGAAGGACGA	Amplification and sequencing of *tdrd6c*
AC_seq_6R	TTGGCTGCGTTTCACTGGAAT	Amplification and sequencing of *tdrd6c*
AC_seq_7F	CCATTGAAGCTTTTGCGTCATGC	Amplification and sequencing of *tdrd6c*
AC_seq_7R	TGTGCAGCTGCGCTTGTTCA	Amplification and sequencing of *tdrd6c*
AC_seq_8F	TGTTGGAGCAGATGTGATTGC	Amplification and sequencing of *tdrd6c*
AC_seq_8R	ACCACAAGCTATCATCTCAATGT	Amplification and sequencing of *tdrd6c*
AC_sg_6	TAGAAGTCTCCTTGAAACCAC	Cloning of CRISPR-gRNAs sequences
AC_sg_6c	AAACGTGGTTTCAAGGAGACT	Cloning of CRISPR-gRNAs sequences
AC_sg_7	TAGAAGCCAGCTGTAACTCC	Cloning of CRISPR-gRNAs sequences
AC_sg_7c	AAACGGAGTTACAGCTGGCT	Cloning of CRISPR-gRNAs sequences

Name	Sequence	Purpose
AC_gt_3F	GGGGACAGCTTTCTTGTACAAAGTGGCGGTGAGCGAGCTGATTAAGGAGAACATGCAC	Gateway Cloning of *tdrd6c-mKate2*
AC_gt_3R	CTCACATGGCCAGTGTACTGGCACTTATCTGTGCCCCAGTTTGCTAGGGAGG	Gateway Cloning of *tdrd6c-mKate2*
AC_gt_4F	TAAGTGCCAGTACACTGGCCATGTGAGGTCGATTTTTAAACTTTTATTTATTGTGGAACAGTGTAAACC	Gateway Cloning of *tdrd6c-mKate2*
AC_gt_4R	GGGGACAACTTTGTATAATAAAGTTGCTGTTATAAATGTTAAAACAACCACAGCAACAAAAGCCC	Gateway Cloning of *tdrd6c-mKate2*
AC_gen_9F	ATCCAGCCAGATCAGTTACGC	Genotyping of $tdrd6c^{mz69}$
AC_gen_9R	TGGTTTTTGCCATGGACCCC	Genotyping of $tdrd6c^{mz69}$
AC_gen_12F	ACCAGTTGGTCAAGCCAGAA	Genotyping of $tdrd6c^{mz69}$
AC_gen_12R	AGTGAATGCTGAACCTTGGGT	Genotyping of $tdrd6c^{mz69}$
Tdrd6a_1441_F	GCCAATGCCTTACCACTATC	Genotyping of $tdrd6a^{Q185}$
Tdrd6a_1444_R	GAAGAATTCAGAGGCAAGTG	Genotyping of $tdrd6a^{Q185}$
AC565_gen_Fw	TGGAAACAATAGAGCTTGGCCT	Genotyping of $tdrd6c^{mz87tg}$
AC568_gen_Rv	GGGAGGTCTGCATTTTG	Genotyping of $tdrd6c^{mz87tg}$
bucGFP_fwd	ATG GTG AGC AAG GGC GAG	Genotyping of *buc-egfp*
bucp106UTR_R	GTG TCC ATG TGT ACA TTT ATA GTG AAG	Genotyping of *buc-egfp*
EC_276	TGAACTCCACGTGCACTTCT	Genotyping of *vasa-egfp*
EC_277	TTCTGCTTGTCGGCCATGAT	Genotyping of *vasa-egfp*
EC_282	CTTGTAGTTGCCGTCGTCCT	Genotyping of *gfp-piRNA*
EC_283	CCTCCCCATCTGCACACTTT	Genotyping of *gfp-piRNA*
AC445_Fw	CAAAAACTACTAATCTAGAGGGCCCGCGGTTC	Cloning for BmN4 transfection
AC446_Rv	GGATTGAACAGGCGGCCGCCTTGTACAG	Cloning for BmN4 transfection

Name	Sequence	Purpose
AC449_Fw	TGAGATTTAATCTAGAGGGCCCGCGGTTC	Cloning for BmN4 transfection
AC450_Rv	AGTCTGTGGCGGCGGCCGCCTTGTACAG	Cloning for BmN4 transfection
AC451_Fw	GGCGGCCGCCGCCACAGACTGCATGTTC	Cloning for BmN4 transfection
AC452_Rv	GCCCTCTAGATTAAATCTCAAAGAATTTATCAGCTGC	Cloning for BmN4 transfection
AC453_Fw	ACCCATGTAATCTAGAGGGCCCGCGGTTC	Cloning for BmN4 transfection
AC454_Rv	CATCCACTAGGGCGGCCGCCTTGTACAG	Cloning for BmN4 transfection
AC455_Fw	GGCGGCCGCCCTAGTGGATGAACCTTTAAAAG	Cloning for BmN4 transfection
AC456_Rv	GCCCTCTAGATTACATGGGTAACATTTGTTTTTC	Cloning for BmN4 transfection
AC457_Fw	AATGGCTTAATCTAGAGGGCCCGCGGTTC	Cloning for BmN4 transfection
AC458_Rv	GGATTGAACAGGCGGCCGCCTTGTACAG	Cloning for BmN4 transfection
AC459_Fw	GGCGGCCGCCTGTTCAATCCCTGGTTTAC	Cloning for BmN4 transfection
AC460_Rv	GCCCTCTAGATTAAGCCATTACTTGTTGC	Cloning for BmN4 transfection
AC461_Fw	TGAGATTTAATCTAGAGGGCCCGCGGTTC	Cloning for BmN4 transfection
AC462_Rv	GCTTTGGATAGGCGGCCGCCTTGTACAG	Cloning for BmN4 transfection
AC463_Fw	GGCGGCCGCCTATCCAAAGCTCACGGAAC	Cloning for BmN4 transfection
AC464_Rv	GCCCTCTAGATTAAATCTCAAAGAATTTATCAGCTG	Cloning for BmN4 transfection
AC531_Fw	GACCAAATAAACAAGTTTGTACAAAAAAGCTGAACG	Cloning the Tdrd6c-epitope
AC532_Rv	GCTCAGGTAAGGGCCCCTGGAACAGAAC	Cloning the Tdrd6c-epitope
AC533_Fw	CCAGGGGCCCTTACCTGAGCCGTGTGAG	Cloning the Tdrd6c-epitope
AC534_Rv	ACAAACTTGTTTATTTGGTCTTGCTCCAC	Cloning the Tdrd6c-epitope

4.2.12 – Anti-Tdrd6c antibody production

With the help of the IMB Protein Production Core Facility, I selected, cloned and expressed the following Tdrd6c-peptide:

H2N-LPEPCELNEWFKNYATDCMFNVVVKLNSSGKLSVEMYDDKTNLNLKIKDL WSKTK-CONH2.

This was fused N-terminally with a His-MBP tag to favor solubility and purification. The tag could be cleaved thanks to a 3C Protease-recognition site.

Expression was performed in BL21DE3 competent cells (Table 2). Cells were lysed with Lysis Buffer (50 mM Tris, 300 mM NaCl, pH 7) and the uncleaved peptide was purified with IMAC and eluted in Elution Buffer (50 mM Tris, 300 mM NaCl, 350 mM Imidazole, pH 7). His-MBP tags were cleaved off o/n with 3C Protease. The cleaved peptide was purified with reverse IMAC and gel filtration.

Tdrd6c antibodies were raised in rabbits with the purified cleaved peptide (Eurogentec). Antisera were subsequently purified against the cleaved peptide by the IMB Protein Production Core Facility.

4.2.13 – Whole mount Immuno-Histochemistry

Zebrafish samples (ovaries, embryos or larvae) stored in MetOH at -20°C were rehydrated in PBS-Tw/MetOH series (50%, 75%, 87.5% and 100%). Two additional washing steps in 1% Triton X-100 in PBS were used for ovaries and larvae. Antigen-retrieval was performed with incubation of the samples in 150 mM Tris (pH 9) solution at RT for 5 min. and then at 70°C for 15 min. Samples were then blocked in Blocking Solution (8% BSA in PBS-Tw) for 90 min. at RT with gentle agitation. After blocking, samples were incubated o/n at 4°C with dilution of primary antibodies (anti-Tdrd6a 1:500, anti-Tdrd6c 1:100 and anti-Ziwi 1:100) in Blocking Solution and with gentle agitation. Samples were washed 6 times (30 min. each wash) in PBS-Tw and then incubated in Blocking Solution with dilution of

Table 3. List of designed Oligonucleotides. (In the previous pages) Name, sequences and purposes of oligonucleotides designed during the work of this Thesis.

secondary antibody (anti-Rabbit 1:500, anti-Rat 1:500) o/n at 4°C with gentle agitation. The next day samples were washed 3 times (20 min. each time) with PBS-Tw. During the second wash, DAPI (Bio-Rad, Cat# 32670) was added to samples containing zebrafish larvae. All samples were then mounted on 8-wells slides (Ibidi, Cat# 80826) in PBS containing ~0.5% Low Gelling agarose. Samples were imaged in the VisiScope system with different objectives (10X, 20X, 25X and 40X).

4.2.14 – Live imaging of Zebrafish embryos

Zebrafish embryos were collected in petri dishes containing E3 water manually de-chorionated. With glass pipettes, embryos at the 1-cell stage were gently transferred to 8-wells slides (Ibidi, Cat# 80826). Gently, E3 in excess was removed keeping the samples under the level of the surface of the solution and PBS containing ~0.5% Low Gelling agarose was added one drop at the time. Samples were imaged in the VisiScope system with 20X objective.

4.2.15 – BmN4 cell transfection and imaging

BmN4 cells grown in 25 mL flasks were re-suspended and counted automatically (Bio-Rad, TC20 Automated Cell Counter). Circa 80 thousands cells were placed in each well of a 8-wells-slides (Ibidi, Cat# 80826) in a volume of 300 µL of IPL-41 medium (Gibco) supplemented with Fetal Bovine Serum (Gibco) and 0.5% Pen-Strep. The next day, 1 µL of each plasmid (from stock of 100 ng/µL) was in solution with 0.5 µl of X-tremeGENE_HP (Roche) and 28.5 µL of IPL-41 (Gibco) medium supplemented with 10% Fetal Bovine Serum (Gibco) for 20-30 min. prior to transfection. Transfected cells were imaged 2 days after transfection at the Leica TCS SP5 Confocal microscope with 63X objective.

4.2.16 – Protein expression and purification

The production of MBP-mCherry-Buc and MBP-GFP-prd was performed by the IMB Protein Production facility (Results – 5.6). In this protocol, 0.5 L of Sf9 culture were grown for circa 48 hours post infection. Cells we re-suspended in 60 mL of Lysis Buffer (pH 8, 30 mM Tris-Cl, 500 mM NaCl, 50 mM Arginine, 50 mM Glutamate, 10 mM imidazole, 5% glycerol, 0.2% Triton X-100, protease inhibitor cocktail, 2 mM MgCl2, 1 mM DTT, Sm nuclease 1:4000) and lysed using sonication (15% duty cycle, output 7 for 2 min.). Lysate was spin for 30 min. at 40000 g.

Proteins were bound to HisTrap with low flow rate (0.5 ml/min). After IMAC, samples were eluted in Elution Buffer (30 mM Tris-Cl, 500 mM NaCl, 50 mM Arginine, 50 mM Glutamate, 5% glycerol, 2.5 mM Desthiobiotin, pH 8.0) and 1 mM DTT was added to eluted fractions which were spin prior to gel filtration (S200 16/60 pg). Protein samples in Gel Filtration Buffer (30 mM Na-Hepes, pH 7.4, 300 mM NaCl, 50 mM Arginine, 50 mM Glutamate, 10% glycerol) were then frozen in liquid nitrogen.

4.3 – Quantification and Statistical Analysis

Quantifications of microscopy images were carried out either manually (counting of PGCs, Results – 5.3.1, batch quantification, Results – 5.3.3, and gfp-silencing, Results – 5.3.4) or with pipelines within the Arivis Sofware (germ plasm features, Results – 5.3.2 , measurements of expression levels in BmN4 cells, Results – 5.5.1).

A two-sided Wilcoxon test was used to calculate significant differences between populations in the following experiments: measurement of PGC and male abundancy (Results – 5.3.1) and quantification of *gfp* silencing (Results – 5.4.1) in in offspring of *tdrd6* mutants.

For the statistical analysis of germ plasm condensate numbers a quasi-Poisson model was used (Results – 5.3.2). Differences between the *control* group and the other groups were assessed with Wald-tests on the model parameters. Tests were corrected for multiple testing within the respective data set.

For the statistical analysis of germ plasm condensate volumes a Gaussian linear mixed effects models (LMM) was used (Results – 5.3.2). Differences between the *control* group and the other groups were assessed with t-tests on the model parameters (Bates et al., 2015). Tests were corrected for multiple testing within the respective data set.

4.4 –Tables of Key Resources

Reagent	**Source**	**Identifier**
Antibodies		
anti-Tdrd6c (from Rabbit)	This Thesis	Epitope: LPEPCELNEWFKNYATDCM FNVVVKLNSSGKLSVEMYD DKTNLNLKIKDLWSKTK
anti-Tdrd6a (from Rabbit)	(Roovers et al., 2018)	Epitope: QAVVHEPESEKEKRD
anti-Ziwi (from Rat)	(Roovers et al., 2018)	Epitope: QLVGRGRQKPAPGAM
anti-Rabbit-Alexa555	Invitrogen	Cat# A21428
anti-Rabbit-Alexa647	Abcam	Cat# ab150075
anti-Rat-Alexa555	Invitrogen	Cat# A21434
anti-Rat-Alexa647	Abcam	Cat# ab150155
Chemicals		
TRIzol	Thermo Fisher	Cat# 15596018
TRIzol LS	Thermo Fisher	Cat# 10296010
Ethyl 3-aminobenzoate methanesulfonate (E10521)	Sigma-Aldrich	Cat# 886-86-2
4%-12% NuPage NOVEX gradient gel	Thermo Fisher	Cat# NP0321
NuPAGE LDS sample (Buffer 4x)	Thermo Fisher	Cat# NP0007

Paraformaldehyde 20%	Sigma-Aldrich	Cat# 252549
PBS	From IMB Media Lab Core Facility	-
Bovine Serum Albumine (BSA)	Sigma-Aldrich	Cat# A7906
Dextran Sulfate	Sigma-Aldrich	Cat# 42867-5G
Vanadyl-ribonucleoside complex	NEB	Cat# S1402S
ProLong_Gold Antifade Mountant	Thermo Fisher	Cat# P10144
Triton X-100	Sigma-Aldrich	Cat# T9284
Tween20	Sigma-Aldrich	Cat# P1379
cOmplete Mini, EDTA-free protease inhibitor cocktail Tablets	Roche	Cat# 11836170001
Ficol PM 400	Sigma-Aldrich	Cat# 26873-85-8
IPL-41 insect medium	Gibco	Cat# 11405057
8-well m-slides	Ibidi	Cat# 80826
9 mL X-tremeGENE_ HP	Roche	Cat# 6365779001
BP clonase II	Thermo Fisher	Cat# 11789020
LR clonase II plus	Thermo Fisher	Cat# 12538120
Critical Commercial Assays		
Sp6 mMESSAGE MACHINE kit	Invitrogen	Cat# AM1340
M-MLV reverse transcriptase, RNase H point mutant	Promega	Cat# M3681
QIAquick PCR Purification Kit	Qiagen	Cat# 28106

Table 4. List of chemicals and kits used in this Thesis.

Name	URL	Reference
Ensembl	http://www.ensembl.org/index.html	(Martin et al., 2023)
CrisprSCAN	https://www.crisprscan.org/	(Moreno-Mateos et al., 2015)
IDT Oligo	https://eu.idtdna.com/pages/products/custom-dna-rna/dna-oligos/custom-dna-oligos	-
PLAAC	http://plaac.wi.mit.edu/	(Lancaster et al., 2014)
IUPred2	https://iupred2a.elte.hu/	(Dosztányi, 2018; Erdős and Dosztányi, 2020; Mészáros et al., 2018)
ClustalOmega	https://www.ebi.ac.uk/Tools/msa/clustalo/	-
NCBI	https://www.ncbi.nlm.nih.gov/Structure/cdd/wrpsb.cgi	(Lu et al., 2020; Marchler-Bauer et al., 2017, 2015, 2011; Marchler-Bauer and Bryant, 2004)
StarSEQ	https://www.starseq.com/life-science/sanger-sequencing/u-mix/	-

Table 5. List of Online resources used in this Thesis.

5 – Results

5.1 – Establishment of zebrafish mutant and transgenic lines

5.1.1 – Analysis of *tdrd6* paralog sequences in zebrafish

Zebrafish belongs to the infraclass of *Teleostei* and, as such, its genome has undergone three events of duplication during the course of evolution: two occurred in a vertebrate ancestor during the Cambrian era and one in the ramification of *Teleostei* during the Carboniferous (Christoffels et al., 2004; Dehal and Boore, 2005; Meyer and Van de Peer, 2005). In fact, the gene *tdrd6* in zebrafish is found as three paralogs in the genome: *tdrd6a* and *tdrd6b* on the chromosome 20 and *tdrd6c* on chromosome 17. Despite their localization on different chromosomes, the structure of the *loci* of *tdrd6b* and *tdrd6c* appear similar, exhibiting 3 exonic regions contributing to their open reading frames (ORFs) in contrast to *tdrd6a* which displays 15 coding exons (Fig. 5A). However, all *tdrd6 loci* of zebrafish interestingly have in common the presence of a large exon of size over 5000 base pairs (bp), encoding for the majority of the produced protein, while all the other coding exons are below 200 bp in size. Furthermore, as can be expected from paralogs, all *tdrd6* genes encode for proteins of similar size and structure, having 7 predicted TDs distributed in their peptide sequence of 2117 amino-acids (aa) for *tdrd6a*, 1883 aa for *tdrd6b* and 1814 aa for *tdrd6c* (Fig. 5B).

As discussed in the introduction (Introduction – 3.2.3), the study of Tdrd6a revealed its role in the regulation of Buc mobility, affecting germ plasm structures and germ cell specification in zebrafish (Roovers et al., 2018). In the same work, it was shown that *tdrd6b* is not expressed in the germline of zebrafish while, on the other hand, the Tdrd6c protein was detected as interactor of both Tdrd6a and Buc in oocytes as well as in embryos. Therefore, the first steps of my Thesis project focused on the design and generation of zebrafish mutant lines that could allow me to study the role of *tdrd6c* during zebrafish development, as I will illustrate in the next paragraphs.

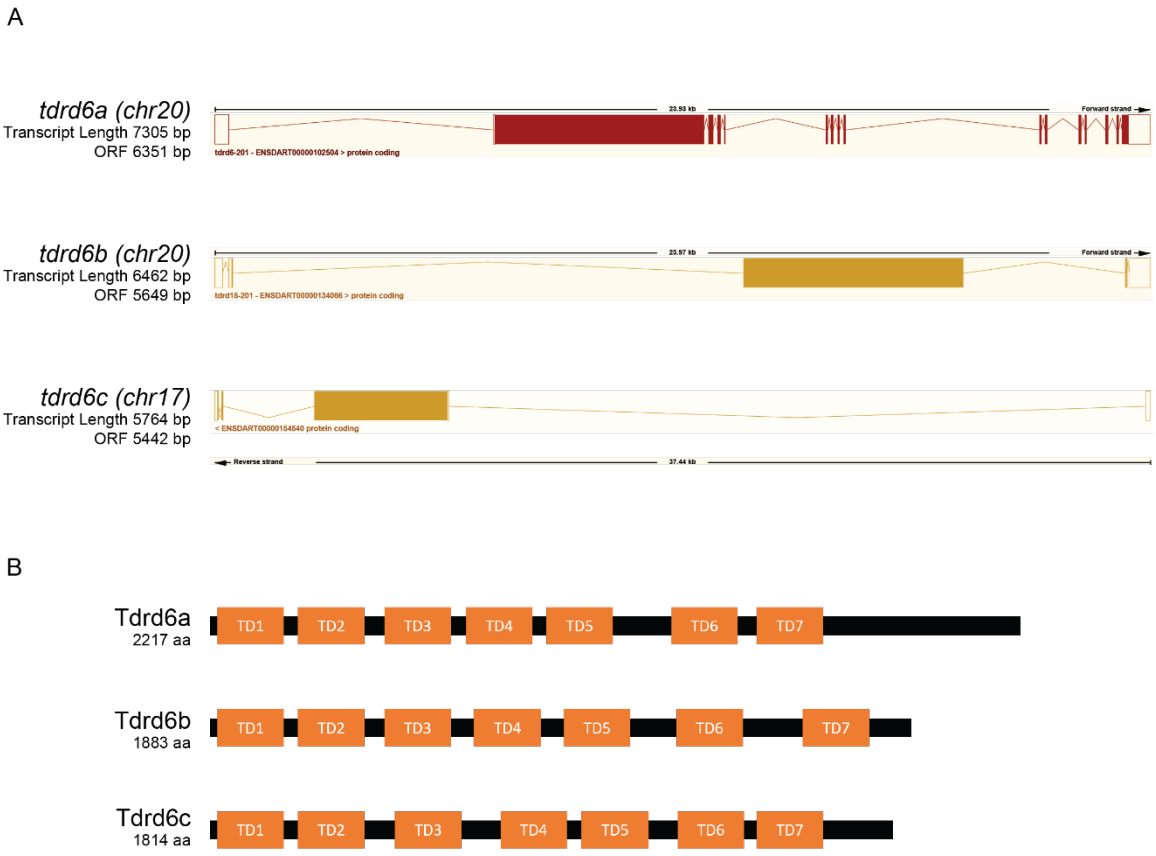

Fig. 5. Overview of *tdrd6 loci* and Tdrd6 proteins in zebrafish. (A) Representation of *tdrd6a, tdrd6b* and *tdrd6c* genomic *loci*. Screenshot from Ensembl database (Martin et al., 2023). (B) Schematic of Tdrd6a, Tdrd6b and Tdrd6c proteins, with highlighted predicted TDs (orange boxes).

5.1.2 – Generation of a *tdrd6c* knock out line

The zebrafish *Danio rerio* reaches sexual maturity approximatively around three months after birth. The common protocols used to induce targeted DNA mutations, in zebrafish, rely on injection of embryonic stages (Hwang et al., 2013; Li et al., 2016). As cell divisions are occurring at a fast rate within the first hours of zebrafish development, depending on the efficiency of the chemicals injected, genetic mutations might occur only in a partial population of cells. This implies that the designed mutation is propagated only in some cell lineages of the multicellular organism, a condition described as genetic mosaicism. Furthermore, genetic information can only be transmitted to the offspring if present in the germ cells, ergo it is crucial that the induced mutation reaches the germline of the

genetically modified organism (GMO) in order to maintain the new genomic feature through generations (Fig. 6).

With the aim of generating a *tdrd6c* knock out line, I used the CRISPR-Cas9 technology to induce double-strand breaks in the zebrafish DNA with specific targeting by guideRNAs (gRNAs) (Hwang et al., 2013; Jinek et al., 2012; Moreno-Mateos et al., 2015). In the attempt to minimize off-target effects and find a more reliable site for CRISPR-mediated DNA cleavage, I designed gRNAs against *tdrd6c* with the accessible framework of CRISPRscan (Moreno-Mateos et al., 2015). My set up aimed at the cleavage of a large sequence of the *tdrd6c* exonic region, possibly causing a knock out by nonsense-mediated decay (NMD). Following my design, I injected the two gRNAs together with the Cas9 protein into wild type embryos at the 1-cell stage (zygote) expecting a deletion of 838 bp within the *tdrd6c* locus accordingly to the supposedly precise CRISPR-Cas9 activity (Fig. 7A). Injected embryos were raised at normal conditions until sexual maturity. From this generation (F0), individual fish were crossed with *wild type* (*wt*) fish and their offspring (F1) was screened for potential mutations within the *tdrd6c* locus. The screening was based on amplification by PCR of genomic material collected from lysates of 48 hpf larvae (Methods – 6.2.2). The primers designed for this PCR amplify a large region (~3 kbp) of the *tdrd6c* first exon, which should enable them to detect any mutation induced by non-precise cleave-and-repair activity on the DNA. In other words, the PCR amplifies both the *wt* allele as well as different possible mutations induced by CRISPR-Cas9 activity and DNA repair (Fig. 7B). This way, one offspring (F1) of an injected female (F0) was recognized to carry a *tdrd6c* allele with an apparent large deletion when compared to the *wt* allele. This female founder was out-crossed with *wt* males again to generate multiple F1 animals. In their adulthood, F1 animals were genotyped and carrier of the *tdrd6c* mutant allele were again out-crossed with *wt* fish in order to reduce possible interference of CRISPR-Cas9 off-targets effects before in-crossing and generation of homozygous *tdrd6c* mutants. The PCR product representing the newly generated *tdrd6c* knock out allele was isolated from agarose gel and characterized with Sanger sequencing (Sanger et al., 1977) (Methods – 6.2.2). This revealed two mutations within the *tdrd6c* exonic region: a first deletion of 5 bp, that causes a frameshift and early stop codon (ORF of 2133 bp), and a second deletion of 1464 bp (Fig. 7C). Fish carrying this allele were in-crossed to generate

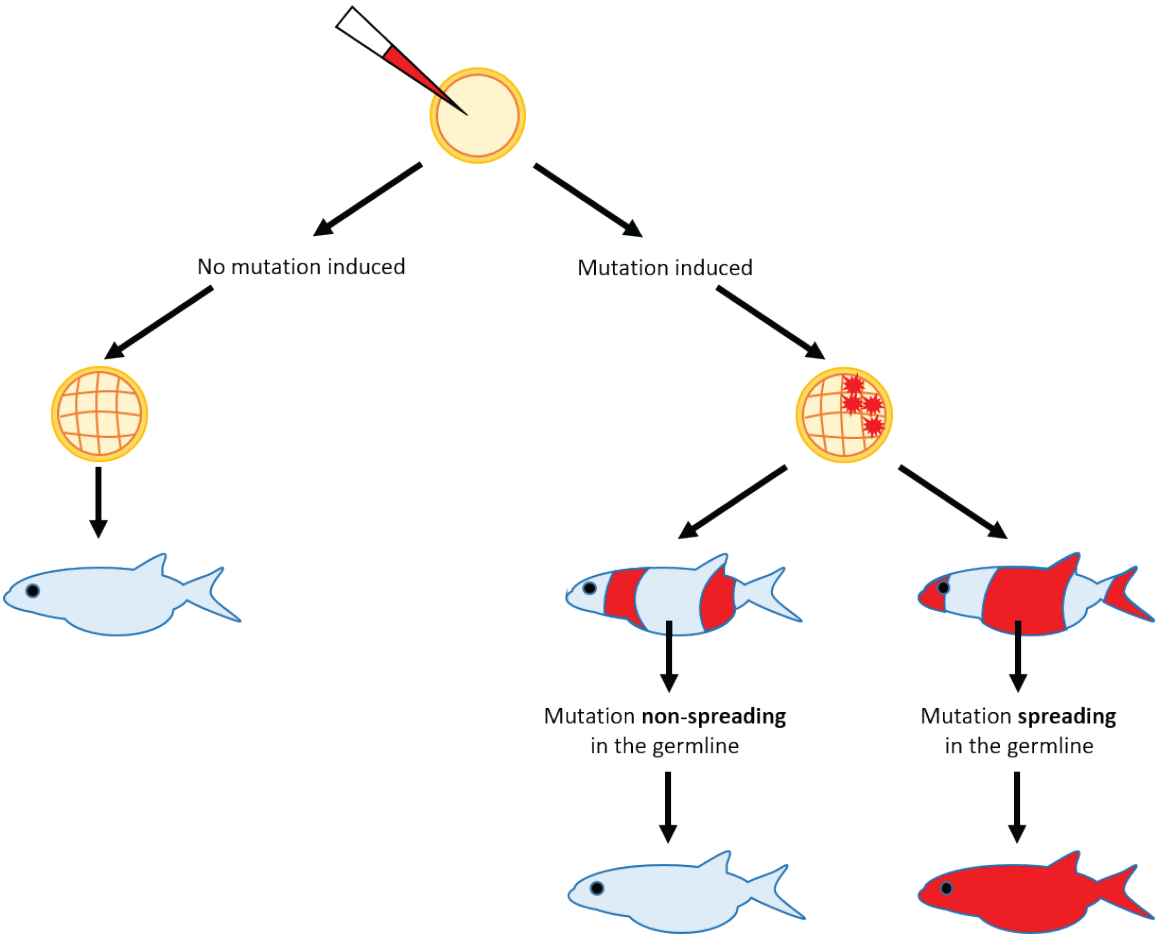

Fig. 6. General overview of GMO generation in zebrafish. On top, portrayal of zebrafish zygote injected with a mutagenic solution (red needle). Following on the left, representation of non-efficient mutagenesis, where cells do not acquire any mutation, resulting in *wt* adult development. Following on the right, portrayal of mutagenesis resulting in mosaicism (red cells in the embryo and red "tissues" in the adult fish). When spread in the germline, the mutation is inherited by all the cell lines of the offspring (red fish).

the first *tdrd6c* population (F3) with both heterozygous and homozygous *tdrd6c* fish (*tdrd6c*$^{+/+}$, *tdrd6c*$^{+/-}$, *tdrd6c*$^{-/-}$).

5.1.2 – Establishment of the *tdrd6c-mKate2* transgenic line

In order to study Tdrd6c localization and interactions, I designed a transgenic line that would express the Tdrd6c protein fused c-terminally to a fluorophore detectable in the red spectrum of emission (wavelength > 590 nm). This range of emission would allow me to

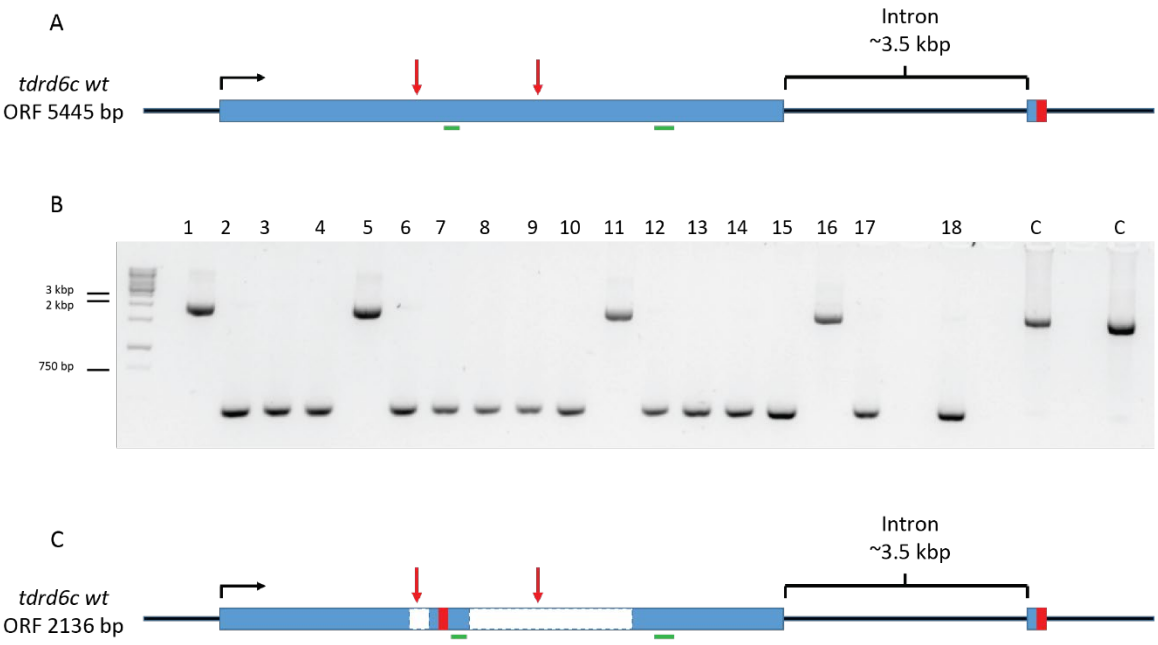

Fig. 7. Characterization of *tdrd6c mutant* allele. (A) Simplified scheme of *tdrd6c locus*, on chromosome 17, peculiarly having only two exonic regions separated by one intron; black arrow symbolizes start of transcription, red box a STOP codon, red arrows the designed CRISPR-Cas9 targeted sites and green lines primers used for genotyping. (B) Genotyping of *tdrd6c* mutant allele in F1 generation, showing high *wt* bands at predicted 1892 bp length and low *mutant* bands at around 500 bp; "c" stands for "control" fish; fish carrying *tdrd6c mutant allele* are: 2, 3, 4, 6, 7, 8, 9, 10, 12, 13, 14, 15, 17, 18. (C) Characterization of the allele, exhibiting two deletions (white boxes) provoked by CRISPR-Cas9 activity, inducing a new and early STOP codon due to frameshift mutation.

combine this fish line with already available GFP-expressing transgenic lines (*e. g. buc-eGFP, vasa-eGFP*) (Krøvel and Olsen, 2002; Riemer et al., 2015). Therefore, I selected the *mKate2* fluorophore, that has emission at a wavelength of 633 nm and a quantum yield of 0.4 (Shcherbo et al., 2009). In the sequence of the designed *tdrd6c-mKate2* transgene I also included the *ziwi promoter*, which is known to drive genetic expression in zebrafish ovaries, and the *tdrd6c-3'UTR*, which could also play an important role in the regulation of the expression of the transgene (Leu and Draper, 2010) (Fig. 8A). Making use of the Gateway multisite cloning technology (Methods – 6.2.3) I combined these four sequences into a destination plasmid that could be injected into zebrafish zygotes (Katzen, 2007) (Fig.

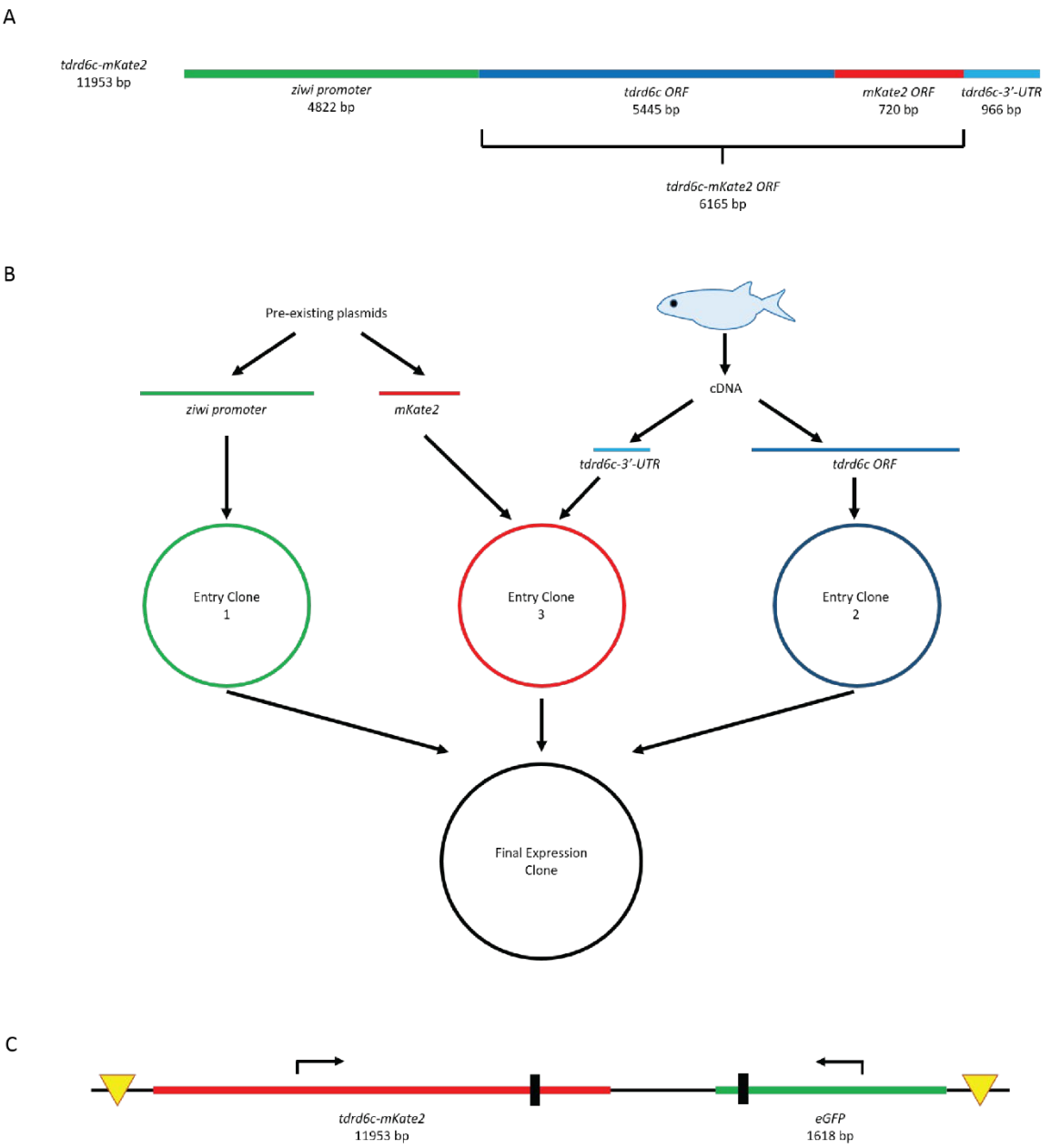

Fig. 8. Design of the *tdrd6c-mKate2* transgene. (A) Representation of the designed *tdrd6c-mKate2* transgene and its features. (B) Scheme of the cloning strategy of the *tdrd6c-mKate2* transgene (Methods – 6.2.3). (C) Representation of the *tol2* cassette used to generate the *tdrd6c-mKate2* transgenic fish; yellow triangles represent *tol2* sites, cleaved from the Tol2 Transposase activity; arrows indicate the start and direction of transcription; black rectangles indicate stop codons.

8B). The resulting plasmid also contains *tol2* sites that can mediate the integration of my designed transgene into the zebrafish genome through a transposition reaction catalyzed

by the Tol2 transposase (Fig. 8C) (Kawakami, 2007; Kwan et al., 2007). Furthermore, the plasmid carries a second gene that drives the expression of the GFP protein specifically in the heart of zebrafish, functioning as a reporter for successful transposase activity. Therefore, screening of injected fish is already possible by the 24 hpf stage after injection, when the heart has already developed sufficiently in zebrafish, with the possibility of measuring the overall efficiency of the injected cocktail. Following this strategy, once cloned and fully sequenced, I injected copies of the complete plasmid into zebrafish *wt* zygotes together with an mRNA encoding for the Tol2 Transposase, a protein that should be able to cut the *tdrd6c-mKate2* transgene from the plasmid and make it available for random insertion into the zebrafish genome. During larval stages, I could observe that part of the injected population (20%-40%) was expressing GFP in their beating hearts. These larvae were isolated and grew further to adulthood (F0). When sexually mature, F0 transgenic fish were crossed to *wt* fish and their offspring was screened for F1 promising carriers. The observation collected in the screen of the F1 generation are summarized in the table below (Table 6).

Mother	**Male**	**mKate2 expression before ZGA (~3 hpf)**	**Heart-GFP expression at 24 hpf**	**Raised**	**Offspring Group**
tdrd6c-mKate2	*wt*	No	No	No	A
		Yes	No	No	B
			Yes	**Yes (1)**	**D**
wt	*tdrd6c-mKate2*	No	No	No	A
			Yes	**Yes (3)**	**C**

Table 6. Scheme of the F1 screening of the transgenic *tdrd6c-mKate2* line. The first two columns indicate which parents (F0) were crossed to each other, while the other columns indicate observation collected on their offspring (F1 generation). Between brackets is specified the number of founders (F0) produced the selected batches (green boxes).

The *ziwi promoter* should drive the expression of *tdrd6c-mKate2* in the germline starting 1-2 weeks after fertilization and then throughout the sexual life of the fish (Leu and Draper, 2010). In particular, in the adult fish, the expression of the transgene should be driven in both female and male gametes, although higher expression has been reported in mature eggs in contrast to spermatozoa. As reported in Table 6, I could only detect Tdrd6c-mKate2 in F1 embryos of transgenic mothers, which was visible already in the first 3 hours of development. This means that the Tdrd6c-mKate2 protein is deposited by the transgenic mother to the zygote, as the zygotic genome is only activated between 3 and 4 hpf in zebrafish, a time window also called zygotic genome activation (ZGA) (Jukam et al., 2017; Vastenhouw et al., 2019). This implies that, although Tdrd6c-mKate2 signal is detectable prior to ZGA, the transgene might not be inherited genetically by the offspring and, according to its promoter, F1-specific expression of *tdrd6c-mKate2* could be checked not earlier than 1-2 weeks post fertilization (wpf), where dissection of the fish would be required (*ergo* an animal sacrifice). However, the *gfp* reporter combined in the designed transgene could be visible already at 24 hpf and would indicate successful genetic transmission of the transgene, which should be selected for breeding (Fig. 9A). With these considerations, I could classify four groups of offspring that I named from A to D as reported in Table 6. This way, I could identify one female and three males from the injected F0 population as transgenic founders. These individuals were isolated and their offspring (belonging to group C and D) were raised in the aquarium. When adults, within these four different F1 populations of siblings, I observed that only females, and not males, from one of these families was able to express and transmit the Tdrd6c-mKate2 protein to the next generation (F2) (Fig. 9B). I could then keep breeding this strain, this way establishing a stable *tdrd6c-mKate2* transgenic line that I could use for further experiments.

5.1.3 – Generation of zebrafish strains with combined genomic features

After successfully generating and maintaining a *tdrd6c* knock out line and the reporter transgenic *tdrd6c-mKate2* line, I crossed these fish with already available zebrafish lines and generated multiple strains, as summarized in the table in the next page (Table 8). These

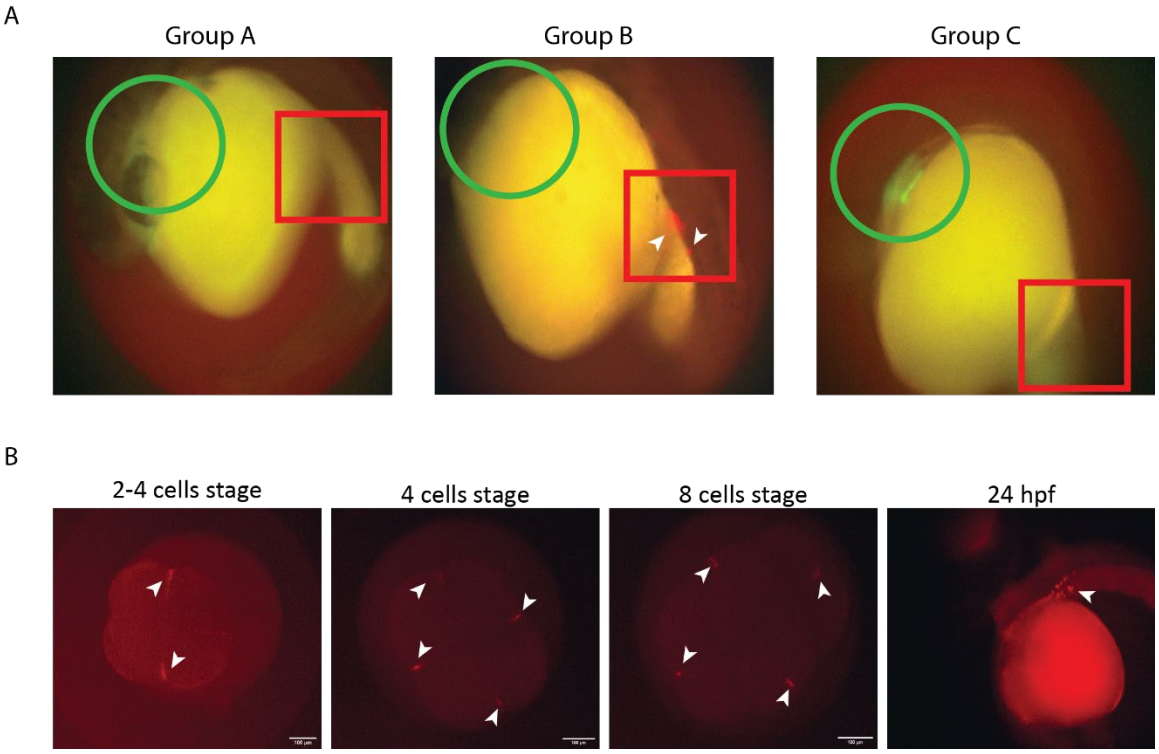

Fig. 9. Tdrd6c-mKate2 expression in offspring of transgenic mothers. (A) Example of larvae assigned to different groups (as explained in Table 6) during the screen of *tdrd6c-mKate2* transgene expression: group A has no transmission of parental Tdrd6c-mKate2 (red box and arrowheads) and no zygotic expression of GFP in the heart (green circle); group B displays transmission of Tdrd6c-mKate2 but no genetic inheritance of the transgene; group C has genetic inheritance of the transgene. Larvae belonging to group D are not reported here because their GFP signal was weak at 24 hpf and only detectable at 48 hpf, when the signal of Tdrd6c-mKate has already faded out significantly. (B) In the established transgenic line, Tdrd6c-mKate2 localizes to cleavage furrows of dividing cells during embryonic stages, similarly to germ plasm foci (arrowheads). Furthermore, the signal is stable over time and visible at 24 hpf, where it is found in cells at the genital ridge (arrowhead), the niche reached by PGCs after migration.

strains are all viable at standard conditions and do not manifest any altered behavior or body-structure defects.

Name	Purpose	References
tdrd6c$^{-/-}$	Characterization of *tdrd6c* function	This thesis
tdrd6a$^{-/-}$*; tdrd6c*$^{-/-}$*; buc-eGFP*	Analysis of oocyte structures and germ plasm in *tdrd6* mutants	(Riemer et al., 2015; Roovers et al., 2018)
tdrd6a$^{-/-}$*; tdrd6c*$^{-/-}$*; vasa-eGFP*	Analysis of PGCs in *tdrd6* mutants	(Krøvel and Olsen, 2002; Roovers et al., 2018)
tdrd6c-mKate2	Visualization of Tdrd6c with live imaging fluorescence techniques;	This thesis
tdrd6c-mKate2; buc-eGFP	Visualization of Tdrd6c and its interaction with Buc	(Riemer et al., 2015)
tdrd6c-mKate2; vasa-eGFP	Visualization of Tdrd6c in PGCs	(Krøvel and Olsen, 2002)
tdrd6a$^{-/-}$*; tdrd6c*$^{-/-}$*; tdrd6c-mKate2; buc-eGFP*	Measuring transgene rescue effect in case of measurable phenotypes	(Riemer et al., 2015; Roovers et al., 2018)
tdrd6a$^{-/-}$*; tdrd6c*$^{-/-}$*; tdrd6c-mKate2; vasa-eGFP*	Measuring transgene rescue effect in case of measurable phenotypes	(Krøvel and Olsen, 2002; Roovers et al., 2018)

Table 7. List of fish lines generated and used for the work of this Thesis. Columns specify names, scopes and references for each combination of transgenes and alleles.

5.2 – Tdrd6c localizes to germ plasm related structures

5.2.1 – Tdrd6c localization during zebrafish oogenesis is restricted to the perinuclear *nuage*

Previous studies have reported evidence of *tdrd6c* expression during zebrafish oogenesis and early embryonic stages (Liu et al., 2022; Roovers et al., 2018). In particular Tdrd6c protein was enriched in pull-down experiments performed against Tdrd6a and Buc-eGFP (Roovers et al., 2018). Altogether, these data suggest that Tdrd6c may be also enriched in

the Bb and the *nuage* structure of oocytes and germ plasm condensates during embryogenesis, similarly to its paralog Tdrd6a. In order to confirm this hypothesis, I used confocal microscopy to analyze eggs from the *tdrd6c-mKate2* line as well as *wt* ovarian tissue stained with antibody against the Tdrd6c protein.

In order to analyze *tdrd6c-mKate2* oocytes, I imaged them in combination with Tdrd6a immuno-staining, which highlights both the *nuage* structure as well as the Bb and vegetal granules (Fig. 10). The Tdrd6c-mKate2 signal only enriched around the *nuclei*, matching the pattern of the *nuage* marked by staining of Tdrd6a. On the other hand, no particular enrichment of Tdrd6c-mKate2 was found in the Bb or vegetal granules, also marked by the detection of Tdrd6a.

This observation would suggest that Tdrd6c localization is restricted only to the perinuclear environment of zebrafish oocytes, in contrast to Tdrd6a, that is also found enriched in the Bb. Furthermore, this observation hints that Tdrd6c could have a different role compared to Tdrd6a during oogenesis, as lack of Tdrd6a resulted in Bb defects (Roovers et al., 2018). However, the expression and localization of the transgenic protein could differ from the one of the *tdrd6c* endogenous gene. Unfortunately, attempted antibody staining-visualization of Tdrd6c in *wt* egg populations (with different stages of oocyte maturation) did not result in the observation of any significant enrichment of endogenous Tdrd6c protein. It may be worth to try to detect endogenous Tdrd6c's localization with the use of different microscopy techniques and set ups, which could be more sensitive in the analysis of large bodies like zebrafish oocytes. Nevertheless, transgenic expression of *tdrd6c-mKate2* in eggs of zebrafish suggests that Tdrd6c localization is restricted to the *nuage* during oogenesis, hinting at the possibility that Tdrd6c role is different to its paralog Tdrd6a.

5.2.2 – Maternally provided Tdrd6c enriches to germ plasm droplets during zebrafish early development

After the fertilization of the oocyte, components of the *nuage* can be found in germ plasm condensates, as for example in the case of the protein Ziwi (Houwing et al., 2007).

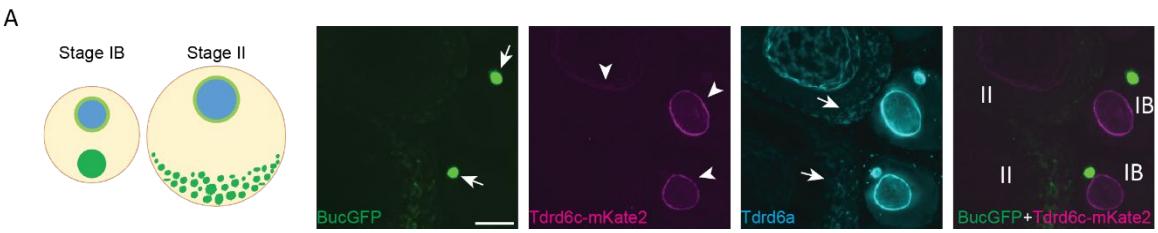

Fig. 10. Tdrd6c localizes to the *nuage* of zebrafish oocytes. On the left, schemes of oocytes structures at different stages of oogenesis: perinuclear *nuage* in light green around the blue nucleus, Bb and vegetal granules in darker green; on the right, panel showing Buc-eGFP (green) marking Bb and vegetal granules (arrows) and Tdrd6c-mKate2 (magenta) localizing to the *nuage* (arrowheads); Tdrd6a antibody-staining (cyan) highlighting all structures (Bb, vegetal granules and *nuage*).

Therefore, I could expect a similar dynamic for Tdrd6c, if the protein is stably inherited by the embryo. Furthermore, as shown at low magnification in the previous paragraph, Tdrd6c-mKate2 protein seems to enrich at cleavage furrows of zebrafish embryo resembling germ plasm localization (Fig. 9B).

In order to validate this observation I generated the *tdrd6c-mKate2; buc-eGFP* line, as the Buc-eGFP signal highlights germ plasm structure throughout zebrafish early development (Riemer et al., 2015). Indeed, the Tdrd6c-mKate2 protein co-localizes with Buc-eGFP during embryonic cleavage stages and the segregation of their germ plasm droplets can be followed nicely over time (Fig. 11A, B). When zooming in to the cleavage furrow area, it is noticeable how germ plasm condensates at the 4-cells stage are spread like droplets in the embryo but particularly enriching in tight proximity of each other within a segment of the furrow (Fig. 11B). At later stages, the germ plasm droplets start fusing into a smaller area, forming a bigger condensate.

Immuno-staining against Tdrd6c performed on Buc-eGFP-positive embryos provided further evidence that endogenous Tdrd6c enriches in condensates marked by Buc-eGFP, confirming that Tdrd6c belongs to germ plasm structures in zebrafish (Fig. 11D). Anti-Tdrd6c antibody was produced as described in the method section (Method – 6.2.4) against a selected unique amino-acidic sequence within of the Tdrd6c peptide and validated on embryos lacking expression of Tdrdc6 (Fig. 11C, E). These data show that Tdrd6c is

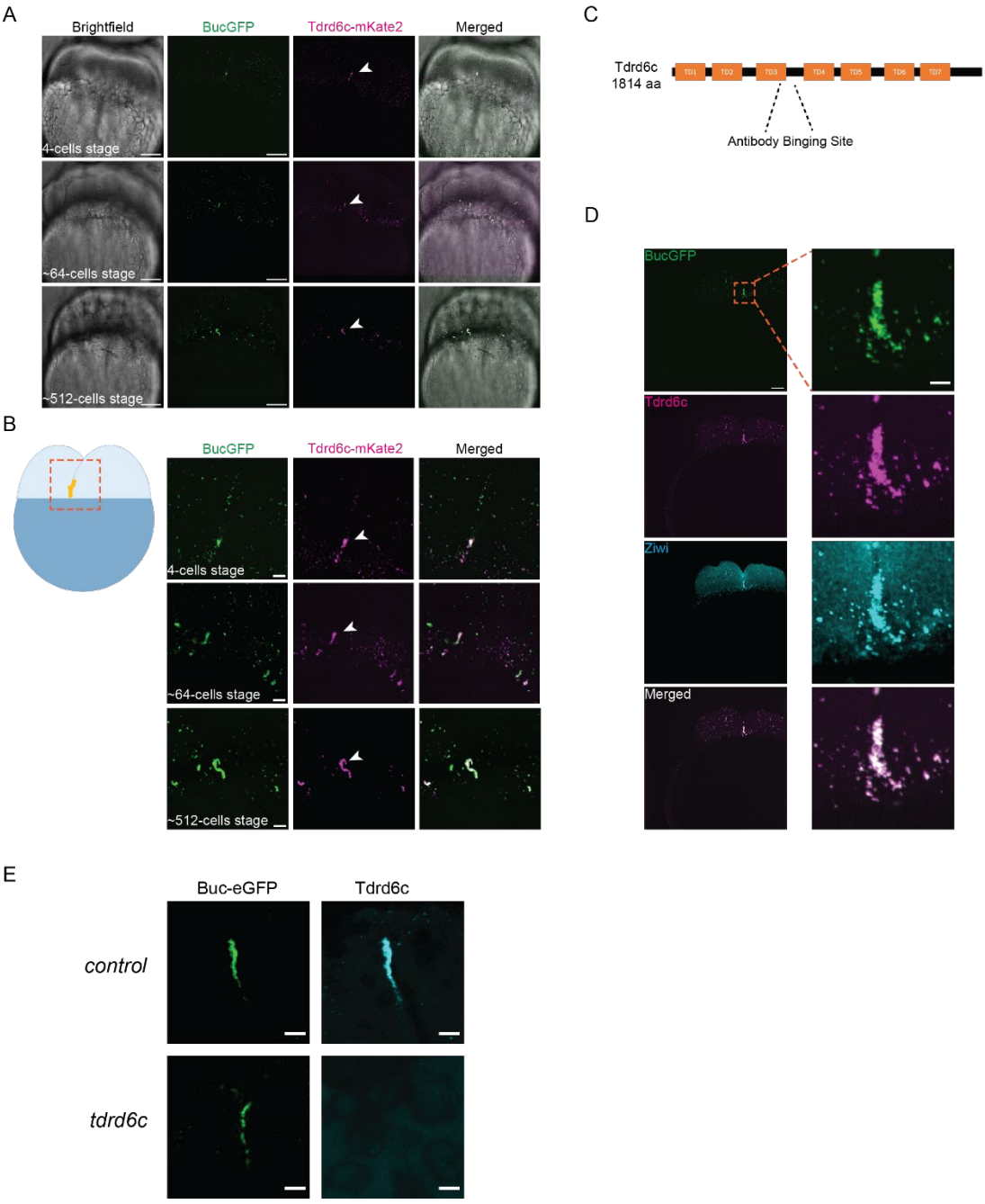

Fig. 11. Tdrd6c localizes to the germ plasm condensates during embryonic stages. (A) Frames collected from a time-lapse video that followed the development of *tdrd6c-mKate2; buc-eGFP* embryos; the selected frames show different embryonic stages, as reported in the left bottom corner of the bright-field images; Tdrd6c-mKate2 in magenta can be found co-localizing with the germ plasm structure (arrowhead) marked by Buc-eGFP (green); (B) Zoom-in of the fluorescent images shown in (A). (C) Scheme representing Tdrd6c protein structure and domain, highlighting the location of the epitope for binding of Tdrd6c antibody.

Figure legend continues in the next page.

present in germ plasm structures during embryonic stages, suggesting that Tdrd6c function may contribute to the regulation of germ plasm integrity and composition.

5.2.3 – Maternally provided Tdrd6c enriches in perinuclear granules of zebrafish PGCs

After the cleavage stages during early embryonic development, the germ plasm ends up in a few cells, where it drives the specification of these cells as primordial germ cells (PGCs). In these cells, known germ plasm components localize into condensates of variable sizes around the nucleus, thus referred to as peri-nuclear germ granules (Knaut et al., 2000; Köprunner et al., 2001; Weidinger et al., 2003). At this stage, the correct composition of these granules is important to control gene expression of the germline, similarly to the *nuage* function in the gametes (D'Orazio et al., 2021).

Consistent with its continuous presence in the germ plasm, observation of mKate2 signal localizing in peri-nuclear granules of cells at the genital ridge in the 24 hpf larvae could suggest that maternally inherited Tdrd6c-mKate2 is stably transferred to PGCs during gastrulation and organogenesis (Fig. 12A). Indeed, I could confirm that the Tdrd6c-mKAte2-positive cells correspond to PGCs using the *tdrd6c-mKate2; vasa-eGFP* line, which at 24 hpf highlights PGCs with the expression of GFP in the germ cells (Fig. 12B). Moreover, immuno-staining on *vasa-eGFP* larvae showed that Tdrd6c is enriched in peri-nuclear granules that also contain Ziwi (Fig. 12C). Altogether, these results indicate that inherited Tdrd6c protein is part of the germ plasm structures also at larval stages when peri-nuclear granules are formed, although I should not exclude that the localization observed

---

(Legend continuation from previous page, **Fig. 11**) (D) Immuno-staining against Tdrd6c (magenta) and Ziwi (cyan) performed on Buc-eGFP (green) positive embryos at the 4-cells stage (zoom in on the side of the panel), further highlighting Tdrd6c presence in the germ plasm of zebrafish. (E) Validation of the specificity of the antibody against Tdrd6c (cyan), as its signal is not detected in embryos lacking Tdrd6c expression (lower row) although presence of germ plasm is visualized by presence of Buc-eGFP. Scale bars = 50 µm for (A) and (D); 20 µm for (B) and 5 µm for zoom in of (D) and for (E).

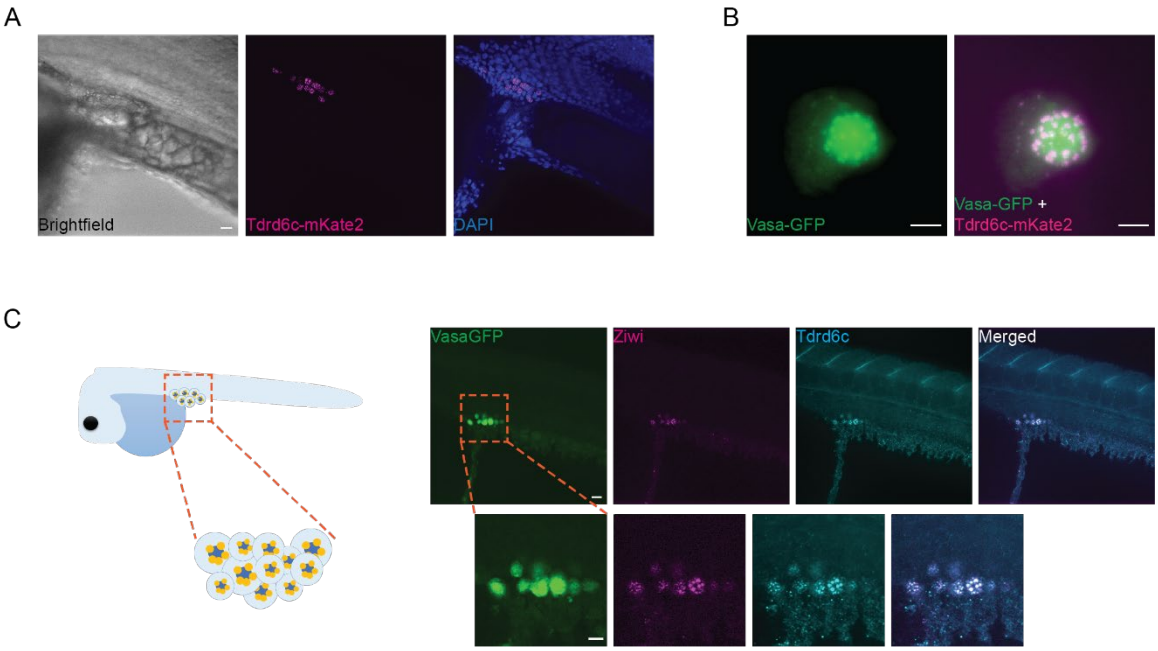

Fig. 12. Tdrd6c localizes to peri-nuclear germ granules during larval stages. (A) At 24 hpf stage, Tdrd6c-mKate2 (magenta) is found in granular structures in cells at the genital ridge of the larva. (B) Tdrd6c-mKate2 (magenta) is found in Vasa-eGFP (green) positive cells. (C) Staining performed on Vasa-eGFP positive larvae revealed that Tdrd6c (cyan) is enriched in Ziwi-positive (magenta) perinuclear granules. Scale bars = 10 µm for (C) and (A); 5 µm for (B) and zoom in of (C).

after ZGA (>3-4 hpf) could also be produced by the *tdrd6c-mKate2* zygotic expression and not the result of maternal inheritance.

5.3 – Tdrd6c, together with Tdrd6a, regulates germ plasm stability and is crucial for PGC specification and fertility of zebrafish

5.3.1 – Tdrd6c is important for PGC abundance and, together with Tdrd6a, essential for zebrafish fertility

As stated previously, all of the zebrafish lines generated for this Thesis are viable and show no apparent phenotype during any stage of their life, growing normally at standard conditions. In particular, *tdrd6c*$^{-/-}$ and *tdrd6a*$^{-/-}$*; tdrd6c*$^{-/-}$ fish have no defects in development and sexual maturity, as they reach fertility after circa three month after birth and can normally mate. Nevertheless, these superficial observation cannot rule out less evident phenotypes and, taken Tdrd6c's localization to embryonic germ plasm and the phenotype scored in the study of the *tdrd6a* gene, I decided to start my analysis with measurements of PGC-related defects in the offspring collected from homozygous mutant females (Roovers et al., 2018). Lack of Tdrd6a expression during oogenesis resulted in a reduced population of PGCs in the offspring, which was quantified by using the *vasa-eGFP* reporter line (Krøvel and Olsen, 2002; Roovers et al., 2018). Following the same strategy, I collected *vasa-eGFP* positive embryos from different crosses (labeling explained in Table 8) and counted GFP-positive cells at the genital ridge in 24 hpf larvae (Fig. 13A, B).

In a first observation, I could confirm that *6a mmut* embryos, at 24hpf, have fewer PGCs compared to the *control* group, as it was shown in previously (Roovers et al., 2018). Likewise, *6c mmut* embryos also showed a drop in number of PGCs compared to *control*, and to a similar extent as *6a mmut* embryos. Interestingly, *6a6c mmut* embryos did not contain any PGCs at 24 hpf, indicating that Tdrd6a and Tdrd6c act in a parallel or partially redundant manner.

Lack of PGCs in zebrafish has been linked to male sex differentiation and obviously affects the fertility of the adult fish (Siegfried and Nüsslein-Volhard, 2008; Weidinger et al., 2003). For this reason, I assessed these aspects in offspring from all crosses by raising them

Mother	Father	Offspring description	Nomenclature
tdrd6a$^{+/-}$*; tdrd6c*$^{+/-}$*;*	*wt*	*From heterozygous mother*	***Control***
tdrd6a$^{-/-}$*; tdrd6c*$^{+/-}$*;*	*wt*	*tdrd6a maternal mutant*	***6a mmut***
tdrd6a$^{+/-}$*; tdrd6c*$^{-/-}$*;*	*wt*	*tdrd6c maternal mutant*	***6c mmut***
tdrd6a$^{-/-}$*; tdrd6c*$^{-/-}$*;*	*wt*	*tdrd6a and tdrd6c maternal mutant*	***6a6c mmut***

Table 8. Nomenclature of offspring of mutant mothers. I will apply this nomenclature to embryos and animals independently of whether they carry or not copies of transgenes (*vasa-eGFP*, *buc-eGFP* or *GFP-piRNA*) but only relatively to the presence, in the mother, of mutant alleles of *tdrd6a* and *tdrd6c*.

to adulthood. At a first glance, following the growth and maturation of these populations, all fish appeared normal and reached a standard size ~3 months after birth, when sexual maturation is usually occurring. However, *6a6c mmut* animals only developed as males, while in the all other populations males and females were found in similar percentages (Fig. 13C). Moreover, *6a6c mmut* adult males were fully sterile: multiple crosses with *wt* females resulted only in unfertilized eggs. On the other hand, *6a mmut* and *6c mmut* males and females did not show any fertility defects.

These results indicate that maternal Tdrd6c is involved in the process of PGC specification in zebrafish, as abundance of PGCs is lower than *control* groups in *6c mmut* population. However, similarly to the observation collected in the study of tdrd6a, maternal Tdrd6c seems to be dispensable for the sexual maturation and fertility of the adult fish. On the other hand, maternal contribution of at least one of the two Tdrd6c proteins, Tdrd6a orTdrd6c, is necessary to ensure PGC development during larval stages and the fertility of the adult individual, as lack of both resulted in the sterility of *6a6c mmut* populations. Following observations collected in the study of *tdrd6a*, PGC defects in *6c mmut* and *6a6c mmut* are likely due to germ plasm structural defects. This, I tested next.

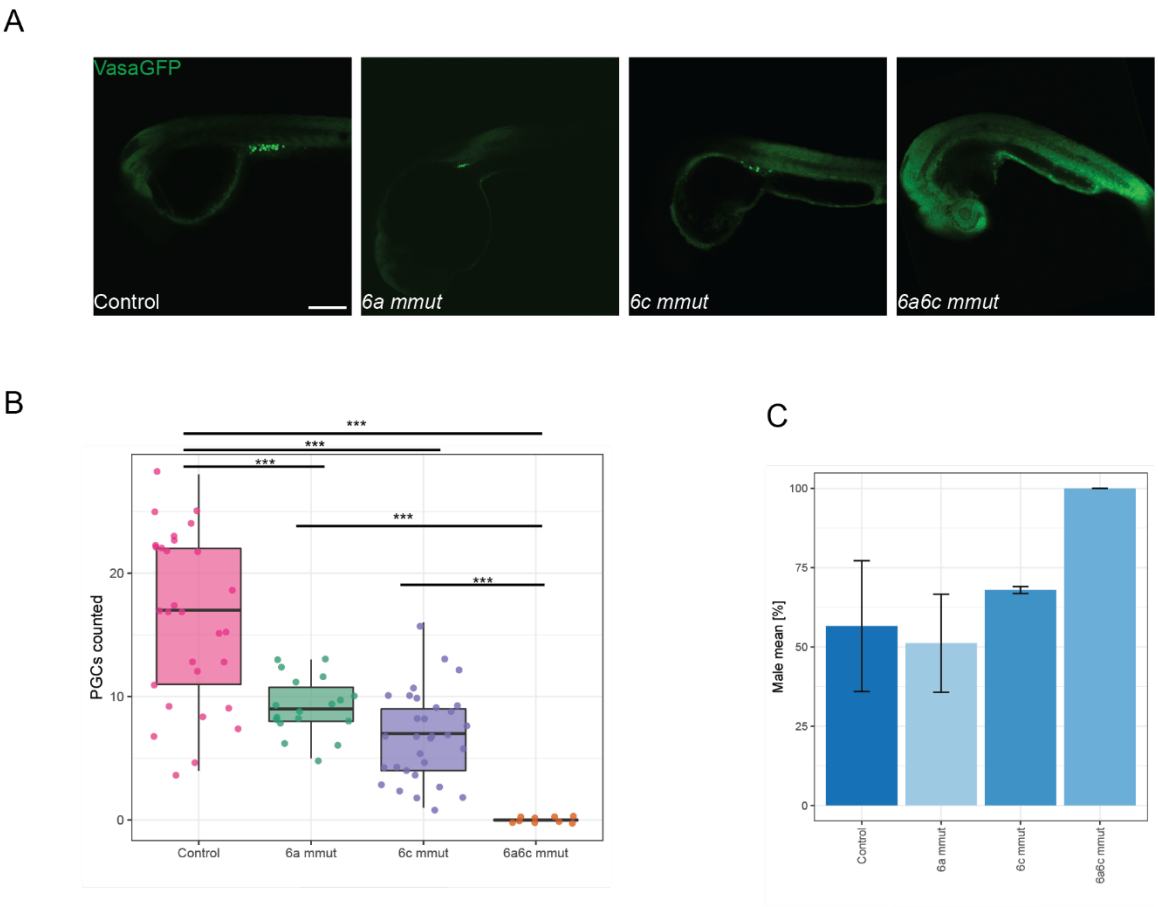

Fig. 13. PGC defects of offspring of *tdrd6a* and *tdrd6c* mutant mothers. (A) PGCs level exhibited in different offspring, highlighted by the Vasa-eGFP signal (green) at the genital ridge of the 24 hpf zebrafish larva. Scale bar = 50 µm. (B) Quantification of PGCs levels in each population. (*** = p-value < 0.005). (C) Quantification of male population over total amount of fish in each population (n = 4).

5.3.2 – Maternally provided Tdrd6 proteins are essential to maintain germ plasm integrity during early embryogenesis

In *6a mmut* larvae, the reduction of PGC abundance has been linked to defects in germ plasm features during early cleavage stages (Roovers et al., 2018). For this reason, combining the *tdrd6* mutant alleles and the *buc-eGFP* transgenic line, I compared germ plasm levels and distribution over time in *6c mmut* and *6a6c mmut* to *6a mmut* and *control* populations (Fig. 14A). Batches belonging to *control*, *6a mmut* and *6c mmut* population did not show any severe germ plasm phenotype within the first 3 hours of development

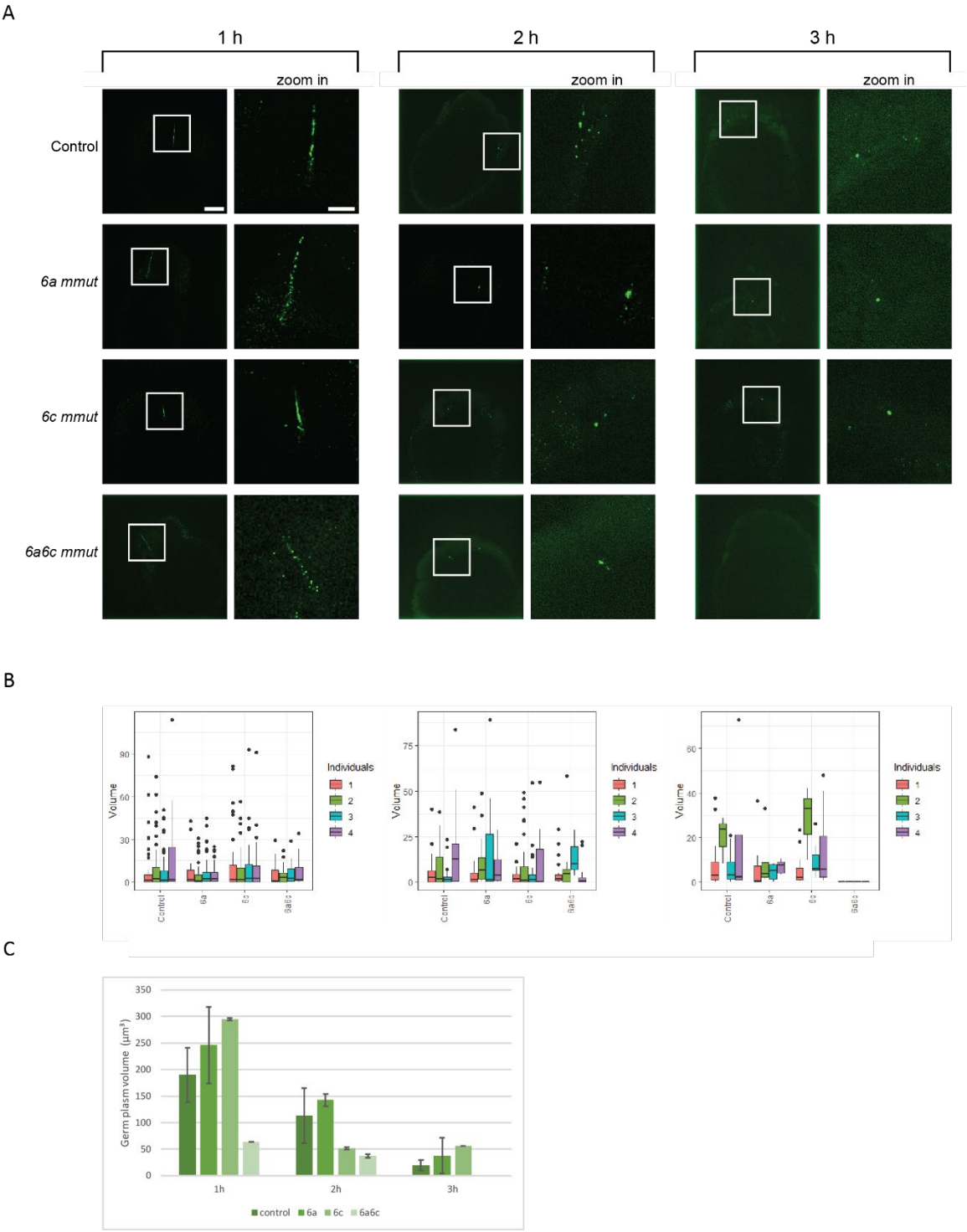

Fig. 14. Defects in germ plasm distribution in *6a6c mmut*. (A) Time lapse performed on embryos from different mutant mothers, following the Buc-eGFP distribution upon ZGA (~3 hpf). (B) Quantification of germ plasm droplets size and numbers in different population of embryos. (C) Quantification of total germ plasm volume detected in each offspring.

(Fig. 14B). It should be considered, however, that data collected from different individuals within each population resulted in a high variance in the quantification of germ plasm droplets numbers and size. Also when measuring the total abundance of the germ plasm, I could see that its decrease in volume over time in *control* population is highly variable (Fig. 14C). Thus, to test the significance of these fluctuations in the *6a mmut* and *6c mmut* more biological replicates would be required. On the other hand, following Buc-eGFP localization in *6a6c mmut* showed that germ plasm enrichment is gradually lost completely during early cell division. In particular, the germ plasm disappears completely between the second and third hour of development, prior to zebrafish ZGA (Vastenhouw et al., 2019). Given that germ plasm is known to be required for PGC specification, this likely explains why PGCs are not formed in *6a6c mmut* embryos: cells are probably lacking the necessary enrichment of determinants for germline specification during a critical time-window when the first cell lineages initiate to differentiate, expressing specific set of genes accordingly to their fate.

5.3.3 – Brood-size drop of Tdrd6a-6c double mutant female zebrafish over time

I noticed a tendency of *tdrd6a*$^{-/-}$*; tdrd6c*$^{-/-}$ female fish to releasing fewer eggs compared to *wt* and single *tdrd6a* and *tdrd6c* mutant females. This seemed to become more consistent with the aging of the animals, as repetition of crosses of *tdrd6a*$^{-/-}$*; tdrd6c*$^{-/-}$ females to *wt* males often resulted in the failure of mating. In order to validate and quantify these qualitative observations I isolated female fish from each genotype, crossed them to *wt* males every two weeks and counted the eggs that were released upon mating. The females were isolated in tanks of 1 L volume together with two companion albino zebrafish, as they are rather social fish and complete isolation could alter their behavior, thus possibly interfering with the mating pattern. On the other hand, these conditions might not reflect the standard situation found in the standard 3.5 L tanks, where fish have more space and belong to a larger community. However, all genotypes received the same treatment, so any bias caused by this strategy should be compensated for in the experiment.

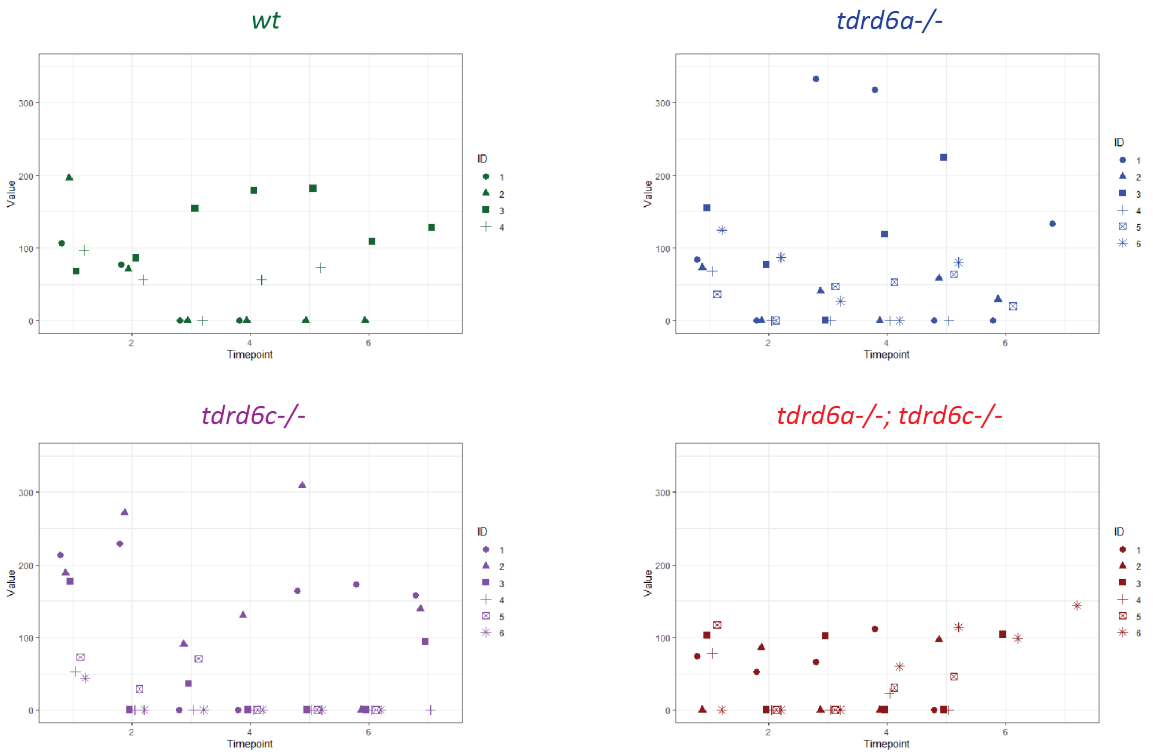

Fig. 15. Quantification of abundancy of different mutant mothers' offspring. Quantification of batches produced by different mothers (each individual corresponding to an ID number from 1 to 6) with different genotypes (*wt* control in green, *tdrd6a*$^{-/-}$ in blue, *tdrd6c*$^{-/-}$ in purple and *tdrd6a*$^{-/-}$*; tdrd6c*$^{-/-}$ in red) when crossed to *wt* males. On the Y-axis, "Value" stands for the count of eggs released by female fish. On the X-axis, each "Time point" unit corresponds to two weeks, which was the selected time between one mating event and the next one.

As stated, I collected batch numbers every two weeks, observing a big variability within different individuals, even in the control *wt* population (Fig. 15). In fact, differences between offspring of different mutant mothers did not provide significant results as more biological replicates would be required to reach statistical significance. However, comparing the trends of each population leads me to speculate that *tdrd6a*$^{-/-}$*; tdrd6c*$^{-/-}$ mutant female fish overall lay less eggs compared to *wt*, seemingly needing more time to repopulate their ovaries with mature eggs between one mating and the next.

5.3.3 – Gene silencing defects in *tdrd6* mutants

In our laboratory we developed a tool with the aim of being able to observe and measure piRNA-driven gene silencing *in vivo* in the zebrafish system. This consists of a Tol2-mediated insertion of a *gfp* copy in the genome of the zebrafish which triggers production of piRNAs against *gfp* sequences (unpublished data from Edoardo Caspani). The provoked interference with the expression of GFP sequences allows for the measurement of germline silencing by piRNAs using reporter transgenic lines like the *vasa-eGFP* line (Fig. 16A, B). In order to quantify potential differences in the functioning of the germline piRNA silencing machinery in *tdrd6a; tdrd6c* mutant females I generated a *tdrd6a; tdrd6c; vasa-eGFP; GFP-piRNA* line (Table 7). Unfortunately, due to the necessity of combining these four alleles as it has been challenging to raise sufficient animals with the required genotype. However, preliminary results hint that the silencing machinery of the germline could be impaired in absence of Tdrd6a and Tdrd6c expression (Fig. 16C). More fish from this line are currently growing and maturing in our laboratory and hopefully will provide consistent data to clarify if and to what extent the silencing machinery is affected in *tdrd6a* and *tdrd6c* mutants.

5.4 – Structural analysis of Tdrd6c Tudor Domains

5.4.1 – Tudor domains of Tdrd6c are extended Tudor domains

The protein Tdrd6c possesses seven TDs, as predicted by alignment in the NCBI domain database (Lu et al., 2020; Marchler-Bauer et al., 2017, 2015, 2011; Marchler-Bauer and Bryant, 2004). However, as discussed in the introduction, TDs can exhibit different functions, as differences in their amino-acidic sequences and 3D structures can reflect on diverse modes of interaction with various targets. For this reason, with the development of

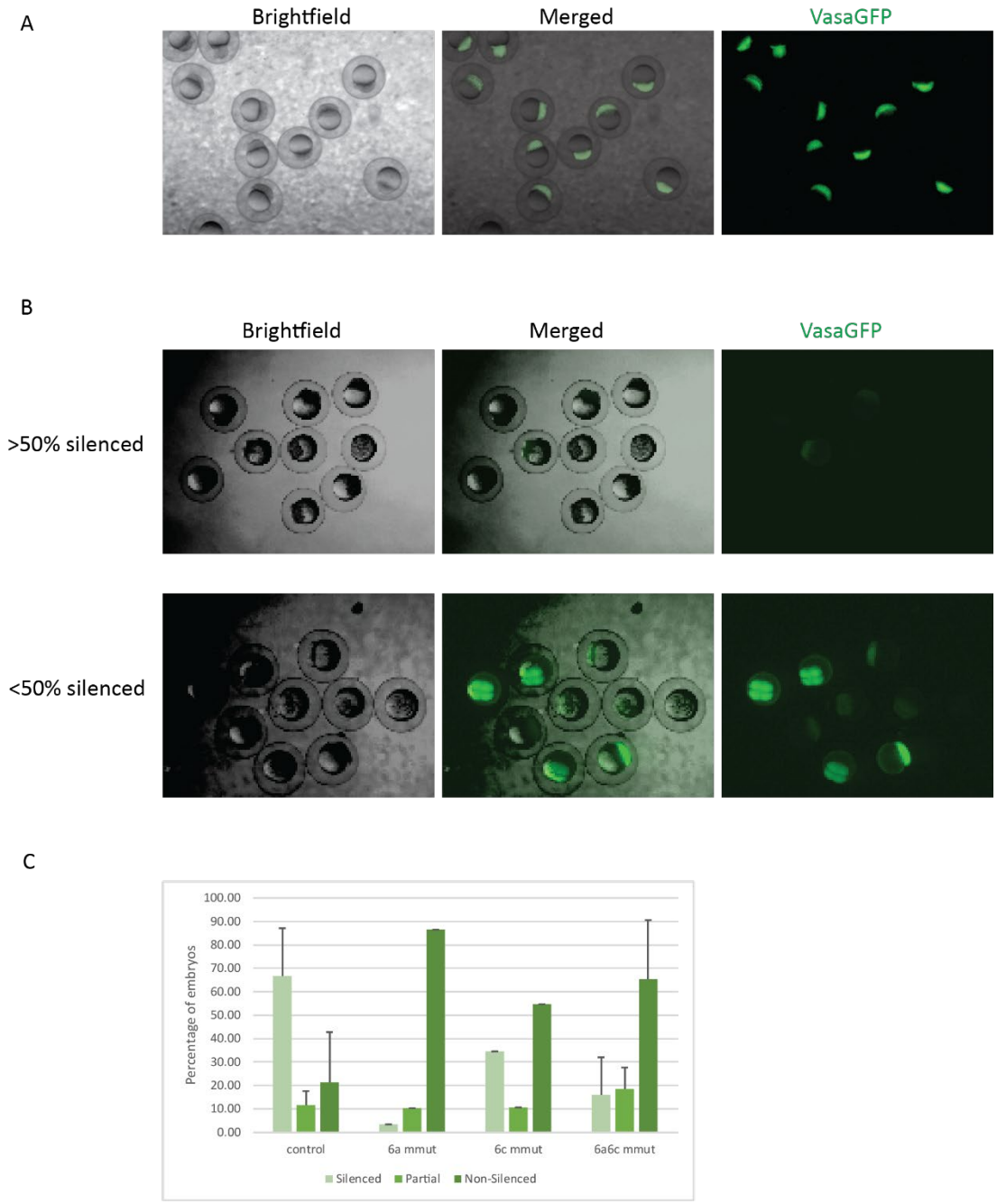

Fig. 16. Quantification of *gfp* silencing in the germline of *tdrd6a* and *tdrd6c* mutant fish. (A) Batch of embryos collected from *vasa-eGFP* positive mother, displaying expression of Vasa-eGFP distributed in all cells of the embryos. (B) Examples of *vasa-eGFP* silencing in different control population collected from two different mothers. (C) Quantification of *vasa-eGFP* silencing in embryos belonging to specific populations. Batches were collected from more than one mother in the *control* (n. = 10) and in the *6a6c mmut* (n. = 2) population of fish, while the other groups were lacking female fish carrying all the necessary alleles to carry out the experiment.

globular structures almost solely represented by TDs, separated by linker loops of at least 21 amino-acids (between TD6 and TD7) to a maximum of 84 amino-acids (between TD3 and TD4) (Fig. 17A).

When observing the structures of the TDs in Tdrd6c, I noticed that, as expected, they all appear to possess the canonical barrel formation formed by five anti-parallel β-sheets with an additional C-terminal α-helix. Furthermore, N-terminally to the barrel structures, they all show two additional β-sheets followed by one α-helix and, following on the c-terminus of the barrel, at least two β-sheets and two α-helices (Fig. 17B). These structures are in agreement with the structure of extended TDs relative to the study of the Survival of Motor Neuros protein (SMN) (P. Selenko, 2001).

Within the barrel structure of the canonical TDs, important residues have been highlighted to be relevant in the interaction between the TD and methylated substrates, as portrayed in the SMN protein (H. Liu et al., 2010; K. Liu et al., 2010). In particular, four aromatic amino-acids have been identified to be essential in constituting an aromatic cage where one Asparagine residue it is exposed for binding of methylated substrates. In the alignment of Tdrd6c eTDs and the reference SMN TD, I could see that not all of the 7 Tdrd6c's eTDs exhibit these conserved residues (Fig. 17C). In fact, eTD1 and eTD2 are missing one out of four aromatic residues, which are required to form a pocket relevant for substrate recognition (H. Liu et al., 2010; K. Liu et al., 2010). Furthermore, the first three eTDs of Tdrd6c do not possess, within this aromatic pocket, the Asparagine (N) residue supposed to interact with methylated Arginines or Lysines of their targeted proteins. Indeed, eTD1, eTD2 and eTD3 of Tdrd6c have their Asparagine residues substituted by, respectively, a Lysine (L), an Isoleucine (I) and an Aspartate (D).

These observations suggest that all TDs of Tdrd6c are extended TDs separated by flexible linker sequences, strengthening the hypothesis of Tdrd6c participating in the interaction with multiple substrates, this way playing a role in the regulation of complex molecular networks such as the germ plasm structures in zebrafish. Moreover, analysis of conserved residues hint at the possibility that the first three eTDs of Tdrd6c could have a different way of interacting with their targets compared to the other eTDs of Tdrd6c, as they display modifications of the residues that build an aromatic cage, conserved in canonical eTDs, required for substrate recognition and interaction.

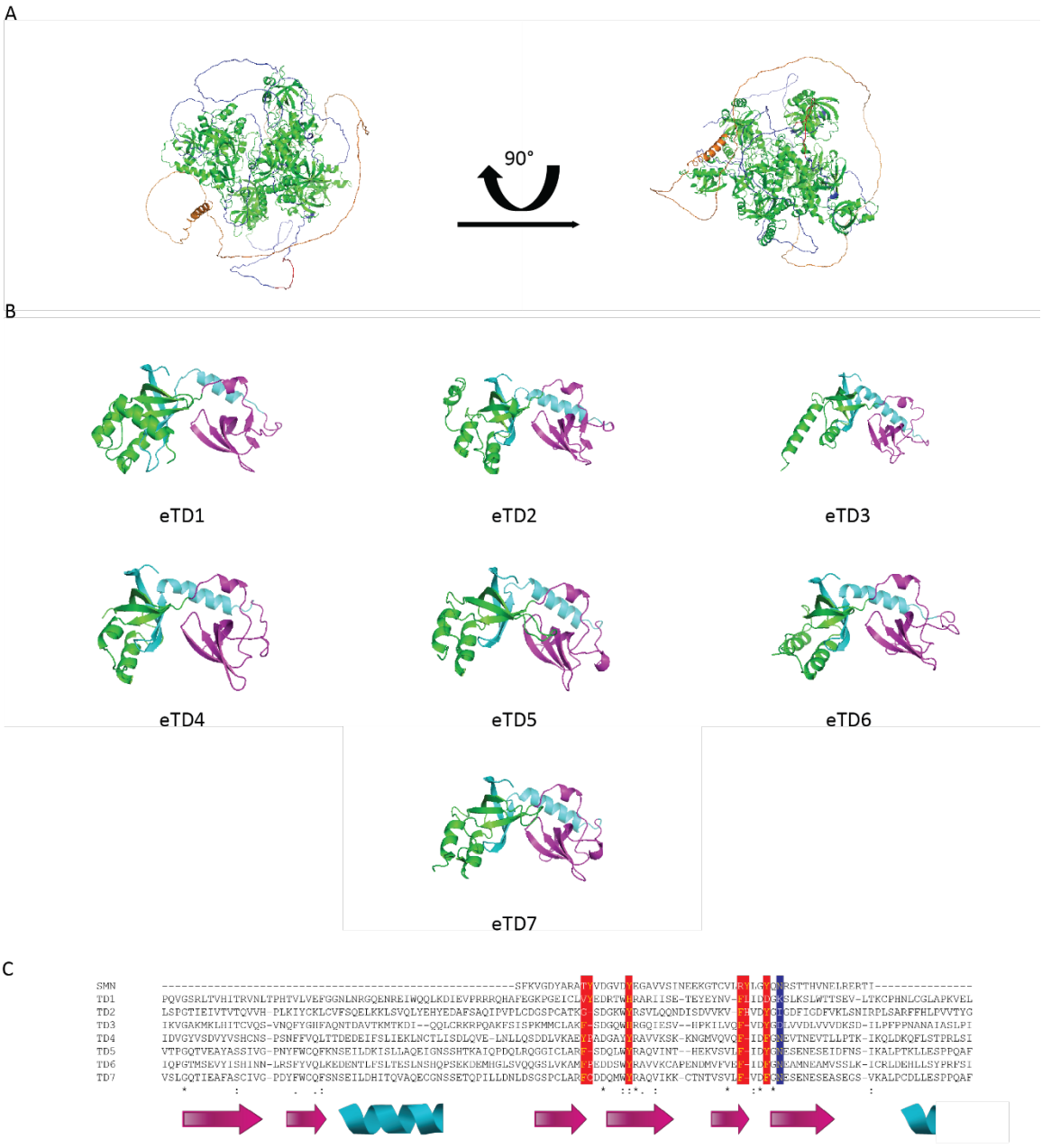

Fig. 17. Structural analysis of Tdrd6c and its TDs. (A) Alpha Fold prediction of Tdrd6c globular structure. TDs are highlighted in green, in blue linker sequences and in orange the unstructured c-terminal sequence. (B) Prediction of the structure of each extended TDs (from 1 to 7); in magenta is the core TD barrel structure, in cyan the N-terminal extension and in green the c-terminal extension. (C) Alignments of each TDs barrel sequence with the SMN protein, highlighting key amino-acids that are supposed to participate to the aromatic cage and recognition of the substrate.

5.4.2 – Tdrd6c peptide sequence exhibits two predicted IDRs and one Prion-like domain

In the study of the structure of Tdrd6c protein I included the analysis of possible IDRs and PrLDs. For this aim, I used the predictor tools provided by IUPred2A and PLAAC (Dosztányi, 2018; Erdős and Dosztányi, 2020; Lancaster et al., 2014; Mészáros et al., 2018). The IUPred2A predictor identified two possible IDRs, one of the size of 43 amino-acids (aa) between TD3 and TD4 (aa 709-751) and one corresponding to 139 aa at the c-terminus of Tdrd6c (aa 1649-1787) (Fig. 18A). These predictions are in agreement with the AF prediction, which identified an unstructured loop of 84 amino-acids between TD3 and TD4 and a large unstructured region following the seventh TD7 of the protein. In addition, within the "first" IDR found between the TD3 and TD4 of Tdrd6c, the PLAAC database predicts the presence of a PrLD (aa 742-759) (Fig. 18B). The difference between IDRs and PrLDs (as discussed in Introduction – 3.1) is that the firsts are flexible unstructured regions, which participate in transient non-specific interaction, while the latter are domain that can also appear as globular and have the potential to form fibrillar structures with their interactors. The predicted PrLD of Tdrd6c is only 18 amino-acids long but relatively enriched in Asparagine (four residues) and with one Glutamine and two Threonines, which are the amino-acids commonly characterizing PrLDs (King et al., 2012). Furthermore, alignment between Tdrd6a and Tdrd6c show how the Tdrd6c PrLD is a unique feature between the two proteins. These observations could be relevant in the study of Tdrd6c contribution to the regulation of germ plasm structure and its modes of interactions with other molecules.

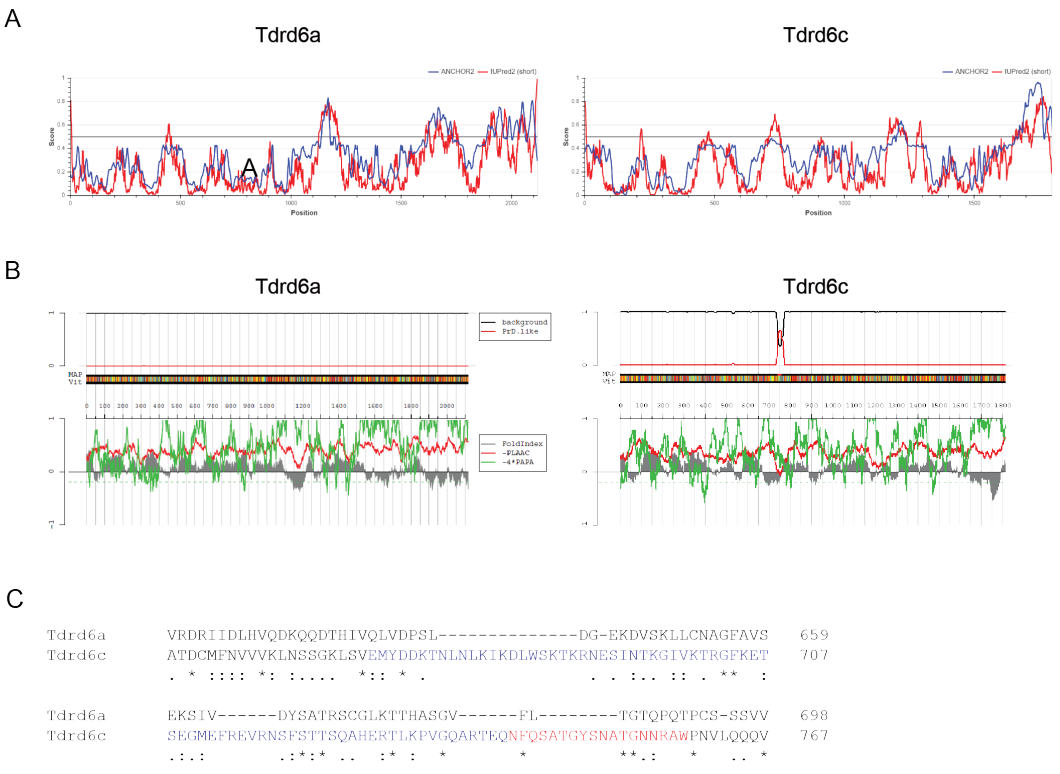

Fig. 18. Analysis of IDRs and PrLD regions within Tdrd6 proteins. (A) IUPred2a prediction of IDRs in Tdrd6a and Tdrd6c. In Tdrd6c two regions are recognized: one between TD3 and TD4 (aa 709-751) and one towards the c-terminus of Tdrd6c. Blue line indicates the ANCHOR2 based prediction, red line indicates IUPred2 based prediction. (B) PLAAC predictions for both Tdrd6a and Tdrd6c. In Tdrd6c a PrLD is recognized within the IDR between the eTD3 and eTD4. Graph on top: black line represents background, red line the PrLD prediction. Bottom graph: red line represents the 4PAPA score, red line the PLAAC score. (C) Alignment of the central peptide sequence of Tdrd6a and Tdrd6c (in blue is highlighted the predicted PrLD, in red the peak of the prediction).

5.5 – Tdrd6c domains, including the PrLD, drive and regulate interacting dynamics of Tdrd6c

5.5.1 – Expression of the PrLD, and not TDs of Tdrd6c, results in peptide self-interaction and cytoplasmic condensates formation

As discussed in the previous structural analysis, the seven eTDs of Tdrd6c exhibit differences in their amino-acidic sequence. These differences could characterize each eTD function and interaction with various substrates. In order to analyze the features of each eTD in a cellular context, I decided to express them in the BmN4 cells. These cells are derived from ovaries of the insect *Bombyx mori* and they are cultured at 28°C, which is the same temperature at which our zebrafish are kept in the aquarium. These characteristics make these cells a suitable environment where to test zebrafish specific peptides and collect valuable information on the way they behave and interact. In fact, this set-up has already provided insights in regard of the Buc-Tdrd6a interaction, which were in agreement with the data collected *in vivo* in the fish (Roovers et al., 2018). Therefore, I transfected BmN4 cells and induced expression of fluorescently tagged zebrafish proteins or peptides in order to study their biophysical properties and investigated their modes of interaction (Fig. 19A). Levels of expression of each transfected plasmid appeared comparable upon quantification of the intensity of their detected fluorescent signal (Fig. 19B). This is important to score in order to assume that any specific observed behavior of each construct is based on its intrinsic structural and biochemical properties and not by its higher or lower concentration within the cell. Knowing the roles of eTDs in multi-valent proteins, I expect that Tdrd6c's eTDs could drive the protein to self-interact, as Tdrd6c if a fairly large protein (1814 aa) with multi-valent capacity. In contrast to these expectations, Tdrd6c full length, as well as shorter fragments expressing different combinations of eTDs, did not show any particular behavior. In fact, their signal was found consistently distributed in the cytoplasm in a homogenous fashion, without an apparent specific localization or enrichment, although not able to diffuse in the nucleus unlike the mCherry control construct (Fig. 19B, C and D).

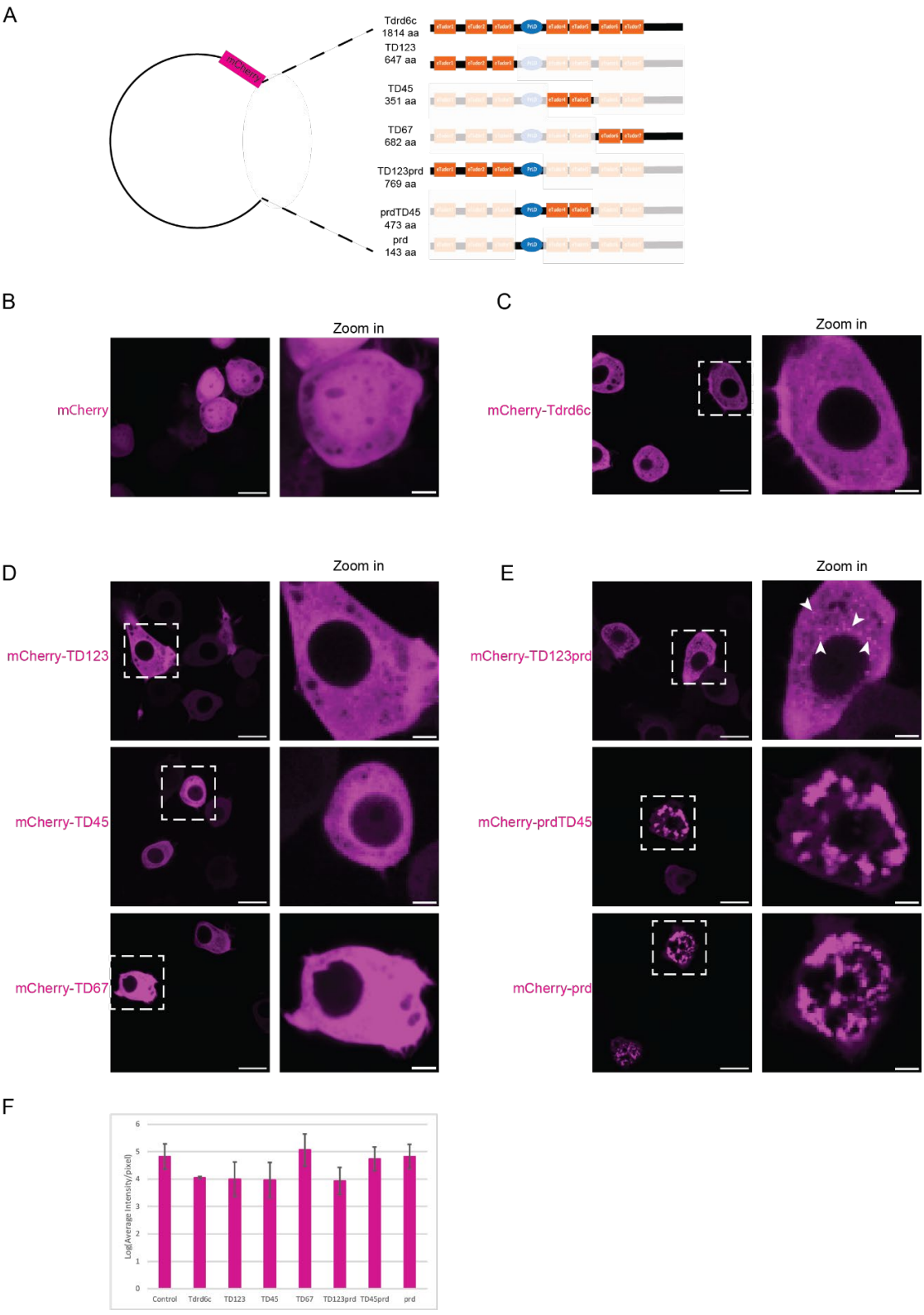

Fig. 19. Expression of Tdrd6c and Tdrd6c-peptides in BmN4. Figure legend continues in the next page.

On the other hand, inclusion of the predicted PrLD in the expressed sequences provokes interesting behaviors of the tagged peptides. In fact, the TD123prd construct, which encodes the first three TDs of Tdrd6c followed by the PrLD, formed small *foci* that were found spread within the cytoplasm of BmN4 cells (Fig. 19E). More interestingly, the prdTD45 peptide, which expresses the PrLD of Tdrd6c in between the N-terminal mCherry-tag and the fourth and fifth TDs of Tdrd6c, triggers formation of large assemblies in the cytoplasm (Fig. 19E). A similar result was obtained by the expression of the PrLD without any eTD, N-terminally tagged by mCherry (Fig. 19E).

These results showed that the PrLD of Tdrd6c has intrinsic self-interacting abilities, independently of whether its positioning is at the c-terminus of a peptide or in between two globular regions of a protein. Additionally, the presence of adjacent TDs 1, 2 and 3 of Tdrd6c modifies the aggregating behavior of the PrLD. Moreover, the Tdrd6c full length protein does not show any particular aggregation behavior in BmN4 cells, hinting that multiple layers of self-regulation affect the aggregation status of Tdrd6c in BmN4 cells.

5.5.2 – Tdrd6c PrLD is sufficient and necessary for interaction with Buc in BmN4 cells

I wanted to address if the dynamics exhibited by Tdrd6c constructs could affect Buc behavior in BmN4 cells. In this system, Buc is able to assemble into spherical condensates which appear rather mobile in the cytoplasm (Fig. 20A) (Roovers et al., 2018).

Fig. 19 (Continued from previous page). Expression of Tdrd6c and Tdrd6c-peptides in BmN4. (A) Schematic representation of vector plasmid carrying the mCherry fluorophore in combination with different Tdrd6c-related inserts. (B) Expression of control plasmid carrying only the mCherry fluorophore, where signal is distributed homogenously in the cytoplasm and in the nucleus of BmN4 cells. (C) Expression of tagged full length Tdrd6c, showing that the signal spreads in the cytoplasm and not in the nucleus. (D) Expression of different TDs combination of Tdrd6c, again with no formation of particular *foci* and with signal cytoplasmic distribution. (E) Expression of Tdrd6c constructs with inclusion of the Tdrd6c PrLD exhibiting formation of condensates in the cytoplasm. Arrowheads highlight smaller condensates. (F) Quantification of average expression levels of the different constructs in BmN4 cells, highlighting comparable levels of intensities per pixel. Scale bars in (B), (C), (D) and (E) = 20 µm and 5 µm for zoom in.

Interestingly, when expressed together, Tdrd6c and Buc co-localize to the same cytoplasmic condensates, although this is not observed consistently in all cells (Fig. 20A). In fact, in the majority of cells the Tdrd6c signal is spread in the cytoplasm while Buc is still able to form small condensates. This dual scenario is possibly caused by different combination of timing and level of expression of the two proteins, which can be critical in phase-separated processes of cellular contexts and indeed was observed to be significant in the study of Tdrd6a-Buc interaction (Roovers et al., 2018).

The interaction between Buc and Tdrd6c was suggested to be triggered by the di-methylation of the Arginine-rich c-terminal region of Buc and consequent recognition by TDs of Tdrd6c (Roovers et al., 2018). However, co-expression of Buc and Tdrd6c eTDs in BmN4 did not result in any co-localization. In fact, in these scenarios, we find Buc behavior unaltered while the Tdrd6c-constructs are dispersed without any particular enrichment in the Buc-positive *foci* (Fig. 20B). On the other hand, when expressing the PrLD of Tdrd6c with various eTDs combination, I find that Buc is able to interact with the tagged-fragments (Fig. 20C). In particular, Buc co-localizes with TD123prd into spherical cytoplasmic granules similar to the ones formed solely by Buc. Instead, when together with prdTD45 or only the PrLD, Buc granules appear to be anchored to the larger mCherry-tagged aggregates made by the PrLD (Fig. 20C, 21B).

These observations suggest that the PrLD of Tdrd6c not only triggers the self-assembly of the Tdrd6c protein but it is also required for the interaction with Buc. Again, this interaction seems to be tuned by the first three TDs of Tdrd6c, as they allow Buc to merge with the Tdrd6c assemblies.

5.5.3 – PrLD induced assemblies affect Buc mobility in BmN4 cells

Live-imaging of Buc-GFP condensates in BmN4 cells shows that these have liquid like properties, as fusion of droplets can be witnessed over a relatively brief time scale of two minutes (Fig. 21A). This observation suggests that Buc, in the specific context of the BmN4 cells cytoplasm, is able to consistently exhibit LLPS features by assembling into droplet-

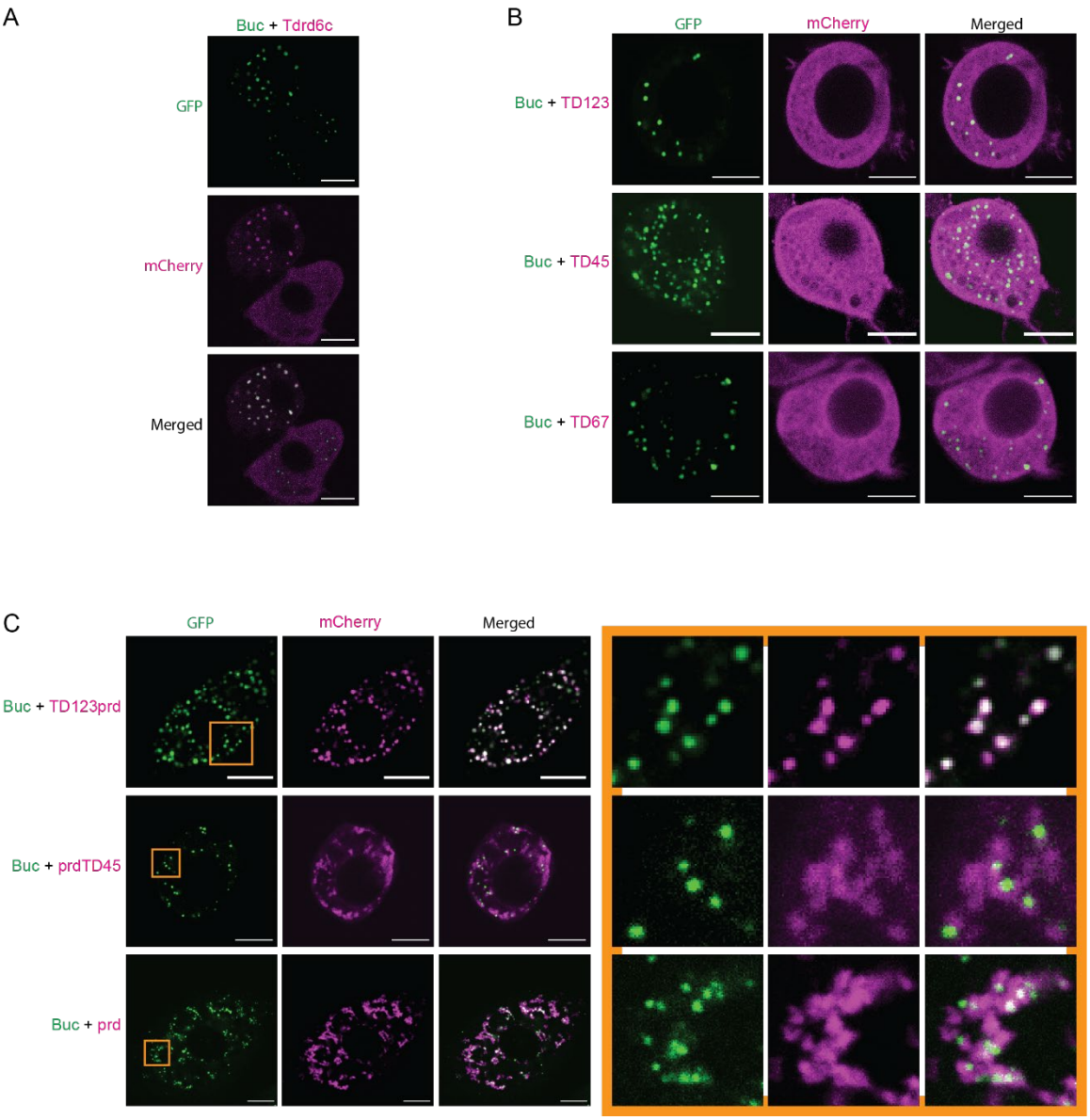

Fig. 20. Buc interaction with Tdrd6c PrLD in BmN4 cells. (A) Co-transfection of BmN4 cells with mCherry-Tdrd6c full length and Buc-GFP resulting in two scenarios: cell on top exhibiting co-localization of the two constructs and cell on the bottom showing Buc *foci* and dispersed Tdrd6c. (B) Co-transfection of mCherry-tagged Tdrd6c constructs without the PrLD together with Buc-GFP, resulting in no apparent interaction. (C) Co-transfection of mCherry-tagged Tdrd6c constructs with the PrLD together with Buc-GFP, resulting in different fashions of interaction. On the right, zoom in view (orange square). Buc-GFP in green; m-Cherry constructs in magenta; scale bars = 10 µm.

like structures. This is partially in contrast to the analysis that reported that Buc is required to confer amyloid properties to the Bb (Boke et al., 2016). However, the two different cellular contexts can influence the behavior of Buc in various ways, as concentrations and interactions of endogenously expressed molecules can be critical in LLPS related behaviors.

Next, I analyzed the mobility of Buc granules in cells that also contain Tdrd6c-prd assemblies (Fig. 21B). As described above, I again observed Buc granules in close proximity of the PrLD-induced aggregates. Interestingly, when followed over time, the GFP-positive droplets appeared immobile (Fig. 21B). Even when in relatively close proximity of the PrLD-induced aggregates. Interestingly, when followed over time, the GFP-positive droplets appeared immobile (Fig. 21B). Even when in relatively close proximity, Buc-positive droplets did not appear to move, nor fuse, within a relatively large time window when compared to the fusion events observed of Buc in absence of Tdrd6c-prd (40 minutes vs 3 minutes, Fig. 21).

These results hint at the fact that Tdrd6c has potential to modulate Buc behavior via its PrLD, which would be in line with reported cases where PrLDs play important roles in LLPS regulation. In facts, as I described in my introduction (Introduction– 3.1.4), PrLD are likely involved in protein-protein interactions, especially in promiscuous affinities with other flexible PrLDs or IDRs. Furthermore, this kind of interaction could highlight the molecular mechanism behind the phenotype scored in *6c mmut* and *6a6c* mmut, where germ plasm stability is likely affected in its LLPS features. As both Tdrd6c and Buc possess PrLDs, it would be interesting to investigate further the contribution of each of them in the regulation of germ plasm dynamics in zebrafish.

5.6 – In vitro analysis of Buc-Tdrd6c interaction

As mentioned in the previous paragraphs, the BmN4 offers a convenient system to address specific interactions between proteins and domains. However, in order to analyze the intrinsic bio-physical properties of Buc and the PrLD of Tdrd6c, I decided to utilize an *in vitro* system using recombinant proteins in solution rather than expressing plasmids in the

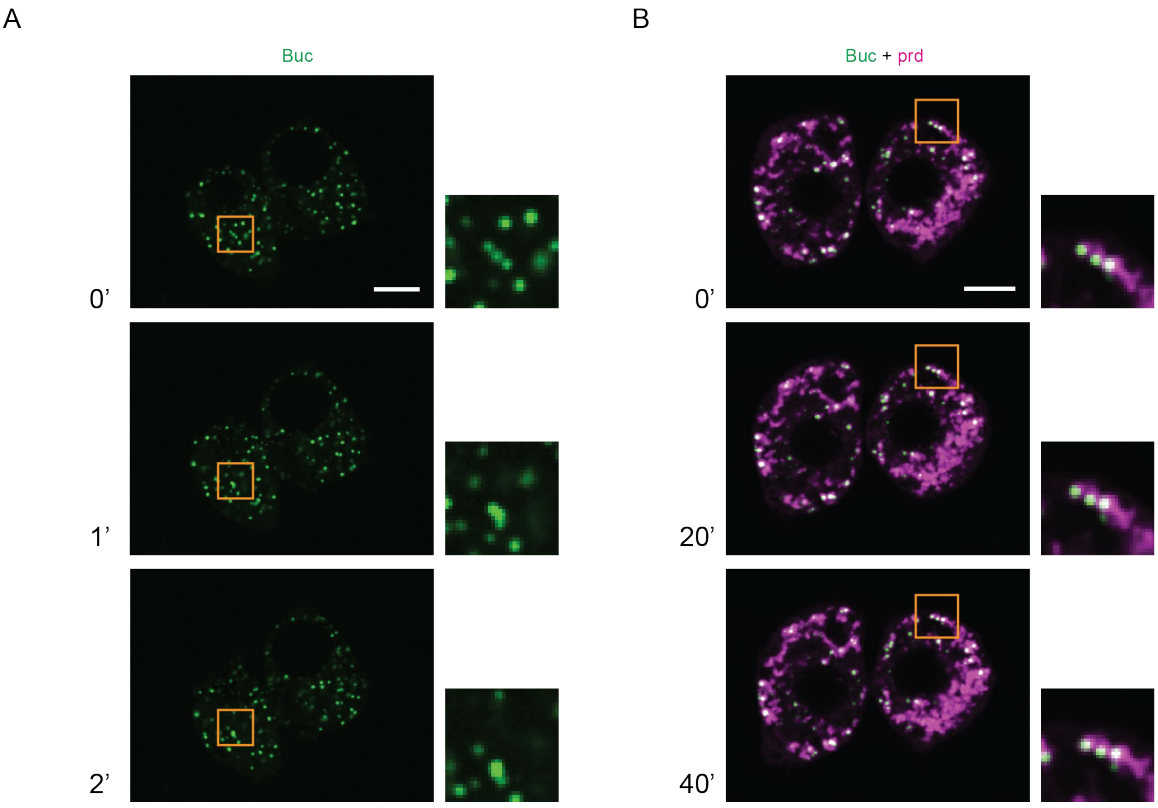

Fig. 21. Buc immobilization over PrLD induced aggregates in BmN4 cells. (A) Live imaging of Buc-GFP, exhibiting fusion of droplets (orange box and zoom in on the right) over a time scale of two minutes (reported on the left as time points 0', 1' and 2'). (B) Live imaging of Buc-GFP (green) and mCherry-prd (magenta), showing immobilization of Buc droplets over the large PrLD induced assemblies (orange box and zoom in on the right) in a time scale of forty minutes (reported on the left as time points 0', 20' and 40'). Scale bars = 10 μm.

cell culture. More in detail, this *in vitro* strategy consists in purifying my proteins and constructs of interest and place them in solution at determined and controlled conditions, in contrast to the cellular environment where I can only control to certain extents factors such gene expression and molecular concentrations. This way, the candidate proteins that I choose to express can be analyzed at various conditions in order to more precisely address their potential in regards of the LLPS processes.

Following this idea, I first cloned the *buc* sequence and the *tdrd6c* sequence encoding for the PrLD into vectors that would drive the expression of the proteins in insect cells (Methods – 6.2.12). To these constructs, sequences translating for Maltose Binding Protein (MBP), Histidine (His) and fluorescent tags were added N-terminally as illustrated in the

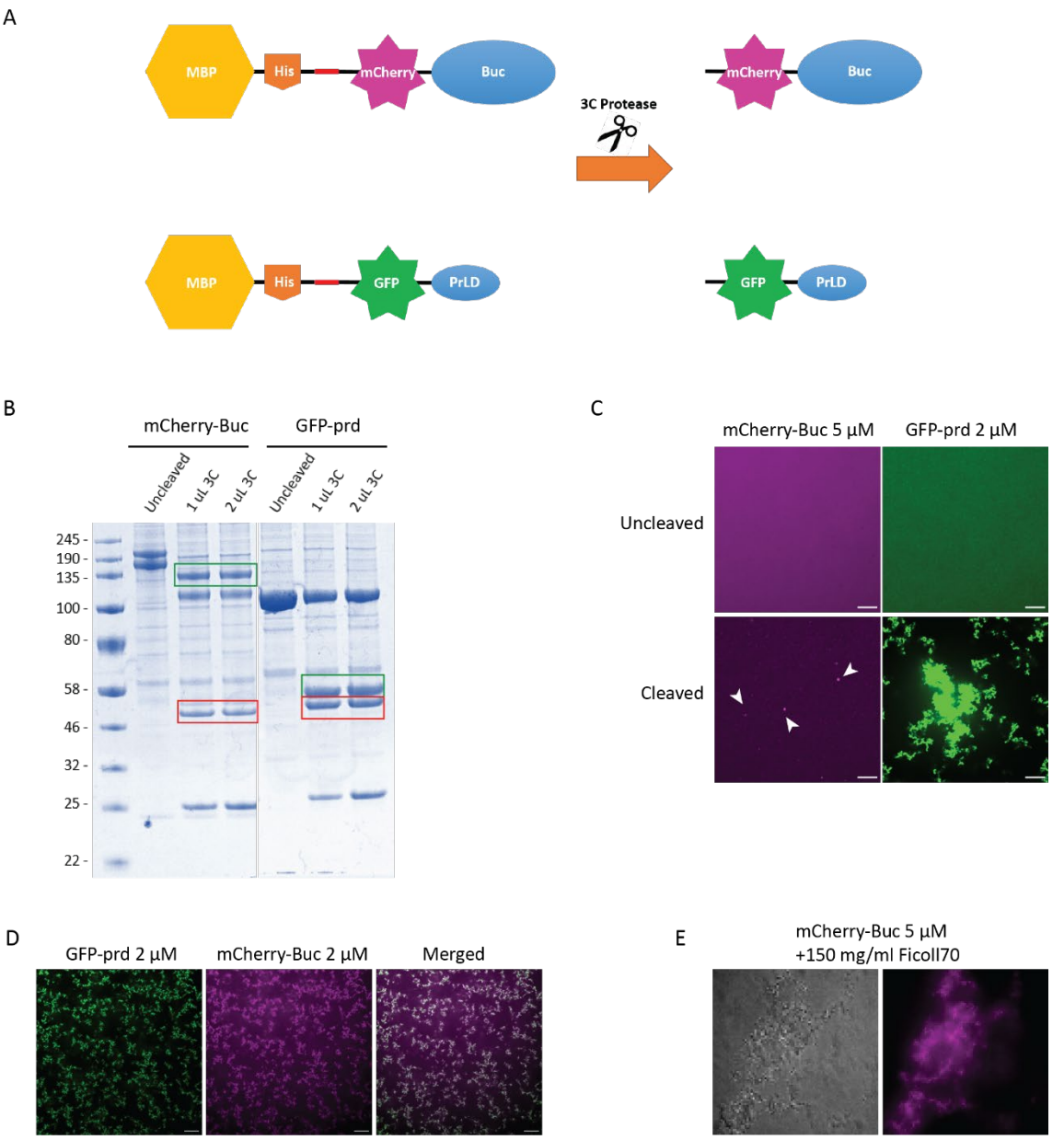

Fig. 22. *In vitro* analysis of Buc and the PrLD of Tdrd6c. (A) Schematic representation of the two constructs designed. (B) Measured activity of the 3C protease on the purified tagged constructs: for each sample I loaded to the gel the uncleaved fraction and fractions cleaved by 1 or 2 µL of Protease. Red boxes indicate cleaved MBP-tag (~42 kDa), while green boxes indicate cleaved mCherry-Buc (~130 kDa) and GFP-prd (~55 kDa) (C) Behavior of the peptides before and after cleavage. After cleavage Buc forms small granules (arrowheads) while the PrLD of Tdrd6c assembles larger structures. (D) Interaction between the two peptides when co-existing in solution, showing co-localization into large granular assemblies. (E) Buc aggregates formation in the presence of crowding reagents (Ficol70), showed in both bright field (left) and fluorescent (right) channel. Scale bars = 20 µm.

figure in the next page (Fig. 22A). The MBP peptide was added to favor solubility of the product, while the His-tag was used for column purification (Methods – 6.2.12). The fluorescent tags were either GFP or mCherry. In between the His-tag and the fluorophore I cloned a sequence recognized by the 3C protease, in order to cleave off the MBP-His-tag peptide, as this was needed for expression and purification but would interfere with the *in vitro* analysis of the Buc and Tdrd6c-prd proteins. Expression and purification of the MBP-His-tagged-fluorescent-proteins was performed by the IMB Protein Production Core Facility (Methods – 6.2.12). Subsequently, I performed the 3C protease-mediated cleavage to remove the MBP-tag from the constructs of my interest and transferred them to small volumes of imaging slides (Fig. 22B). Within this set up, I let the samples rest for 30 minutes in buffer (30 mM Na-Hepes pH 7.4, 300 mM NaCl, 50 mM Arginine, 50 mM Glutamate, 10% Glycerol and 1 mM DTT) prior to observing the behavior of the protein-constructs via detection of the fluorescent tags (Fig. 22C). Interestingly, when freed from the MBP-His-tag, both Buc and the PrLD are able to form condensates, although for Buc these are hardly visible while for the PrLD of Tdrd6c they quickly form large aggregates (Fig. 22C). However, the PrLD aggregation seems to assist Buc in its phase-separating fashion, as when the two proteins are placed to the same well I could observe co-localization of Buc to the Tdrd6c's PrLD-formed aggregates (Fig. 22D). Similarly, I could observe that Buc alone also forms similar condensates when a crowding reagent (Ficol70) is added to the solution (Fig. 22E), suggesting that Tdrd6c's PrLD may function as a biological crowding reagent during zebrafish embryogenesis. However, these preliminary observations should be followed up with a more detailed analysis, first aiming at the understanding of which concentrations and conditions are critical for the phase-separation of each individual construct. Then, I could more precisely address the LLPS features of the two constructs and especially to which extent they affect each other behavior and dynamics.

It is interesting to point out that the data collected in these experiments (despite being preliminary for the explained reasons) are in agreement with the assays performed in the BmN4 cells, suggesting that indeed the PrLD of Tdrd6c suffices to drive the interaction between Buc and Tdrd6c and, more importantly, affects Buc-condensates behavior.

6 – Discussion

6.1 – Roles and functions of Tdrd6c within zebrafish germline-specific condensates

6.1.1 – Possible roles of Tdrd6c in the composition and functioning of the *nuage* of zebrafish oocytes

The first data I collected in my work regarded the localization of Tdrd6c in the zebrafish organism, which provides initial evidence over possible functions of the protein. Combination of a tagged reporter line (*tdrd6c-mKate2*) and antibody staining showed that Tdrd6c is present in germline phase-separated structures of zebrafish (Fig. 9, 10, 11 and 12). In oocytes, Tdrd6c enriches at the perinuclear *nuage*, in contrast to its paralog Tdrd6a that concentrate in the *nuage* but also in the Bb of stage IB oocytes and vegetal granules of stage II oocytes (Fig. 10) (Roovers et al., 2018). However, this does not exclude that Tdrd6c could be present within the Bb and vegetal granules assemblies with levels of abundancy too low to be detected over the background of the cytoplasm. Nevertheless, the comparison with Tdrd6a's localization data is striking, especially considering the similar structure of the two proteins. It is important to consider that timing and levels of expression could influence the different behavior of the two proteins during oogenesis. Therefore, a precise quantification of Tdrd6a and Tdrd6c protein abundancy at different stages of oogenesis could provide insights towards the understanding their different enrichment. This could be achieved by Western Blot analysis, comparing Tdrd6c and Tdrd6a levels of expression in lysates of total ovaries versus the ones extracted from filtered stage I oocytes (smaller than 150 μm in diameter). However, it is likely that Tdrd6a is more abundant throughout oogenesis, as its transcript was detected with higher levels in a recent single-cell sequencing study of zebrafish ovary (Liu et al., 2022). Besides focusing on its level of expression, a parallel analysis of Tdrd6c domains, their interactions and dynamics could provide insights in regards to its different localization to Tdrd6a. In my work, I collected preliminary structural-prediction data of Tdrd6c and I will dedicate a specific section to recapitulate and discuss them more in detail (Discussion – 6.2).

In my analysis based on microscopy-techniques, I could not highlight any phenotype when looking at *tdrd6c* knock-out mutant eggs, where I did not detect any significant defect in oocyte-specific structures. However, speculating over Tdrd6c particular enrichment within the perinuclear environment, I suggest that Tdrd6c may have an impact in the structure and functioning of the *nuage*. As discussed in the introduction (Introduction –3.2.4), the *nuage* is an important environment for gene expression regulation in germ cells where multi-Tudor containing proteins have shown to be relevant with their direct interaction with Argonaute proteins (Chen et al., 2009; Huang et al., 2011; Reuter et al., 2009; Siomi et al., 2010; Vrettos et al., 2021; Wang et al., 2009; Zhang et al., 2017, 2018). Following these observations, it would be interesting to perform immuno-precipitation (IP) experiments of *nuage*-specific proteins (*e.g.* Zili, Tdrd1) and combine them with Mass Spectrometry (MS) analysis, comparing *tdrd6c* knock-out mutant to *wt* oocytes. This set-up could highlight Tdrd6c possible function in the stabilization and control over the *nuage*-specific protein network.

In the study of Tdrd6a, which is also present within the *nuage*, minor defects in RNA populations where measured in absence of *tdrd6a* expression (Roovers et al., 2018). Therefore, similar RNA sequencing experiments conducted in *tdrd6c* mutants may reveal an impact of Tdrd6c on the regulation of RNA levels during oogenesis. Moreover, in my work I started collecting preliminary data using a transgenic line (currently unpublished from Edoardo Caspani) which allows for measurements of the functioning of the piRNAs-mediated silencing machinery via levels of expression of a GFP-reporter (Fig. 16). These data are currently lacking replicates to reach significance but could lead to first measurements of piRNAs-related defects in *tdrd6c* populations of zebrafish that could further justify the design of RNA sequencing experiments. These should aim at highlighting differences in the abundancy of mRNAs but also other classes of RNAs, in particular piRNAs, in the different mutant backgrounds.

Indeed, it is also important to stress that all the discussed experiments should also be performed on populations of fish mutant for both *tdrd6a* and *tdrd6c* genes, in order to clarify to which extent the function of the two Tdrd6 proteins might overlap in the regulation of the perinuclear environment of zebrafish oocytes. It is likely that experiments conducted on *tdrd6a; tdrd6c* double mutant fish will highlight deeper defects in the *nuage*

interactome, providing more insights regarding the importance of the *tdrd6* paralogs in the correct organization and functioning of the perinuclear environment of zebrafish eggs.

6.1.2 – Tdrd6c as a shuttle-protein: guiding Ziwi from the *nuage* to the germ plasm

After fertilization, Tdrd6c is found in the embryo within germ plasm structures, as exhibited by co-localization with the Buc-eGFP marker (Fig. 11). It is interesting to notice that the pattern of localization of Tdrd6c during oogenesis and embryogenesis matches the one of Ziwi, which also enriches in the *nuage* and is then collected within the embryonic germ plasm condensates (Houwing et al., 2007). Furthermore, it was revealed that, when Buc is absent during embryogenesis, Tdrd6a loses its interaction with both Tdrd6c and Ziwi (Roovers et al., 2018).

Considering these data and observations, I speculate that Tdrd6c, also in light of its multi-valent module of action, could function as a shuttle for Ziwi. Tdrd6c may start its interaction with Ziwi within the *nuage* of oocytes and, later during the zygote formation, guide Ziwi to the embryonic germ plasm when simultaneously interacting with Buc (Fig. 23). In order to validate this hypothesis, quantification of Ziwi enrichment in the *nuage* and in the germ plasm in presence and absence of Tdrd6c would be crucial. This quantification could be carried out with combination of microscopy, analyzing data obtained by Ziwi-stained oocytes and embryos, as well as with Western Blot analysis comparing IPs of *nuage*-specific components (*e.g.* Zili, Tdrd1) to IPs of germ plasm-specific components (*e.g.* Buc). In this quantitative analysis, first it would be important to assess whether or not the global levels of expression of the Ziwi protein are affected by the absence of Tdrd6c. If that were the case, it would imply that Tdrd6c is important for the overall stabilization of the Ziwi protein in zebrafish, which would not be necessarily dependent on its mis-localization. On the other hand, if Ziwi protein levels would be similar in presence or absence of Tdrd6c, I could then distinguish three plausible read-outs from the quantitative IP-Western Blot analysis. I summarize these scenarios in the Table 9 (in the next page).

	***Nuage*-specific measurements**	**Germ plasm-specific measurements**	**Interpretation**
1	Ziwi levels in absence of Tdrd6c are similar compared to *wt*	Ziwi levels in absence of Tdrd6c are similar compared to *wt*	Tdrd6c is **not** needed for enrichment of Ziwi to germline condensates
2	Ziwi levels in absence of Tdrd6c are similar compared to *wt*	Ziwi levels in absence of Tdrd6c are **reduced** compared to *wt*	Tdrd6c is needed for the shuttling of Ziwi from the *nuage* to the germ plasm
3	Ziwi levels in absence of Tdrd6c are **reduced** compared to *wt*	Ziwi levels in absence of Tdrd6c are **reduced** compared to *wt*	Tdrd6c is needed for the enrichment of Ziwi to germline condensates

Table 9. Plausible read-outs of quantification of Ziwi expression in presence or absence of Tdrd6c.

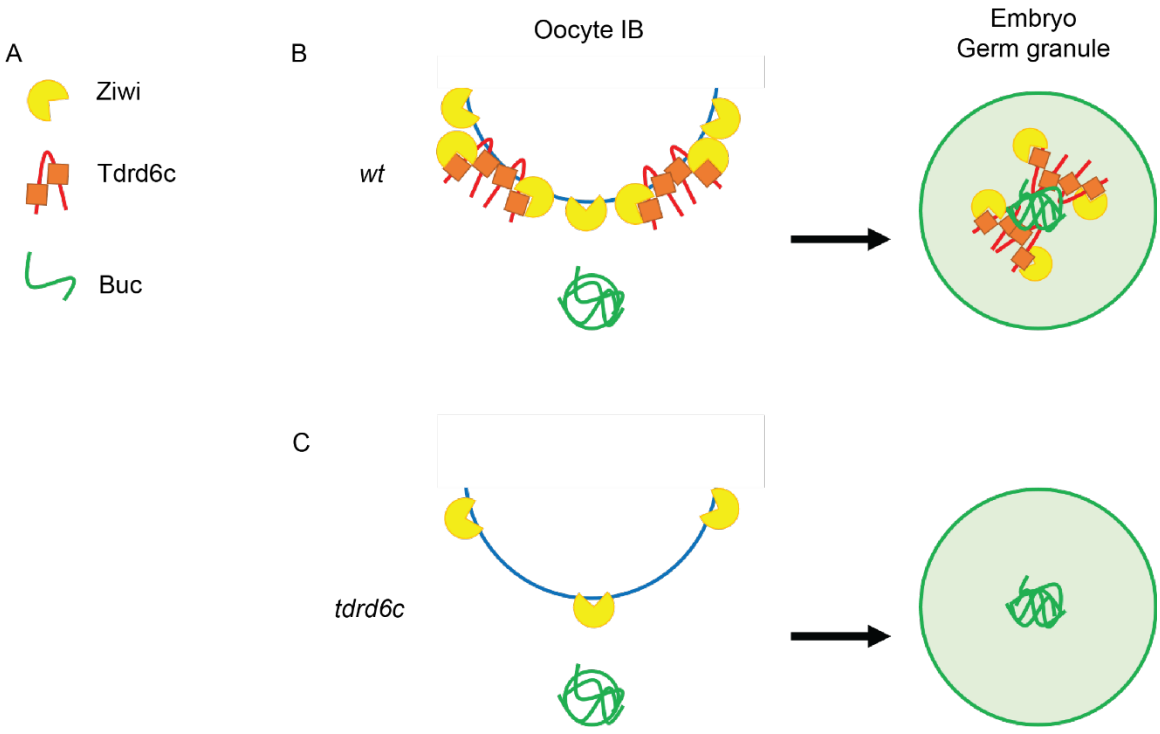

Fig. 23. Model of the possible shuttling-role of Tdrd6c during oocyte-to-embryo transition. (A) Legend of symbols assigned to each protein. (B) *Wt* scenario represented where within the *nuage* (blue line) Tdrd6c favors Ziwi enrichment, while Buc organizes the Bb (green). In the embryo, Ziwi is brought to the Buc-organized germ granules via Tdrd6c. (Legend continues in the next page)

6.1.3 – Maternally provided Tdrd6c is important for PGC specification in the zebrafish embryo

Tdrd6c pattern of localization during embryogenesis resembles the one of Tdrd6a, which is a protein that shares structural similarities with Tdrd6c, hinting at the possibility that the roles of the two molecules are similar during embryogenesis (Fig. 9, 11 and 12).

Indeed, in the offspring of *tdrd6c* mutant female fish, I could measure significant defects in relation to the PGC specification, as *6c mmut* larvae exhibited a reduction of PGC numbers at the genital ridge of the 24 hpf stage (Fig. 13). This reduction appeared comparable to the defects of *6a mmut* larvae that I analyzed, in agreement with previous reports (Roovers et al., 2018). What was more striking to observe was that simultaneous absence of both Tdrd6a and Tdrd6c during embryogenesis led to complete absence of PGCs at the 24 hpf larval stage (Fig. 13A, B).

Subsequently, these populations of *6a6c mmut* larvae were kept at standard conditions and were able to grow normally compared to *wt* fish. However, I could observe that all *6a6c mmut* populations matured only as males (Fig. 13C), a phenotype that in zebrafish has been linked with scarce PGC abundancy (Dranow et al., 2013; Tzung et al., 2015; Weidinger et al., 2003). In fact, the juvenile gonads in zebrafish initially develops as ovaries, producing eggs which are needed to produce signals to maintain the ovarian fate (Dranow et al., 2013; Tzung et al., 2015). When these signals are not sufficient due to reduced egg numbers (less germ cells), the juvenile ovary can switch fate and develop as testis instead (Dranow et al., 2013). In agreement with this model, different experiments that have lowered PGC abundancy have resulted in the growth of only-male population in zebrafish (Tzung et al., 2015; Weidinger et al., 2003). Interestingly, not only I could observe that *6a6c mmut* fish mature only as males, but also that they are sterile, meaning that the complete depletion of PGCs at the larval stages cannot be recovered in adulthood, severely affecting the fertility of the fish.

(Continued legend from previous page) (C) In absence of Tdrd6c, lower levels of Ziwi are found in the *nuage*, while the Bb is not affected in its composition. After fertilization, Ziwi fails to be recruited to the germ plasm due to lack of Tdrd6c.

These observations reveal an important role for the Tdrd6c protein in the regulation of early PGC specification in zebrafish and the requirement of expression of at least one Tdrd6 protein during oogenesis in order to ensure sufficient PGC abundancy and fertility of the offspring. However, these PGC defects may be in principle caused by various molecular and cytological processes, which I briefly listed in Table 10. In the next paragraphs, I will discuss my proposition of a model where the scored phenotypes in maternal mutant embryos are due to defects in the early segregation of determinants, involving germ plasm instability during the first hours of cell division.

Developmental phase	**Defective process**	**Impact on PGCs**
Early segregation of determinants	Defects in segregation of determinants; insufficient levels of expressions of determinants	Cells do not acquire sufficient determinants or sufficient levels of determinants and cannot initiate differentiation
Expression of PGC-specific genes	Incorrect chromatin state; presence of unwanted regulator of gene expression (repressors of germ-specific genes or activators of somatic-specific genes	Although having sufficient determinants to initiate differentiation, the PGC status is not reached due to insufficient expression of germline-specific genes or overexpression of somatic-specific genes
Migration of PGCs	Unfavorable environment; incorrect gastrulation and patterning of the larva; lack of signals from surrounding tissues	PGCs cannot reach their final location and will either redirect their differentiation into a different cellular state or undergo apoptosis

Early PGC maintenance and survivability	Occurrence of mutations during proliferation; Defects in piRNA-mediated gene silencing; Unfavorable environment	Even when migration occurs correctly, PGCs can encounter problems during their proliferation and maturation, eventually leading to their apoptosis

Table 10. List and brief description of molecular and cytological processes that occur within the first 24 hours of zebrafish germline specification.

6.1.4 – Tdrd6 proteins regulate germ plasm maintenance during cleavage stages of zebrafish embryogenesis

The observed defects in PGC abundancy at the 24 hpf stage could be caused by the malfunctioning of different early developmental processes (Table 10). However, due to the fact that I measured these phenotypes not in mutant larvae, but in offspring of mutant female fish, the causes should be tracked prior to the ZGA, which in zebrafish initiates during the stages between 3 hpf and the 4 hpf (Jukam et al., 2017; Vastenhouw et al., 2019). Indeed, until that window of time, zebrafish development is directed by parental determinants that can regulate different processes. Among those, germline specification in zebrafish is known to rely, during the first hours of development, on the presence of germ plasm condensates that collect specific maternally expressed proteins and RNAs that contribute to PGC differentiation, as I described in the introduction of this work (Introduction – 3.2.3). For these reasons, I decided to measure possible defects in the germ plasm dynamics during the cleavage stages.

Following the localization of the Buc-eGFP reporter during the first 3 hours of development I could observe that in *6a6c mmut* animals the germ plasm is gradually lost from the cleavage plains (Fig. 14). In fact, when compared to the *control* group, the germ plasm marked by Buc-eGFP of *6a6c mmut*, was not detectable by ~3 hpf, despite exhibiting a correct localization to the furrows at ~1 hpf. This was in stark contrast to the bright *foci* that could be observed in *control* samples. This observation nicely links the absence of

PGCs in *6a6c mmut* larvae and the sterility of *6a6c mmut* fish to defects in germ plasm early distribution, as the maintenance of germ plasm is a crucial process to ensure germline development in zebrafish (Hashimoto et al., 2004).

However, loss of germ plasm enrichment in *6a6c mmut* embryos was stated based solely on measurements on the localization of the reporter Buc-eGFP. Knowing that the germ plasm serves to collect different proteins and RNAs, many of which are yet to be characterized (or even discovered), it is possible that some of them could localize and distribute correctly in absence of Tdrd6a, Tdrd6c and Buc in *6a6c mmut* embryos. Electron microscopy approaches could be used to clarify whether the germ plasm is lost as a whole in these populations of fish or only certain molecules (*e.g.* Buc) are unstable and mis-localize out of the condensates. On the other hand, Buc is recognized as the main organizer of these structures in zebrafish (as reported in studies of the last 20 years), making it plausible that in *6a6c mmut* animals Buc destabilization causes the dispersal of all the other germ plasm components (Bontems et al., 2009; Riemer et al., 2015; Rostam et al., 2022). At the very least, considering the absence of PGC formation in the *6a6c mmut* larvae, I can propose a model for which, in absence of both Tdrd6 proteins, destabilization of the germ plasm during embryogenesis results in the mis-localization of required determinants for PGC specification and/or maintenance (hence sterility). Indeed, different studies have highlighted the importance of certain proteins in the regulation of early PGC differentiation, with their depletion during embryogenesis resulting in scarce of PGC levels by interfering with PGC migration and maintenance processes (D'Orazio et al., 2021; Gross-Thebing et al., 2017; Liao et al., 2018; Weidinger et al., 2003; Westerich et al., 2023). I will discuss these possible scenarios and different processes in the next paragraph.

6.1.5 – Possible links between loss of specific factors within the germ plasm and the early absence of PGCs in *6a6c mmut* larvae

As summarized in Table 10, different molecular processes can interfere with normal germline establishment in zebrafish. Interestingly, they could all be linked to defects in the germ plasm composition, as these condensates collect several determinant that have various functions in the biology of germ cells and their determination (Fig. 24). Hereby, as

examples, I will report two well characterized cases, although it is important to consider that many factors belonging to the germ plasm network are still unknown or have their functions yet to be understood.

For several years it was thought that the gene *dead end* (*dnd*), first characterized in 2003, played a role in zebrafish PGC migration, as its knock down during embryogenesis resulted in mis-localized PGCs (Weidinger et al., 2003). However, recent studies have revealed that in absence of Dnd protein, PGCs undergo trans-differentiation between 10 and 18 hpf, during the time window of PGC migration, reprogramming themselves as somatic cells (Gross-Thebing et al., 2017; Westerich et al., 2023). This process of trans-differentiation is caused by the mis-localization of *nanos3* transcripts at the periphery of perinuclear germ granules in PGCs during gastrulation, impairing the translation of the Nanos3 protein, which is essential to inhibit somatic gene expression (Köprunner et al., 2001; Westerich et al., 2023).

Another interesting study was carried out recently in the analysis of Tdrd7, another multi-Tudor containing protein in zebrafish, showing the requirement of this molecule to regulate gene expression in PGCs after their migration (D'Orazio et al., 2021; Strasser et al., 2008). It was revealed that PGCs gain specific epigenetic traits during migration, which could be linked to the suppression of somatic genes via remodeling of chromatin accessibility (D'Orazio et al., 2021). This process is impaired when *tdrd7* is knocked-down with Morpholino (MO) injections into zebrafish zygotes, causing loss of PGC-specific epigenetic state after migration, and hence the expression of somatic genes. As Tdrd7 is also enriched within the germ plasm condensates, these phenotypes would link the germ plasm structural composition to the regulation of the chromatin state in PGCs, although the mechanism behind this cross-talk has not been analyzed in detail.

The transcripts of *dnd* and *tdrd7* (but also *nanos3*) are known to be enriched within the germ plasm in zebrafish, although their function is carried out in germ cells in later stages upon their translation (Köprunner et al., 2001; Strasser et al., 2008; Weidinger et al., 2003). Therefore, the examples displayed by the studies of *dnd* and *tdrd7* nicely indicate possible scenarios where defects in the structure and composition of germ plasm observed in *6a6c mmut* could trigger early germline defects even when initial PGC specification occurs correctly. Therefore, it would be important to check if PGCs can be observed, in *6a6c mmut*

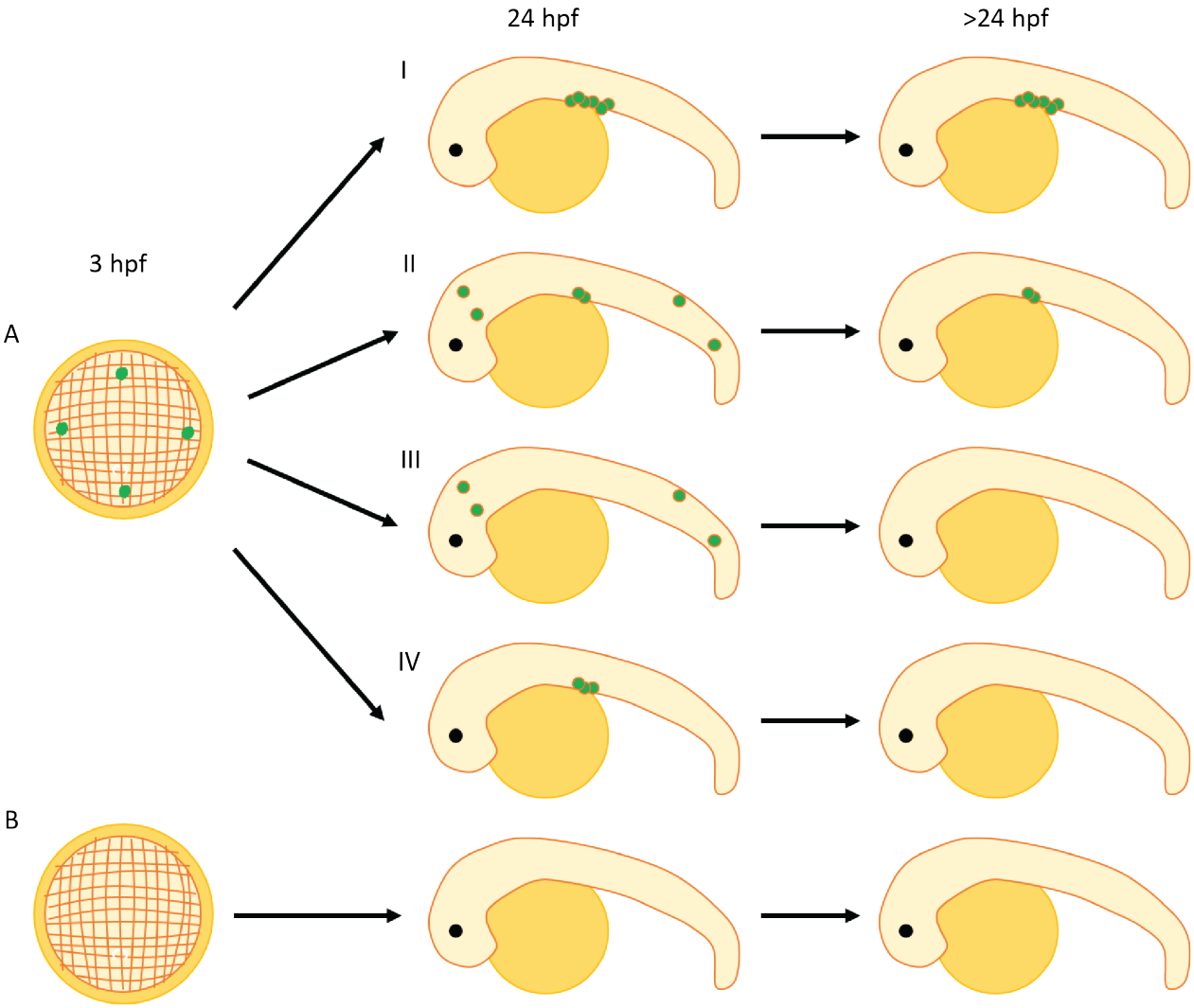

Fig. 24. Possible causes to early PGC abundancy defects in zebrafish. (A) Germ plasm structure (green blobs) is not lost as a whole. (I) Only non-crucial factors are lost and PGC specification and development in not altered. (II) Factors important for PGC migration are not enriched in the germ plasm, causing mis-migration. This usually results in transient visualization of ectopic PGCs in different location than the genital ridge of the larva. However, stochastically, few PGCs can end up to the genital ridge and establish the germline of the individual. (III) Factors required for PGC specification or for suppression of somatic fate are lacking within the germ plasm, hence favoring trans-differentiation of PGCs to somatic cells. Germ cell-specific markers can be transiently be present within these cells, despite their somatic localization, morphology and other traits that could be characterized molecularly (*e.g.* somatic-gene expression) (IV) Factors required for PGC maintenance are lost from the germ plasm network, causing gradual loss of identity during or after PGC migration. In this case, it is likely that few PGCs could be observed within the larval stages, as reversing the cell fate is a process that requires some time. (B) Complete loss of germ plasm, thus germline determinants enrichments, impairs PGC specification.

embryos, at different stages between the ZGA and the 24 hpf utilizing different markers in order to state if PGCs in these populations never acquire the PGC identity, lose it in later stages due to trans-differentiation or mis-migration, or undergo programmed cell death.

6.1.6 – Possible molecular mechanisms behind whole germ plasm instability of *6a6c mmut* embryos

Besides the considerations of the previous paragraph, the most plausible explanation behind the phenotype exhibited by *6a6c mmut* fish is that the germ plasm is unstable and lost as a whole during the first cell divisions of the zebrafish embryo. This statement is supported by the measured loss of Buc enrichment, which is widely recognized as the main organizer of the germ plasm structures in zebrafish, suggesting the complete mis-localization of all other germ plasm components (Bontems et al., 2009; Riemer et al., 2015). Moreover, transient PGC specification, which would be lost due to either mis-migration or trans-differentiation by the 24 hpf stage, would have been difficult to escape my attention during my analysis, with Vasa-eGFP highlighting PGCs from the shield stage onwards (>6 hpf) (Krøvel and Olsen, 2002). However, the instability of Buc, which would trigger germ plasm disruption, can be explained with different molecular mechanisms, which should be hereby discussed.

The germ plasm in *6a6c mmut* is clearly formed in the zygote, meaning that Buc at first is able to organize condensates which are also correctly localizing to the cleavage furrows in spite of the absence of Tdrd6a and Tdrd6c (Fig. 15). How and why is then this material lost at later time points? The gradual loss of germ plasm could be caused by mechanical stress, produced by cell division, which could be sufficient to disrupt condensates that, although assembled correctly, are missing important scaffold that would stabilize them. Similarly, changes in the environment proximal to the germ plasm droplets (reduced cellular volumes, changes in molecular concentrations) could also disturb the state of a biological condensate. To address these possible scenarios, a deeper analysis of Buc properties *in vitro* could assess how the material properties of Buc condensates may be affected by the presence and absence of Tdrd6 proteins. Following the data collected in zebrafish, I could

speculate that Buc-induced condensates *in vitro* should be more stable in presence of Tdrd6 proteins, resisting to different sources of mechanical and/or chemical stress.

On the other hand, Buc localization could be impaired because Tdrd6 interactions might mediate the contact with important scaffolds on the cleavage furrows (Fig. 25). It has been shown that genes involved in the assembly of the cytoskeleton and formation of tight junctions are crucial to assist germ plasm distribution in zebrafish (Campbell et al., 2015; Eno et al., 2018; Eno and Pelegri, 2018; Miranda-Rodríguez et al., 2017). In these scenarios, however, germ plasm condensates are stable but mis-localized within the cytoplasm of the embryonic cells and they eventually contribute to correct establishment of PGC, resulting in normal fertility of the adult animal. This means that anchoring of germ plasm to cleavage furrows is dispensable for PGC specification, although making the process likely more robust. Stability of the condensate structure, despite mis-localization within the cytoplasm, may be more important to sequester determinants from the environment, ensuring their sufficient abundancy upon ZGA and the start of germline differentiation. In my work, when following the germ plasm droplets *in vivo* in the different populations of embryos, I did not observe a difference in the ratio of dispersed Buc-condensates over the furrow-anchored Buc-condensates. However, quantification of numbers and features of dispersed Buc-condensates is not as reliable as the one of the anchored germ plasm, as their mobility within the volume is difficult to track. Therefore, a quantification of Buc-positive condensates in fixed samples could address more precisely if these are more abundant in the cytoplasmic regions not in proximity of the furrows in *6a6c mmut* fish. Furthermore, it would be interesting to carry out a proteomic analysis addressing how the Buc-interactome changes in absence of both Tdrd6 proteins at different times of development. This could lead us to a clearer picture of whether or not multi-Tudor proteins are involved in the anchoring to cleavage furrows molecular assemblies. This analysis could also highlight unwanted interactors that might be targeting Buc in the absence of Tdrd6 proteins, potentially affecting Buc behavior and disrupting the germ plasm condensates. In a parallel but similar analysis, quantification of Buc proteins levels at different time points could clarify if condensate instability leads to Buc dispersion or Buc degradation.

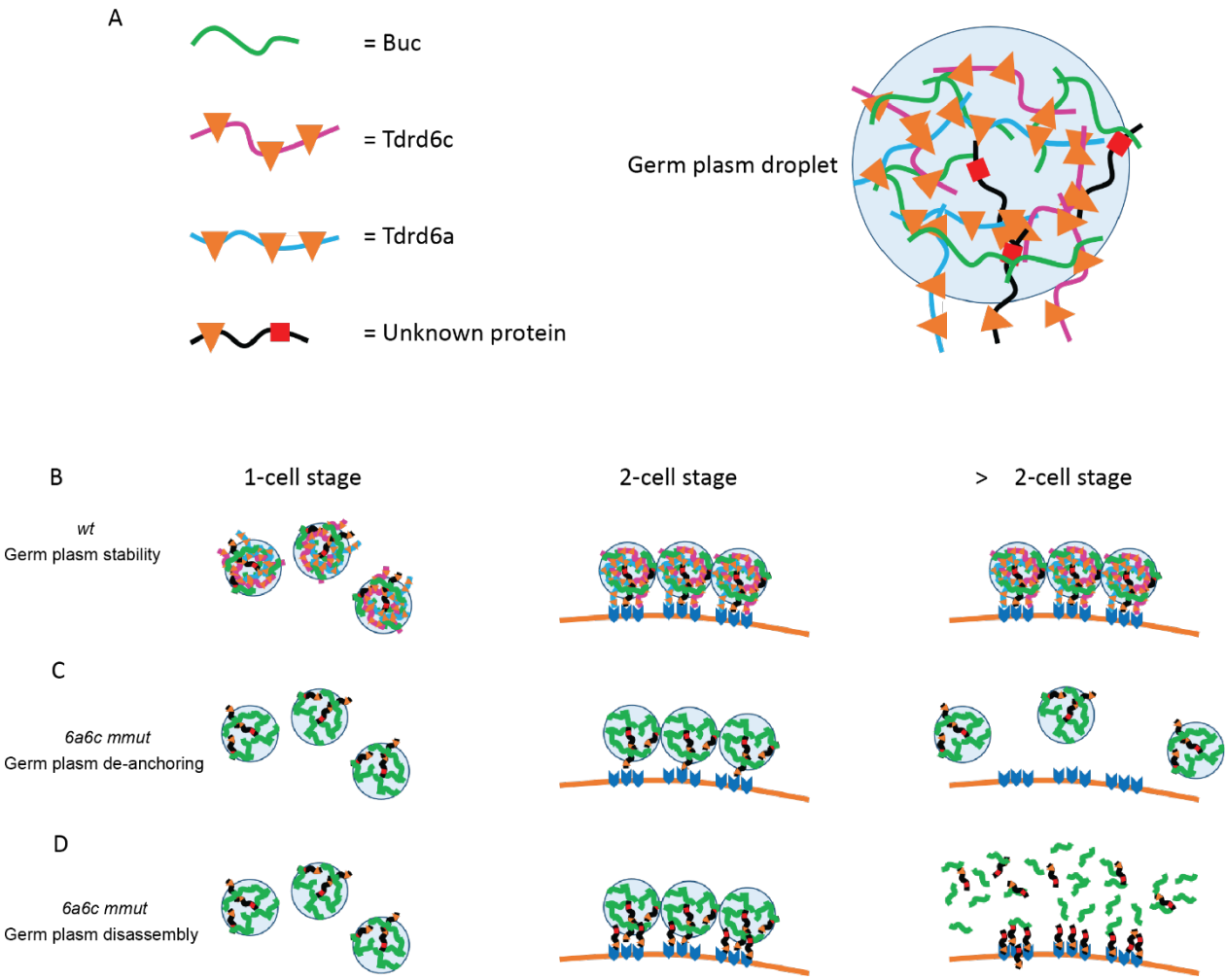

Fig. 25. Examples of models behind germ plasm instability of *6a6c mmut* embryos. (A) Schematic representations of Buc, Tdrd6a and Tdrd6c simplified protein structures and an example of additional interactor, forming a molecular network resulting in the assembly a droplet structure. (B) Wild type scenario where droplets are formed in the zygote of zebrafish, then anchored on the cleavage furrow (orange line with blue anchor-proteins) through proteins interaction, forming a stable contact governing germ plasm enrichment upon ZGA. (C) In the absence of Tdrd6a and Tdrd6c proteins, droplets are formed and can dock over cleavage furrows, but perhaps do not form enough stable contacts with the cleavage furrow anchors, resulting in dispersion of droplets that might become unstable for different reasons (passive disassembly or interactions with other molecules). (D) Lack of Tdrd6a and Tdrd6c does not influence the anchoring of germ plasm droplets but influences Buc-driven LLPS, triggering disassembly of the condensates and the release of the molecular components in the cytoplasm.

6.2 – Analysis of Tdrd6c protein domains

Presence of Tdrd6c in the embryonic germ plasm has been validated both with the analysis of the *tdrd6c-mKate2* line as well as with immuno-staining performed against the endogenous Tdrd6c protein in *wt* zebrafish strains (Fig. 9, 11 and 12). Although Tdrd6c does not seem to be part of Buc-organized structures in the oocytes (Fig. 10), its recruitment to the germ plasm of embryos may be driven by direct interaction with Buc. Tdrd6a-IP experiments performed on embryos where *buc* was not expressed revealed loss of Tdrd6c enrichment, suggesting that Buc is required to bring the two Tdrd6 proteins together into zebrafish embryonic condensates (Roovers et al., 2018). Indeed, in the analysis conducted by transfection of BmN4 cells, I could observe Tdrd6c and Buc co-localization within cytoplasmic condensates (Fig. 20).

As Tdrd6c possesses 7 eTDs and no other annotated domain, I initially hypothesized that its interaction with Buc could be mediated by one of these structured domains. However, in my analysis of different Tdrd6c constructs expressed in BmN4 cells, I could detect interaction between Tdrd6c protein and Buc only when the PrLD of Tdrd6c was included in the expressed proteins, and not with any construct that lacked the PrLD (Fig. 20). Furthermore, Tdrd6c's PrLD is able to form cytoplasmic condensates while the other parts of Tdrd6c were typically detected with dispersed in the cytoplasm, when expressed in isolation (Fig. 19). These data, surprisingly, suggest that the PrLD of Tdrd6c is the main driver of the interaction between Tdrd6c and Buc, and not Tdrd6c's eTDs as I expected based on the data relative to the Tdrd6a-Buc interaction (Roovers et al., 2018). Moreover, they suggest that the PrLD of Tdrd6c could have an important role in the regulation of LLPS in the germ plasm structure, due to its aggregation-prone nature and its affinity for Buc, the main organizer of germ plasm in zebrafish. These observations were confirmed with preliminary analysis of recombinant proteins, where the PrLD of Tdrd6c could form granular aggregates to which Buc co-localized (Fig. 22). However, these affinities should be investigated further, aiming at the understanding of the molecular grammar driving them, with an analysis of the amino-acidic composition of the two proteins and their domains involved in these dynamics.

In agreement with the description of PrLDs given in the introduction (Introduction – 3.1.4), Tdrd6c's PrLD displays the canonical enrichment in polar residues, with a high representation of Threonines, Serines and Asparagines which compose for 33% of the amino-acidic sequence (Fig. 26). Furthermore, c-terminally to the predicted PrLD lays a QQQ-motif which should not escape some consideration, as poly-Q stretches have been measured to govern phase-separation processes in different systems (Boncella et al., 2020; Burke et al., 2015; Jung et al., 2020; Langdon et al., 2018). Polar amino-acids not only are sites for interaction and binding with substrates due to their electron distribution but, for similar chemical reasons, are also targets of post-translational modifications (PTMs) which often regulate the folding and function of protein domains. Considering the flexible nature of PrLD and the different phases of zebrafish development to which Tdrd6c is involved, PTMs should be considered to be playing a role in the regulation of Tdrd6c's PrLD. However, first it would be important to detect the contribution of specific combination of amino-acids (in absence of PTMs) within Tdrd6c's PrLD sequence in the regulation of its own phase-separation capabilities. This could be assessed both in solution and with transfection of BmN4 cells, modifying each class of residues and measuring changes in the dynamics of the expressed construct. Polar residues could be mutated to hydrophobic amino-acids such as Leucine, Isoleucine and Alanine. The QQQ-motif could be removed or extended by addition of more Glutamines residues, following a similar strategy as the one adopted in the examination of *Arabidopsis* ELF3 (Jung et al., 2020). These mutated constructs should then be observed within the same conditions and levels of expression in order to clarify which amino-acidic composition can promote, impair or change the intrinsic phase-separation features of Tdrd6c's PrLD. The same proteins could then be co-expressed with Buc to investigate which molecular grammar can modulate the interaction with Buc and in which way in regards to LLPS dynamics.

Following the same analytical approach, it would be also important to examine the aromatic amino-acids of Tdrd6c's PrLD, although they are not found particularly enriched within its sequence (9% of amino-acid composition). Nevertheless, even if few, they could still contribute to the dynamics of the PrLD via cation-π or π-π interactions, which could represent relevant drivers of germ plasm formation and stability (Banani et al., 2016; Das et al., 2020; Pak et al., 2016; Qamar et al., 2018; Vernon et al., 2018; Wang et al., 2018).

A

N-ter - A T D C M F N V V V K L N S S G K L S V

E M Y D D K T N L N L K I K D L W S K T K R N E S I N T K G I

V K T R G F K E T S E G M E F R E V R N S F S T T S Q A H E R

T L K P V G Q A R T E Q N F Q S A T G Y S N A T G N N R A W

P N V L Q Q Q V M A Y P K L T E L P L R T I D V G Y V – C-ter

B

Amino-Acid	Representation within Tdrd6c's PrLD	Class representation
T	11 (12%)	31 (34%)
S	7 (8%)	
N	9 (10%)	
Q	4 (4%)	
F	4 (4%)	8 (9%)
Y	2 (2%)	
W	2 (2%)	
R	7 (8%)	16 (17%)
K	9 (10%)	

Fig. 26. Overview of the amino-acid composition of Tdrd6c's PrLD. (A) Highlights of Tdrd6c's PrLD amino-acids, with the predicted Prion-like domain underlined, but also reporting N-terminal and c-terminal linker sequences. In blue are polar amino-acids (T for Threonines, S for Serines, N for Asparagines and Q for Glutamines), in red aromatic residues (F for Phenylalanines, Y for Tyrosines and W for Tryptophanes) and green positively charged amino-acids (R for Arginines and K for Lysines). (B) Table recapitulating how many of each residues and class of amino-acids enrich within the PrLD of Tdrd6c (which is represented by a total of 92 aa).

Mutating the aromatic residues of Tdrd6c's PrLD to similar but non-aromatic amino-acids (*e.g.* Phenylalanine to Alanine, Tyrosine to Serine, Tryptophan to Leucine) could address if the behavior of the PrLD is driven by π-π interactions.

Furthermore, seven Arginines and nine Lysines residues are found in the PrLD of Tdrd6c, making up for 17% of its protein sequence. These amino-acids are also known to participate in cation-π interactions, but also to be substrates for eTDs upon methylation, as both residues can be targeted by methyl-transferases. Especially Arginines are observed to be methylated often when found within RGG/RG-motifs. Indeed, one of these Arginine residues of Tdrd6c's PrLD is followed by a Glycine, composing for an RG-site that could be available for methylation by PRMTs and recognition by eTDs. Interestingly, in my work I observed how the first 3 eTDs of Tdrd6c have an effect over the aggregating fashion displayed by the PrLD of Tdrd6c, suggesting a possible action in *cis*- between these domains. However, within the structure of these 3 eTDs I detected substitutions of some amino-acids proposed to be required for the formation of the aromatic pocket necessary for the interaction with methylated substrates (Fig. 17). This would imply that these 3 eTDs of Tdrd6c should exhibit a different fashion of target recognition. Accordingly, eTDs have been already reported to have various ways of interaction with substrates, also with non-methylated Arginines and Lysines, although these affinities have not been described on a molecular resolution (Kawale and Burmann, 2021; Liu et al., 2018; Zhang et al., 2017). With these considerations, I suggest that it could be important to test positively-charged Arginines and Lysines within the PrLD of Tdrd6c and modify them into negatively charged residues (Threonine and Serine) in order to address their relevance in the regulation of the dynamics of Tdrd6c phase-separation features and modes of interaction.

In the light of Buc-Tdrd6c interaction, it would be also interesting to investigate the relevance of Buc's PrLD, which is present in Buc N-terminal sequence, especially considering that PrLDs are known to drive promiscuous interactions with other molecules (Introduction – 3.1.4). This could be tested *in vitro* making use of purified recombinant proteins followed up by their analysis in solution. However, first it would be important to determine the critical concentrations and conditions at which Buc undergoes phase-separation, in order to be able to measure significant changes in Buc LLPS features when the PrLD of Tdrd6c is added to the environment. After this, it would be interesting to

analyze the Buc amino-acidic sequence with the same approach that I have described for Tdrd6c's PrLD, aiming to clarify the contribution of specific combination of residues to the interaction between Buc and Tdrd6c and to the LLPS features of Buc.

Overall, the study of single amino-acids within Tdrd6c's PrLD may reveal interesting insights regarding its molecular regulation and its interaction with Buc. After collection of significant data *in vitro*, interesting amino-acidic sequences or mutations of Tdrd6c could be further analyzed *in vivo* with either mRNA injections or the establishment of new GMOs. Injection of mRNAs into zygote could be used to visualize integration of specific domains (*e.g.* the PrLD of Tdrd6c tagged with a fluorophore) into germ plasm condensates, which could even alter the germ plasm dynamics in a measurable fashion (mis-localization of determinants, Buc-eGFP mobility, expression levels germ plasm-specific transcript). However, expression of injected mRNA may occur not early enough, not allowing for collection of significant observations in relation to germ plasm segregation (<3 hpf). This consideration is particularly important as the first 3 hours of development correspond to the time-window where germ plasm dynamics are likely influenced by the function of Tdrd6c (Discussion – 6.1.4). Alternatively, injection of proteins may be attempted, although the read-out of such procedure could be affected by protein mis-folding and mis-localization, which can cause complications during embryogenesis. On the other hand, establishment of GMOs (mutant or transgenic zebrafish lines) would require an intense work of screening through at least 2 generations of fish (6 months). For these reason, an accurate *in vitro* analysis of protein sequences and mutations of Tdrd6c and Buc should narrow down few solid candidates prior to tests conducted *in vivo* in the zebrafish organism.

6.3 – Concluding remarks

In the work of this Thesis I addressed the role of Tdrd6 proteins in regulation of germ cell specification in zebrafish. As described in the introduction (Introduction – 3.2.5), multi-Tudor containing proteins have been observed to contribute to germ cell biology in various ways, from governing of the structure and activity of the *nuage* to the regulation of the

dynamics and functioning of germ plasm condensates in different organisms (Arkov et al., 2006; Bose et al., 2022; Brennecke et al., 2008; Chen et al., 2009; Handler et al., 2011; Hosokawa et al., 2007; Houwing et al., 2007; Huang et al., 2011; Nishida et al., 2009; Reuter et al., 2009; Roovers et al., 2018; Sato et al., 2015; Vagin et al., 2009; Vrettos et al., 2021; Wang et al., 2009).

In the first part of discussion of this Thesis (Discussion – 6.1), I described various possible interpretations of the data collected during my analysis of *tdrd6c* localization and the phenotypes observed during development of *tdrd6c* mutant fish and *tdrd6a; tdrd6c* double mutant fish. According to my elaborations, I speculate that Tdrd6 proteins both function as important scaffold for germ plasm assemblies through regulation of Buc LLPS dynamics during embryogenesis (Fig. 25). In the absence of Tdrd6 proteins, germ plasm is severely destabilized, which in turn leads to impaired PGC specification and finally sterility of the adult fish. In this context, it would be important to follow up my work with the analysis of the molecular regulation of the interaction between Tdrd6c and Buc and measure its relevance towards LLPS features of the germ plasm. Live imaging and molecular tracking tools in the field of microscopy and related software should provide a solid platform to investigate these dynamics and unveil more details regarding LLPS characteristics of germ plasm droplets in zebrafish. Also, electron microscopy should be utilized to confirm the hypothesis of complete loss of germ plasm in *6a6c mmut* by the stage of ZGA. Furthermore, PGC characterization in *6a6c mmut* embryos should be carried out at stages between right after ZGA, between 3 and 6 hpf to determine whether or not PGC are initially specified and present before being lost at the 24 hpf due to different mechanisms (Fig. 24). This would be interesting to be addressed by single-cell RNA sequencing and profiling of PGC-specific gene expression patterns between 3 and 6 hpf. In this time window, *wt* PGCs should enrich in several known transcripts that are part of the germ plasm, most notably the *nanos*, *dazl* and *vasa*, which are among the most conserved germline-specific genes in evolution (Howley and Ho, 2000; Knaut et al., 2000; Köprunner et al., 2001; Maegawa et al., 2002). With these references, it should be feasible to characterize a specific transcriptome of zebrafish PGCs at the onset of ZGA. This analysis could be then compared to results obtained with single-cell RNA sequencing performed on *6a6c mmut*, measuring

the alterations in gene expression of PGCs (if distinguishable) that lacked correct germ plasm inheritance.

When examining Tdrd6c role during oogenesis, I could only collect data regarding its localization and not its function, as no phenotype was characterized in *tdrd6c* mutant eggs. As its perinuclear enrichment would suggest, however, Tdrd6c could play a role in the structure and function of the *nuage* (Fig. 10). Following this speculation, a proteomic and RNA sequencing analysis could reveal significant changes in the molecular composition of the *nuage* and its related control over gene expression patterns. One hypothesis is that Tdrd6c is involved in the mechanism of Ziwi enrichment to condensates (Fig. 23), which could be highlighted in a proteomic analysis (Discussion – 6.1.2). The same methods should then be applied in the analysis of *tdrd6a; tdrd6c* knock-out mutant oocytes in order to explore the extent of Tdrd6a and Tdrd6c overlapping function in the regulation of the perinuclear environment formation and functioning.

Additionally to unveiling the roles of Tdrd proteins in the biology of zebrafish, it would be important to assess the molecular mechanics behind their interactions within the germline condensates and their influence over LLPS features. In my work, I started collecting data in this regards, especially in the context of the interaction between Tdrd6c and Buc, with approaches both in cell culture and in solution (Results – 5.6 and 5.7). However, deeper level of molecular resolution could be achieved towards the understanding of zebrafish germ plasm LLPS regulation. The accurate analysis of each Tudor domain (TD) present within the sequences of Tdrd6a and Tdrd6c could highlight important various mode of interactions of the Tdrd proteins, contributing to the comprehension of protein-protein affinities governed by specific amino-acidic sequences of different TDs. In fact, Tdrd6a and Tdrd6c expresses each 7 TDs, which are likely involved in the recognition of different substrates, offering a solid molecular set-up for the comprehension of TDs biochemistry. This knowledge could then be transferred to the study of other TDs expressed in other proteins and systems, contributing to areas of research that focus on processes regulated by protein-protein interactions via TDs.

What was also addressed in the work of this Thesis was the role of the PrLD of Tdrd6c, which is represented by 92 amino-acids within the total 1814 residues of the Tdrd6c protein (Fig. 18). The expression of this domain was interesting to be followed both in BmN4 cells

as well as in solution, as in both systems it displayed self-interaction capabilities, forming large protein aggregates visualized by confocal microscopy (Fig. 19 and 22). Furthermore, its presence seemed to be required to drive the interaction between constructs of Tdrd6c and Buc, the germ plasm organizer in zebrafish (Fig. 20). Interestingly, upon interaction with Tdrd6c's PrLD, Buc-condensates appeared to lose their mobility within the cytoplasm of BmN4 cells, as they looked anchored to the Tdrd6c's PrLD-induced aggregate (Fig. 21). These observations suggest that the PrLD of Tdrd6c is involved in the regulation of Buc mobility. It would be interesting to validate these results *in vivo* with experiments in the zebrafish embryo (Discussion – 6.2). PrLDs have been reported to be important regulators of MLOs, but their mode of interactions are various and often transient due to the flexible nature of these domains (Introduction – 3.1.4). However, different areas of research are investing projects and efforts in order to clarify the molecular grammar behind their biological regulation. Furthermore, this knowledge can contribute not only to the understanding of the composition and functioning of MLOs, but also to the study of degenerative diseases where mis-regulation of the folding and interaction of PrLDs triggers formation of amyloid structure that causes cell death with severe consequences for the organism (Aguzzi and Altmeyer, 2016).

Altogether this Thesis has elucidated the role of Tdrd6 proteins in the regulation of germ plasm stability during early development of zebrafish, playing a crucial role for PGC formation and for the fertility of the animal. Also, I provided preliminary data in relation to specific domains of Tdrd6c, highlighting its first 3 eTDs and the PrLD as a possible regulators of Buc LLPS dynamics, an aspect that would be crucial to be addressed experimentally in the zebrafish organism. Therefore, the knowledge collected within this work hopefully can contribute not only to the germ cell biology but also to studies of processes regulated by protein-protein interaction via TDs as well as Prion-related area of research.

7 – List of References

Aguzzi, A., Altmeyer, M., 2016. Phase Separation: Linking Cellular Compartmentalization to Disease. Trends in Cell Biology 26, 547–558. https://doi.org/10.1016/j.tcb.2016.03.004

Aguzzi, A., De Cecco, E., 2020. Shifts and drifts in prion science. Science 370, 32–34. https://doi.org/10.1126/science.abb8577

al-Mukhtar K.A., Webb A.C., 1971. An ultrastructural study of primordial germ cells, oogonia and early oocytes in Xenopus laevis. J Embryol Exp Morphol. Oct;26(2):195-217. PMID: 5168216.

Alberti, S., 2017. Phase separation in biology. Current Biology 27, R1097–R1102. https://doi.org/10.1016/j.cub.2017.08.069

Alberti, S., Halfmann, R., King, O., Kapila, A., Lindquist, S., 2009. A Systematic Survey Identifies Prions and Illuminates Sequence Features of Prionogenic Proteins. Cell 137, 146–158. https://doi.org/10.1016/j.cell.2009.02.044

Amaya, J., Ryan, V.H., Fawzi, N.L., 2018. The SH3 domain of Fyn kinase interacts with and induces liquid–liquid phase separation of the low-complexity domain of hnRNPA2. Journal of Biological Chemistry 293, 19522–19531. https://doi.org/10.1074/jbc.RA118.005120

André, J., and Rouiller, C., 1956 . L'ultrastructure de la membrane nucléaire des ovocytes de l'Araignée (Tegenaria domestica Clark) . Electron Microsc. Proc. Stockholm Conf. 162 .

Arkov, A.L., Wang, J.-Y.S., Ramos, A., Lehmann, R., 2006. The role of Tudor domains in germline development and polar granule architecture. Development 133, 4053–4062. https://doi.org/10.1242/dev.02572

Balbiani, E. G., 1864. Sur la constitution du germe dans l'oeuf animal avant la fecondation. C. R. Hebd. Seances Acad. Sci. D 58, 584.

Banani, S.F., Lee, H.O., Hyman, A.A., Rosen, M.K., 2017. Biomolecular condensates: organizers of cellular biochemistry. Nature Reviews Molecular Cell Biology 18, 285–298. https://doi.org/10.1038/nrm.2017.7

Banani, S.F., Rice, A.M., Peeples, W.B., Lin, Y., Jain, S., Parker, R., Rosen, M.K., 2016. Compositional Control of Phase-Separated Cellular Bodies. Cell 166, 651–663. https://doi.org/10.1016/j.cell.2016.06.010

Banerjee, P.R., Milin, A.N., Moosa, M.M., Onuchic, P.L., Deniz, A.A., 2017. Reentrant Phase Transition Drives Dynamic Substructure Formation in Ribonucleoprotein Droplets. Angewandte Chemie International Edition 56, 11354–11359. https://doi.org/10.1002/anie.201703191

Banjade, S., Wu, Q., Mittal, A., Peeples, W.B., Pappu, R.V., Rosen, M.K., 2015. Conserved interdomain linker promotes phase separation of the multivalent adaptor protein Nck. Proc. Natl. Acad. Sci. U.S.A. 112. https://doi.org/10.1073/pnas.1508778112

Bates, D., Mächler, M., Bolker, B., Walker, S., 2015. Fitting Linear Mixed-Effects Models Using lme4. Journal of Statistical Software, 67(1), 1–48. doi:10.18637/jss.v067.i01.

Beutel, O., Maraspini, R., Pombo-García, K., Martin-Lemaitre, C., Honigmann, A., 2019. Phase Separation of Zonula Occludens Proteins Drives Formation of Tight Junctions. Cell 179, 923-936.e11. https://doi.org/10.1016/j.cell.2019.10.011

Boke, E., Ruer, M., Wühr, M., Coughlin, M., Lemaitre, R., Gygi, S.P., Alberti, S., Drechsel, D., Hyman, A.A., Mitchison, T.J., 2016. Amyloid-like Self-Assembly of a Cellular Compartment. Cell 166, 637–650. https://doi.org/10.1016/j.cell.2016.06.051

Boncella, A.E., Shattuck, J.E., Cascarina, S.M., Paul, K.R., Baer, M.H., Fomicheva, A., Lamb, A.K., Ross, E.D., 2020. Composition-based prediction and rational manipulation of prion-like domain recruitment to stress granules. Proc. Natl. Acad. Sci. U.S.A. 117, 5826–5835. https://doi.org/10.1073/pnas.1912723117

Bontems, F., Stein, A., Marlow, F., Lyautey, J., Gupta, T., Mullins, M.C., Dosch, R., 2009. Bucky Ball Organizes Germ Plasm Assembly in Zebrafish. Current Biology 19, 414–422. https://doi.org/10.1016/j.cub.2009.01.038

Bose, M., Lampe, M., Mahamid, J., Ephrussi, A., 2022. Liquid-to-solid phase transition of oskar ribonucleoprotein granules is essential for their function in Drosophila embryonic development. Cell 185, 1308-1324.e23. https://doi.org/10.1016/j.cell.2022.02.022

Boswell', R.E., Mahowaldt, A.R., n.d. fudor, A Gene Required for Assembly of the Germ Plasm in Drosophila melanogaster 8.

Boterenbrood E.C., Nieuwkoop, P.D., 1973 The formation of the mesoderm in urodelean amphibians : V. Its regional induction by the endoderm. Wilhelm Roux Arch Entwickl Mech Org. 1973 Dec;173(4):319-332. doi: 10.1007/BF00575837. PMID: 28304800.

Bounoure, L., 1939. L'origine des cellules reproductrices et le probl~me de la lign6e germinale. Paris, Gauthier Villars, 1939.

Brangwynne, C.P., Eckmann, C.R., Courson, D.S., Rybarska, A., Hoege, C., Gharakhani, J., Julicher, F., Hyman, A.A., 2009. Germline P Granules Are Liquid Droplets That Localize by Controlled Dissolution/Condensation. Science 324, 1729–1732. https://doi.org/10.1126/science.1172046

Brangwynne, C.P., Mitchison, T.J., Hyman, A.A., 2011. Active liquid-like behavior of nucleoli determines their size and shape in *Xenopus laevis* oocytes. Proc. Natl. Acad. Sci. U.S.A. 108, 4334–4339. https://doi.org/10.1073/pnas.1017150108

Brennecke, J., Malone, C.D., Aravin, A.A., Sachidanandam, R., Stark, A., Hannon, G.J., 2008. An Epigenetic Role for Maternally Inherited piRNAs in Transposon Silencing. Science 322, 1387–1392. https://doi.org/10.1126/science.1165171

Burke, K.A., Janke, A.M., Rhine, C.L., Fawzi, N.L., 2015. Residue-by-Residue View of In Vitro FUS Granules that Bind the C-Terminal Domain of RNA Polymerase II. Molecular Cell 60, 231–241. https://doi.org/10.1016/j.molcel.2015.09.006

Callebaut, I., Mornon, J.P., 1997. The human EBNA-2 coactivator p100: multidomain organization and relationship to the staphylococcal nuclease fold and to the tudor protein involved in *Drosophila melanogaster* development. Biochemical Journal 321, 125–132. https://doi.org/10.1042/bj3210125

Cajal, S.R., 1903. Un sencillo metodo de coloracion selectiva del reticulo protoplasmico y sus efectos en los diversos organos nerviosos de vertebrados e invertebrados. Trab Lab Investig Biol Univ Madr. 2: 129–221.

Calnan, B.J., Tidor, B., Biancalana, S., Hudson, D., Frankel, A.D., 1991. Arginine-Mediated RNA Recognition: the Arginine Fork. Science 252, 1167–1171. https://doi.org/10.1126/science.252.5009.1167

Campbell, P.D., Heim, A.E., Smith, M.Z., Marlow, F.L., 2015. Kinesin-1 interacts with Bucky ball to form germ cells and is required to pattern the zebrafish body axis. Development dev.124586. https://doi.org/10.1242/dev.124586

Chen, C., Jin, J., James, D.A., Adams-Cioaba, M.A., Park, J.G., Guo, Y., Tenaglia, E., Xu, C., Gish, G., Min, J., Pawson, T., 2009. Mouse Piwi interactome identifies binding mechanism of Tdrkh Tudor domain to arginine methylated Miwi. Proc. Natl. Acad. Sci. U.S.A. 106, 20336–20341. https://doi.org/10.1073/pnas.0911640106

Christoffels, A., Koh, E.G.L., Chia, J., Brenner, S., Aparicio, S., Venkatesh, B., 2004. Fugu Genome Analysis Provides Evidence for a Whole-Genome Duplication Early During the Evolution of Ray-Finned Fishes. Molecular Biology and Evolution 21, 1146–1151. https://doi.org/10.1093/molbev/msh114

Côté, J., Richard, S., 2005. Tudor domains bind symmetrical dimethylated arginines. J Biol Chem. 2005 Aug 5;280(31):28476-83. doi: 10.1074/jbc.M414328200. Epub 2005 Jun 6. PMID: 15955813.

Courchaine, E.M., Barentine, A.E.S., Straube, K., Lee, D.-R., Bewersdorf, J., Neugebauer, K.M., 2021. DMA-tudor interaction modules control the specificity of in vivo condensates. Cell 184, 3612-3625.e17. https://doi.org/10.1016/j.cell.2021.05.008

Cox, D.N., Chao, A., Baker, J., Chang, L., Qiao, D., Lin, H., 1998. A novel class of evolutionarily conserved genes defined by *piwi* are essential for stem cell self-renewal. Genes Dev. 12, 3715–3727. https://doi.org/10.1101/gad.12.23.3715

Das, S., Lin, Y.-H., Vernon, R.M., Forman-Kay, J.D., Chan, H.S., 2020. Comparative roles of charge, π , and hydrophobic interactions in sequence-dependent phase separation of intrinsically disordered proteins. Proc. Natl. Acad. Sci. U.S.A. 117, 28795–28805. https://doi.org/10.1073/pnas.2008122117

Dehal, P., Boore, J.L., 2005. Two Rounds of Whole Genome Duplication in the Ancestral Vertebrate. PLoS Biol 3, e314. https://doi.org/10.1371/journal.pbio.0030314

Ditlev, J.A., Case, L.B., Rosen, M.K., 2018. Who's In and Who's Out—Compositional Control of Biomolecular Condensates. Journal of Molecular Biology 430, 4666–4684. https://doi.org/10.1016/j.jmb.2018.08.003

D'Orazio, F.M., Balwierz, P.J., González, A.J., Guo, Y., Hernández-Rodríguez, B., Wheatley, L., Jasiulewicz, A., Hadzhiev, Y., Vaquerizas, J.M., Cairns, B., Lenhard, B., Müller, F., 2021. Germ cell differentiation requires Tdrd7-dependent chromatin and transcriptome reprogramming marked by germ plasm relocalization. Developmental Cell 56, 641-656.e5. https://doi.org/10.1016/j.devcel.2021.02.007

Dosch, R., Wagner, D.S., Mintzer, K.A., Runke, G., Wiemelt, A.P., Mullins, M.C., 2004. Maternal Control of Vertebrate Development before the Midblastula Transition: Mutants from the Zebrafish I 10.

Dosztányi, Z., 2018. Prediction of protein disorder based on IUPred: Prediction of Protein Disorder Based on IUPred. Protein Science 27, 331–340. https://doi.org/10.1002/pro.3334

Dranow, D.B., Tucker, R.P., Draper, B.W., 2013. Germ cells are required to maintain a stable sexual phenotype in adult zebrafish. Developmental Biology 376, 43–50. https://doi.org/10.1016/j.ydbio.2013.01.016

Elkouby, Y.M., Jamieson-Lucy, A., Mullins, M.C., 2016. Oocyte Polarization Is Coupled to the Chromosomal Bouquet, a Conserved Polarized Nuclear Configuration in Meiosis. PLoS Biol 14, e1002335. https://doi.org/10.1371/journal.pbio.1002335

Eno, C., Gomez, T., Slusarski, D.C., Pelegri, F., 2018. Slow calcium waves mediate furrow microtubule reorganization and germ plasm compaction in the early zebrafish embryo. Development dev.156604. https://doi.org/10.1242/dev.156604

Eno, C., Pelegri, F., 2018. Modulation of F-actin dynamics by maternal mid1ip1L controls germ plasm aggregation and furrow recruitment in the zebrafish embryo. Development dev.156596. https://doi.org/10.1242/dev.156596

Ephrussi, A., Dickinson, L.K., Lehmann, R., 1991. Oskar organizes the germ plasm and directs localization of the posterior determinant nanos. Cell 66, 37–50.

Erdős, G., Dosztányi, Z., 2020. Analyzing Protein Disorder with IUPred2A. Current Protocols in Bioinformatics 70. https://doi.org/10.1002/cpbi.99

Extavour, C.G., 2003. Mechanisms of germ cell specification across the metazoans: epigenesis and preformation. Development 130, 5869–5884. https://doi.org/10.1242/dev.00804

Folkmann, A.W., Putnam, A., Lee, C.F., Seydoux, G., 2021. Regulation of biomolecular condensates by interfacial protein clusters. Science 373, 1218–1224. https://doi.org/10.1126/science.abg7071

Frey, S., Görlich, D., 2007. A Saturated FG-Repeat Hydrogel Can Reproduce the Permeability Properties of Nuclear Pore Complexes. Cell 130, 512–523. https://doi.org/10.1016/j.cell.2007.06.024

Friedman, J.R., Nunnari, J., 2014. Mitochondrial form and function. Nature 505, 335–343. https://doi.org/10.1038/nature12985

Gallo, C.M., Wang, J.T., Motegi, F., Seydoux, G., 2010. Cytoplasmic Partitioning of P Granule Components Is Not Required to Specify the Germline in *C. elegans*. Science 330, 1685–1689. https://doi.org/10.1126/science.1193697

Gibson, D.G., Young, L., Chuang, R.-Y., Venter, J.C., Hutchison, C.A., Smith, H.O., 2009. Enzymatic assembly of DNA molecules up to several hundred kilobases. Nat Methods 6, 343–345. https://doi.org/10.1038/nmeth.1318

Gilks, N., Kedersha, N., Ayodele, M., Shen, L., Stoecklin, G., Dember, L.M., Anderson, P., 2004. Stress Granule Assembly Is Mediated by Prion-like Aggregation of TIA-1□D. Molecular Biology of the Cell 15.

Gross-Thebing, T., Yigit, S., Pfeiffer, J., Reichman-Fried, M., Bandemer, J., Ruckert, C., Rathmer, C., Goudarzi, M., Stehling, M., Tarbashevich, K., Seggewiss, J., Raz, E., 2017. The Vertebrate Protein Dead End Maintains Primordial Germ Cell Fate by Inhibiting Somatic Differentiation. Developmental Cell 43, 704-715.e5. https://doi.org/10.1016/j.devcel.2017.11.019

Gupta, T., Marlow, F.L., Ferriola, D., Mackiewicz, K., Dapprich, J., Monos, D., Mullins, M.C., 2010. Microtubule Actin Crosslinking Factor 1 Regulates the Balbiani Body and Animal-Vegetal Polarity of the Zebrafish Oocyte. PLoS Genetics 6, e1001073. https://doi.org/10.1371/journal.pgen.1001073

Han, T.W., Kato, M., Xie, S., Wu, L.C., Mirzaei, H., Pei, J., Chen, M., Xie, Y., Allen, J., Xiao, G., McKnight, S.L., 2012. Cell-free Formation of RNA Granules: Bound RNAs Identify Features and Components of Cellular Assemblies. Cell 149, 768–779. https://doi.org/10.1016/j.cell.2012.04.016

Handler, D., Olivieri, D., Novatchkova, M., Gruber, F.S., Meixner, K., Mechtler, K., Stark, A., Sachidanandam, R., Brennecke, J., 2011. A systematic analysis of *Drosophila* TUDOR domain-containing proteins identifies Vreteno and the Tdrd12 family as essential primary piRNA pathway factors: TUDOR domain-containing proteins in *Drosophila*. The EMBO Journal 30, 3977–3993. https://doi.org/10.1038/emboj.2011.308

Harmon, T.S., Holehouse, A.S., Rosen, M.K., Pappu, R.V., 2017. Intrinsically disordered linkers determine the interplay between phase separation and gelation in multivalent proteins. eLife 6, e30294. https://doi.org/10.7554/eLife.30294

Hashimoto, Y., Maegawa, S., Nagai, T., Yamaha, E., Suzuki, H., Yasuda, K., Inoue, K., 2004. Localized maternal factors are required for zebrafish germ cell formation. Developmental Biology 268, 152–161. https://doi.org/10.1016/j.ydbio.2003.12.013

Hirakata, S., Ishizu, H., Fujita, A., Tomoe, Y., Siomi, M.C., 2019. Requirements for multivalent Yb body assembly in transposon silencing in *Drosophila*. EMBO Reports 20, e47708. https://doi.org/10.15252/embr.201947708

Hoege, C., Hyman, A.A., 2013. Principles of PAR polarity in Caenorhabditis elegans embryos. Nat Rev Mol Cell Biol 14, 315–322. https://doi.org/10.1038/nrm3558

Hogan B.L., 1996. Bone morphogenetic proteins in development. Curr Opin Genet Dev. 1996 Aug;6(4):432-8. doi: 10.1016/s0959-437x(96)80064-5. PMID: 8791534.

Hosokawa, M., Shoji, M., Kitamura, K., Tanaka, T., Noce, T., Chuma, S., Nakatsuji, N., 2007. Tudor-related proteins TDRD1/MTR-1, TDRD6 and TDRD7/TRAP: Domain composition, intracellular localization, and function in male germ cells in mice. Developmental Biology 301, 38–52. https://doi.org/10.1016/j.ydbio.2006.10.046

Houwing, S., Kamminga, L.M., Berezikov, E., Cronembold, D., Girard, A., van den Elst, H., Filippov, D.V., Blaser, H., Raz, E., Moens, C.B., Plasterk, R.H.A., Hannon, G.J., Draper, B.W., Ketting, R.F., 2007. A Role for Piwi and piRNAs in Germ Cell Maintenance and Transposon Silencing in Zebrafish. Cell 129, 69–82. https://doi.org/10.1016/j.cell.2007.03.026

Howley, C., Ho, R.K., 2000. mRNA localization patterns in zebra®sh oocytes. Mechanisms of Development.

Huang, H.-Y., Houwing, S., Kaaij, L.J.T., Meppelink, A., Redl, S., Gauci, S., Vos, H., Draper, B.W., Moens, C.B., Burgering, B.M., Ladurner, P., Krijgsveld, J., Berezikov, E., Ketting, R.F., 2011. Tdrd1 acts as a molecular scaffold for Piwi proteins and piRNA targets in zebrafish: Tdrd1 as a scaffold for Piwi-pathway activity. The EMBO Journal 30, 3298–3308. https://doi.org/10.1038/emboj.2011.228

Huang, X.A., Yin, H., Sweeney, S., Raha, D., Snyder, M., Lin, H., 2013. A Major Epigenetic Programming Mechanism Guided by piRNAs. Developmental Cell 24, 502–516. https://doi.org/10.1016/j.devcel.2013.01.023

Hwang, W.Y., Fu, Y., Reyon, D., Maeder, M.L., Tsai, S.Q., Sander, J.D., Peterson, R.T., Yeh, J.-R.J., Joung, J.K., 2013. Efficient genome editing in zebrafish using a CRISPR-Cas system. Nature Biotechnology 31, 227–229. https://doi.org/10.1038/nbt.2501

Hyman, A.A., Weber, C.A., Jülicher, F., 2014. Liquid-Liquid Phase Separation in Biology. Annual Review of Cell and Developmental Biology 30, 39–58. https://doi.org/10.1146/annurev-cellbio-100913-013325

Ishiguro, T., Sato, N., Ueyama, M., Fujikake, N., Sellier, C., Kanegami, A., Tokuda, E., Zamiri, B., Gall-Duncan, T., Mirceta, M., Furukawa, Y., Yokota, T., Wada, K., Taylor, J.P., Pearson, C.E., Charlet-Berguerand, N., Mizusawa, H., Nagai, Y., Ishikawa, K., 2017. Regulatory Role of RNA Chaperone TDP-43 for RNA Misfolding and Repeat-Associated Translation in SCA31. Neuron 94, 108-124.e7. https://doi.org/10.1016/j.neuron.2017.02.046

Jinek, M., Chylinski, K., Fonfara, I., Hauer, M., Doudna, J.A., Charpentier, E., 2012. A Programmable Dual-RNA–Guided DNA Endonuclease in Adaptive Bacterial Immunity. Science 337, 816–821. https://doi.org/10.1126/science.1225829

Jukam, D., Shariati, S.A.M., Skotheim, J.M., 2017. Zygotic Genome Activation in Vertebrates. Developmental Cell 42, 316–332. https://doi.org/10.1016/j.devcel.2017.07.026

Jung, J.-H., Barbosa, A.D., Hutin, S., Kumita, J.R., Gao, M., Derwort, D., Silva, C.S., Lai, X., Pierre, E., Geng, F., Kim, S.-B., Baek, S., Zubieta, C., Jaeger, K.E., Wigge, P.A., 2020. A prion-like domain in ELF3 functions as a thermosensor in Arabidopsis. Nature 585, 256–260. https://doi.org/10.1038/s41586-020-2644-7

Katzen, F., 2007. Gateway® recombinational cloning: a biological operating system, Expert Opinion on Drug Discovery, 2:4, 571-589 DOI: 10.1517/17460441.2.4.571

Kawakami, K., 2007. Tol2: a versatile gene transfer vector in vertebrates. Genome Biology 8, S7. https://doi.org/10.1186/gb-2007-8-s1-s7

Kawale, A.A., Burmann, B.M., 2021. Inherent backbone dynamics fine-tune the functional plasticity of Tudor domains. Structure 29, 1253-1265.e4. https://doi.org/10.1016/j.str.2021.06.007

Kazazian, H.H., 2004. Mobile Elements: Drivers of Genome Evolution. Science 303, 1626–1632. https://doi.org/10.1126/science.1089670

Kemphues, K.J., Priess, J.R., Morton, D.G., Cheng, N., 1988. Identification of genes required for cytoplasmic localization in early C. elegans embryos. Cell 52, 311–320. https://doi.org/10.1016/S0092-8674(88)80024-2

Kim, C.A., Bowie, J.U., 2003. SAM domains: uniform structure, diversity of function.

Kim, J., Daniel, J., Espejo, A., Lake, A., Krishna, M., Xia, L., Zhang, Y., Bedford, M.T., 2006. Tudor, MBT and chromo domains gauge the degree of lysine methylation. EMBO Rep 7, 397–403. https://doi.org/10.1038/sj.embor.7400625

King, O.D., Gitler, A.D., Shorter, J., 2012. The tip of the iceberg: RNA-binding proteins with prion-like domains in neurodegenerative disease. Brain Research 1462, 61–80. https://doi.org/10.1016/j.brainres.2012.01.016

Kitamura, A., Nakayama, Y., Shibasaki, A., Taki, A., Yuno, S., Takeda, K., Yahara, M., Tanabe, N., Kinjo, M., 2016. Interaction of RNA with a C-terminal fragment of the amyotrophic lateral sclerosis-associated TDP43 reduces cytotoxicity. Sci Rep 6, 19230. https://doi.org/10.1038/srep19230

Kloc, M., Bilinski, S., Etkin, L.D., 2004. The Balbiani Body and Germ Cell Determinants: 150 Years Later, in: Current Topics in Developmental Biology. Elsevier, pp. 1–36. https://doi.org/10.1016/S0070-2153(04)59001-4

Knaut, H., Pelegri, F., Bohmann, K., Schwarz, H., Nüsslein-Volhard, C., 2000. Zebrafish vasa RNA but Not Its Protein Is a Component of the Germ Plasm and Segregates Asymmetrically before Germline Specification. Journal of Cell Biology 149, 875–888. https://doi.org/10.1083/jcb.149.4.875

Köprunner, M., Thisse, C., Thisse, B., Raz, E., 2001. A zebrafish *nanos* -related gene is essential for the development of primordial germ cells. Genes Dev. 15, 2877–2885. https://doi.org/10.1101/gad.212401

Kroschwald, S., Maharana, S., Mateju, D., Malinovska, L., Nüske, E., Poser, I., Richter, D., Alberti, S., 2015. Promiscuous interactions and protein disaggregases determine the material state of stress-inducible RNP granules. eLife 4. https://doi.org/10.7554/eLife.06807

Krøvel, A.V., Olsen, L.C., 2002. Expression of a vas::EGFP transgene in primordial germ cells of the zebrafish. Mechanisms of Development 116, 141–150. https://doi.org/10.1016/S0925-4773(02)00154-5

Kwan, K.M., Fujimoto, E., Grabher, C., Mangum, B.D., Hardy, M.E., Campbell, D.S., Parant, J.M., Yost, H.J., Kanki, J.P., Chien, C.-B., 2007. The Tol2kit: A multisite gateway-based construction kit forTol2 transposon transgenesis constructs. Developmental Dynamics 236, 3088–3099. https://doi.org/10.1002/dvdy.21343

Lancaster, A.K., Nutter-Upham, A., Lindquist, S., King, O.D., 2014. PLAAC: a web and command-line application to identify proteins with prion-like amino acid composition. Bioinformatics 30, 2501–2502. https://doi.org/10.1093/bioinformatics/btu310

Langdon, E.M., Qiu, Y., Ghanbari Niaki, A., McLaughlin, G., Weidmann, C., Gerbich, T., Smith, J.A., Crutchley, J.M., Termini, C.M., Weeks, K.M., Myong, S., Gladfelter, A., 2018. mRNA structure determines specificity of a polyQ-driven phase separation. https://doi.org/10.1101/233817

Lehmann, R., Nüsslein-Volhard, C., 1986. Abdominal segmentation, pole cell formation, and embryonic polarity require the localized activity of oskar, a maternal gene in drosophila. Cell 47, 141–152. https://doi.org/10.1016/0092-8674(86)90375-2

Leu, D.H., Draper, B.W., 2010. The ziwi promoter drives germline-specific gene expression in zebrafish. Developmental Dynamics 239, 2714–2721. https://doi.org/10.1002/dvdy.22404

Li, M., Zhao, L., Page-McCaw, P.S., Chen, W., 2016. Zebrafish Genome Engineering Using the CRISPR–Cas9 System. Trends in Genetics 32, 815–827. https://doi.org/10.1016/j.tig.2016.10.005

Li, P., Banjade, S., Cheng, H.-C., Kim, S., Chen, B., Guo, L., Llaguno, M., Hollingsworth, J.V., King, D.S., Banani, S.F., Russo, P.S., Jiang, Q.-X., Nixon, B.T., Rosen, M.K., 2012. Phase transitions in the assembly of multivalent signalling proteins. Nature 483, 336–340. https://doi.org/10.1038/nature10879

Liao, H., Chen, Y., Li, Y., Xue, S., Liu, M., Lin, Z., Liu, Y., Chan, H.C., Zhang, X., Sun, H., 2018. CFTR is required for the migration of primordial germ cells during zebrafish early embryogenesis. Reproduction 156, 261–268. https://doi.org/10.1530/REP-17-0681

Liemann, S., Glockshuber, R., 1998. Transmissible Spongiform Encephalopathies. BIOCHEMICAL AND BIOPHYSICAL RESEARCH COMMUNICATIONS 250.

Lin, H., Spradling, A.C., 1997. A novel group of *pumilio* mutations affects the asymmetric division of germline stem cells in the *Drosophila* ovary. Development 124, 2463–2476. https://doi.org/10.1242/dev.124.12.2463

Lin, Y., Protter, D.S.W., Rosen, M.K., Parker, R., 2015. Formation and Maturation of Phase-Separated Liquid Droplets by RNA-Binding Proteins. Molecular Cell 60, 208–219. https://doi.org/10.1016/j.molcel.2015.08.018

Liu, H., Wang, J.-Y.S., Huang, Y., Li, Z., Gong, W., Lehmann, R., Xu, R.-M., 2010. Structural basis for methylarginine-dependent recognition of Aubergine by Tudor. Genes & Development 24, 1876–1881. https://doi.org/10.1101/gad.1956010

Liu, J., Zhang, S., Liu, M., Liu, Y., Nshogoza, G., Gao, J., Ma, R., Yang, Y., Wu, J., Zhang, J., Li, F., Ruan, K., 2018. Structural plasticity of the TDRD3 Tudor domain probed by a fragment screening hit. The FEBS Journal 285, 2091–2103. https://doi.org/10.1111/febs.14469

Liu, K., Chen, C., Guo, Y., Lam, R., Bian, C., Xu, C., Zhao, D.Y., Jin, J., MacKenzie, F., Pawson, T., Min, J., 2010. Structural basis for recognition of arginine methylated Piwi proteins by the extended Tudor domain. Proceedings of the National Academy of Sciences 107, 18398–18403. https://doi.org/10.1073/pnas.1013106107

Liu, Y., Kossack, M.E., McFaul, M.E., Christensen, L.N., Siebert, S., Wyatt, S.R., Kamei, C.N., Horst, S., Arroyo, N., Drummond, I.A., Juliano, C.E., Draper, B.W., 2022. Single-cell transcriptome reveals insights into the development and function of the zebrafish ovary. eLife 11, e76014. https://doi.org/10.7554/eLife.76014

Lu, S., Wang, J., Chitsaz, F., Derbyshire, M.K., Geer, R.C., Gonzales, N.R., Gwadz, M., Hurwitz, D.I., Marchler, G.H., Song, J.S., Thanki, N., Yamashita, R.A., Yang, M., Zhang, D., Zheng, C., Lanczycki, C.J., Marchler-Bauer, A., 2020. CDD/SPARCLE: the conserved domain database in 2020. Nucleic Acids Research 48, D265–D268. https://doi.org/10.1093/nar/gkz991

Luteijn, M.J., Ketting, R.F., 2013. PIWI-interacting RNAs: from generation to transgenerational epigenetics. Nat Rev Genet 14, 523–534. https://doi.org/10.1038/nrg3495

Luzio, J.P., Pryor, P.R., Bright, N.A., 2007. Lysosomes: fusion and function. Nat Rev Mol Cell Biol 8, 622–632. https://doi.org/10.1038/nrm2217

Maegawa, S., Yamashita, M., Yasuda, K., Inoue, K., 2002. Zebrafish DAZ-like protein controls translation via the sequence 'GUUC': zDAZL is a translational activator. Genes to Cells 7, 971–984. https://doi.org/10.1046/j.1365-2443.2002.00576.x

Maharana, S., Wang, J., Papadopoulos, D.K., Richter, D., Pozniakovsky, A., Poser, I., Bickle, M., Rizk, S., Guillén-Boixet, J., Franzmann, T., Jahnel, M., Marrone, L., Chang, Y.-T., Sterneckert, J., Tomancak, P., Hyman, A.A., Alberti, S., 2018. RNA buffers the phase separation behavior of prion-like RNA binding proteins. Science eaar7366. https://doi.org/10.1126/science.aar7366

Mahowald, A.P., 1972. Ultrastructural observations on oogenesis inDrosophila. J. Morphol. 137, 29–48. https://doi.org/10.1002/jmor.1051370103

Malinovska, L., Kroschwald, S., Alberti, S., 2013. Protein disorder, prion propensities, and self-organizing macromolecular collectives. Biochimica et Biophysica Acta (BBA) - Proteins and Proteomics 1834, 918–931. https://doi.org/10.1016/j.bbapap.2013.01.003

Malone, C.D., Hannon, G.J., 2009. Small RNAs as Guardians of the Genome. Cell 136, 656–668. https://doi.org/10.1016/j.cell.2009.01.045

Marchler-Bauer, A., Bo, Y., Han, L., He, J., Lanczycki, C.J., Lu, S., Chitsaz, F., Derbyshire, M.K., Geer, R.C., Gonzales, N.R., Gwadz, M., Hurwitz, D.I., Lu, F., Marchler, G.H., Song, J.S., Thanki, N., Wang, Z., Yamashita, R.A., Zhang, D., Zheng, C., Geer, L.Y., Bryant, S.H., 2017. CDD/SPARCLE: functional classification of proteins via subfamily domain architectures. Nucleic Acids Res 45, D200–D203. https://doi.org/10.1093/nar/gkw1129

Marchler-Bauer, A., Bryant, S.H., 2004. CD-Search: protein domain annotations on the fly. Nucleic Acids Research 32, W327–W331. https://doi.org/10.1093/nar/gkh454

Marchler-Bauer, A., Derbyshire, M.K., Gonzales, N.R., Lu, S., Chitsaz, F., Geer, L.Y., Geer, R.C., He, J., Gwadz, M., Hurwitz, D.I., Lanczycki, C.J., Lu, F., Marchler, G.H., Song, J.S., Thanki, N., Wang, Z., Yamashita, R.A., Zhang, D., Zheng, C., Bryant, S.H., 2015. CDD: NCBI's conserved domain database. Nucleic Acids Research 43, D222–D226. https://doi.org/10.1093/nar/gku1221

Marchler-Bauer, A., Lu, S., Anderson, J.B., Chitsaz, F., Derbyshire, M.K., DeWeese-Scott, C., Fong, J.H., Geer, L.Y., Geer, R.C., Gonzales, N.R., Gwadz, M., Hurwitz, D.I., Jackson, J.D., Ke, Z., Lanczycki, C.J., Lu, F., Marchler, G.H., Mullokandov, M., Omelchenko, M.V., Robertson, C.L., Song, J.S., Thanki, N., Yamashita, R.A., Zhang, D., Zhang, N., Zheng, C., Bryant, S.H., 2011. CDD: a Conserved Domain Database for the functional annotation of proteins. Nucleic Acids Research 39, D225–D229. https://doi.org/10.1093/nar/gkq1189

Marlow, F.L., Mullins, M.C., 2008. Bucky ball functions in Balbiani body assembly and animal–vegetal polarity in the oocyte and follicle cell layer in zebrafish. Developmental Biology 321, 40–50. https://doi.org/10.1016/j.ydbio.2008.05.557

Martin, F.J., Amode, M.R., Aneja, A., Austine-Orimoloye, O., Azov, A.G., Barnes, I., Becker, A., Bennett, R., Berry, A., Bhai, J., Bhurji, S.K., Bignell, A., Boddu, S., Branco Lins, P.R., Brooks, L., Ramaraju, S.B., Charkhchi, M., Cockburn, A., Da Rin Fiorretto, L., Davidson, C., Dodiya, K., Donaldson, S., El Houdaigui, B., El Naboulsi, T., Fatima, R., Giron, C.G., Genez, T., Ghattaoraya, G.S., Martinez, J.G., Guijarro, C., Hardy, M., Hollis, Z., Hourlier, T., Hunt, T., Kay, M., Kaykala, V., Le, T., Lemos, D., Marques-Coelho, D., Marugán, J.C., Merino, G.A., Mirabueno, L.P., Mushtaq, A., Hossain, S.N., Ogeh, D.N., Sakthivel, M.P., Parker, A., Perry, M., Piližota, I., Prosovetskaia, I., Pérez-Silva, J.G., Salam, A.I.A., Saraiva-Agostinho, N., Schuilenburg, H., Sheppard, D., Sinha, S., Sipos, B., Stark, W., Steed, E., Sukumaran, R., Sumathipala, D., Suner, M.-M., Surapaneni, L., Sutinen, K., Szpak, M., Tricomi, F.F., Urbina-Gómez, D., Veidenberg, A., Walsh, T.A., Walts, B., Wass, E., Willhoft, N., Allen, J., Alvarez-Jarreta, J., Chakiachvili, M., Flint, B., Giorgetti, S., Haggerty, L., Ilsley,

G.R., Loveland, J.E., Moore, B., Mudge, J.M., Tate, J., Thybert, D., Trevanion, S.J., Winterbottom, A., Frankish, A., Hunt, S.E., Ruffier, M., Cunningham, F., Dyer, S., Finn, R.D., Howe, K.L., Harrison, P.W., Yates, A.D., Flicek, P., 2023. Ensembl 2023. Nucleic Acids Research 51, D933–D941. https://doi.org/10.1093/nar/gkac958

Mészáros, B., Erdős, G., Dosztányi, Z., 2018. IUPred2A: context-dependent prediction of protein disorder as a function of redox state and protein binding. Nucleic Acids Research 46, W329–W337. https://doi.org/10.1093/nar/gky384

Meyer, A., Van de Peer, Y., 2005. From 2R to 3R: evidence for a fish-specific genome duplication (FSGD). Bioessays 27, 937–945. https://doi.org/10.1002/bies.20293

Miranda-Rodríguez, J.R., Salas-Vidal, E., Lomelí, H., Zurita, M., Schnabel, D., 2017. RhoA/ROCK pathway activity is essential for the correct localization of the germ plasm mRNAs in zebrafish embryos. Developmental Biology 421, 27–42. https://doi.org/10.1016/j.ydbio.2016.11.002

Mittag, T., Pappu, R.V., 2022. A conceptual framework for understanding phase separation and addressing open questions and challenges. Molecular Cell 82, 2201–2214. https://doi.org/10.1016/j.molcel.2022.05.018

Mohanty, P., Kapoor, U., Sundaravadivelu Devarajan, D., Phan, T.M., Rizuan, A., Mittal, J., 2022. Principles Governing the Phase Separation of Multidomain Proteins. Biochemistry 61, 2443–2455. https://doi.org/10.1021/acs.biochem.2c00210

Molliex, A., Temirov, J., Lee, J., Coughlin, M., Kanagaraj, A.P., Kim, H.J., Mittag, T., Taylor, J.P., 2015. Phase Separation by Low Complexity Domains Promotes Stress Granule Assembly and Drives Pathological Fibrillization. Cell 163, 123–133. https://doi.org/10.1016/j.cell.2015.09.015

Montgomery Jr, Tho S.H., 1898. "Comparative cytological studies, with especial regard to the morphology of the nucleolus." *Journal of morphology* 15.2 (1898): 265-582.

Moreno-Mateos, M.A., Vejnar, C.E., Beaudoin, J.-D., Fernandez, J.P., Mis, E.K., Khokha, M.K., Giraldez, A.J., 2015. CRISPRscan: designing highly efficient sgRNAs for CRISPR-Cas9 targeting in vivo. Nat Methods 12, 982–988. https://doi.org/10.1038/nmeth.3543

Nieuwkoop P.D., Sutasurya L.A., 1976. Embryological evidence for a possible polyphyletic origin of the recent amphibians. J Embryol Exp Morphol. Feb;35(1):159-67. PMID: 1083885.

Nishida, K.M., Okada, T.N., Kawamura, T., Mituyama, T., Kawamura, Y., Inagaki, S., Huang, H., Chen, D., Kodama, T., Siomi, H., Siomi, M.C., 2009. Functional involvement of Tudor and dPRMT5 in the piRNA processing pathway in Drosophila germlines. EMBO J 28, 3820–3831. https://doi.org/10.1038/emboj.2009.365

Pak, C.W., Kosno, M., Holehouse, A.S., Padrick, S.B., Mittal, A., Ali, R., Yunus, A.A., Liu, D.R., Pappu, R.V., Rosen, M.K., 2016. Sequence Determinants of

Intracellular Phase Separation by Complex Coacervation of a Disordered Protein. Molecular Cell 63, 72–85. https://doi.org/10.1016/j.molcel.2016.05.042

Plummer, P.J.G., 1946. Scrapie -A Disease of Sheep.

Ponting, C. P., 1997. Tudor domains in proteins that interact with RNA. *Trends Biochem. Sci.* 22, 51-52.

Protter, D.S.W., Rao, B.S., Van Treeck, B., Lin, Y., Mizoue, L., Rosen, M.K., Parker, R., 2018. Intrinsically Disordered Regions Can Contribute Promiscuous Interactions to RNP Granule Assembly. Cell Reports 22, 1401–1412. https://doi.org/10.1016/j.celrep.2018.01.036

Prusiner, S.B., 1991. Molecular Biology of Prion Diseases 252.

Prusiner, S.B., 1982. Novel Proteinaceous Infectious Particles Cause Scrapie. Science 216, 136–144. https://doi.org/10.1126/science.6801762

Qamar, S., Wang, G., Randle, S.J., Ruggeri, F.S., Varela, J.A., Lin, J.Q., Phillips, E.C., Miyashita, A., Williams, D., Ströhl, F., Meadows, W., Ferry, R., Dardov, V.J., Tartaglia, G.G., Farrer, L.A., Kaminski Schierle, G.S., Kaminski, C.F., Holt, C.E., Fraser, P.E., Schmitt-Ulms, G., Klenerman, D., Knowles, T., Vendruscolo, M., St George-Hyslop, P., 2018. FUS Phase Separation Is Modulated by a Molecular Chaperone and Methylation of Arginine Cation-π Interactions. Cell 173, 720-734.e15. https://doi.org/10.1016/j.cell.2018.03.056

Reuter, M., Chuma, S., Tanaka, T., Franz, T., Stark, A., Pillai, R.S., 2009. Loss of the Mili-interacting Tudor domain–containing protein-1 activates transposons and alters the Mili-associated small RNA profile. Nat Struct Mol Biol 16, 639–646. https://doi.org/10.1038/nsmb.1615

Riemer, S., Bontems, F., Krishnakumar, P., Gömann, J., Dosch, R., 2015. A functional Bucky ball-GFP transgene visualizes germ plasm in living zebrafish. Gene Expression Patterns 18, 44–52. https://doi.org/10.1016/j.gep.2015.05.003

Romero, P., Obradovic, Z., Li, X., Garner, E.C., Brown, C.J., Dunker, A.K., 2001. Sequence complexity of disordered protein. Proteins 42, 38–48. https://doi.org/10.1002/1097-0134(20010101)42:1<38::AID-PROT50>3.0.CO;2-3

Roovers, E.F., Kaaij, L.J., Redl, S., Bronkhorst, A.W., Wiebrands, K., de Jesus Domingues, A.M., Huang, H.-Y., Han, C.-T., Salvenmoser, W., Gruen, D., Butter, F., van Oudenaarden, A., Ketting, R.F., 2018. Tdrd6a regulates the aggregation of Buc into functional subcellular compartments that drive germ cell specification. https://doi.org/10.1101/267971

Rostam, N., Goloborodko, A., Riemer, S., Hertel, A., Riedel, D., Vorbrüggen, G., Dosch, R., 2022. The germ plasm is anchored at the cleavage furrows through interaction with tight junctions in the early zebrafish embryo. Development 149, dev200465. https://doi.org/10.1242/dev.200465

Saha, S., Weber, C.A., Nousch, M., Adame-Arana, O., Hoege, C., Hein, M.Y., Osborne-Nishimura, E., Mahamid, J., Jahnel, M., Jawerth, L., Pozniakovski, A., Eckmann,

C.R., Jülicher, F., Hyman, A.A., 2016. Polar Positioning of Phase-Separated Liquid Compartments in Cells Regulated by an mRNA Competition Mechanism. Cell 166, 1572-1584.e16. https://doi.org/10.1016/j.cell.2016.08.006

Sanders, D.W., Kedersha, N., Lee, D.S.W., Strom, A.R., Drake, V., Riback, J.A., Bracha, D., Eeftens, J.M., Iwanicki, A., Wang, A., Wei, M.-T., Whitney, G., Lyons, S.M., Anderson, P., Jacobs, W.M., Ivanov, P., Brangwynne, C.P., 2020. Competing Protein-RNA Interaction Networks Control Multiphase Intracellular Organization. Cell 181, 306-324.e28. https://doi.org/10.1016/j.cell.2020.03.050

Sanger, F., Nicklen, S., Coulson, A.R., 1977. DNA sequencing with chain-terminating inhibitors. Proc. Natl. Acad. Sci. U.S.A. 74, 5463–5467. https://doi.org/10.1073/pnas.74.12.5463

Sato, K., Iwasaki, Y.W., Siomi, H., Siomi, M.C., 2015. Tudor-domain containing proteins act to make the piRNA pathways more robust in Drosophila. Fly 9, 86–90. https://doi.org/10.1080/19336934.2015.1128599

Schwartz, J.C., Wang, X., Podell, E.R., Cech, T.R., 2013. RNA Seeds Higher-Order Assembly of FUS Protein. Cell Reports 5, 918–925. https://doi.org/10.1016/j.celrep.2013.11.017

Selenko P., Sprangers R., Stier G., Bühler D., Fischer U., Sattler M., 2001. SMN tudor domain structure and its interaction with the Sm proteins. Nat Struct Biol. 2001 Jan;8(1):27-31. doi: 10.1038/83014. PMID: 11135666.

Shcherbo, D., Murphy, C.S., Ermakova, G.V., Solovieva, E.A., Chepurnykh, T.V., Shcheglov, A.S., Verkhusha, V.V., Pletnev, V.Z., Hazelwood, K.L., Roche, P.M., Lukyanov, S., Zaraisky, A.G., Davidson, M.W., Chudakov, D.M., 2009. Far-red fluorescent tags for protein imaging in living tissues. Biochemical Journal 418, 567–574. https://doi.org/10.1042/BJ20081949

Shelkovnikova, T.A., Robinson, H.K., Southcombe, J.A., Ninkina, N., Buchman, V.L., 2014. Multistep process of FUS aggregation in the cell cytoplasm involves RNA-dependent and RNA-independent mechanisms. Human Molecular Genetics 23, 5211–5226. https://doi.org/10.1093/hmg/ddu243

Shin, Y., Brangwynne, C.P., 2017. Liquid phase condensation in cell physiology and disease. Science 357, eaaf4382. https://doi.org/10.1126/science.aaf4382

Shorter, J., Lindquist, S., 2005. Prions as adaptive conduits of memory and inheritance. Nature Reviews Genetics 6, 435–450. https://doi.org/10.1038/nrg1616

Siegfried, K.R., Nüsslein-Volhard, C., 2008. Germ line control of female sex determination in zebrafish. Developmental Biology 324, 277–287. https://doi.org/10.1016/j.ydbio.2008.09.025

Siomi, M.C., Mannen, T., Siomi, H., 2010. How does the Royal Family of Tudor rule the PIWI-interacting RNA pathway? Genes & Development 24, 636–646. https://doi.org/10.1101/gad.1899210

Smith, J., Calidas, D., Schmidt, H., Lu, T., Rasoloson, D., Seydoux, G., 2016. Spatial patterning of P granules by RNA-induced phase separation of the intrinsically-disordered protein MEG-3. eLife 5, e21337. https://doi.org/10.7554/eLife.21337

Sprunger, M.L., Jackrel, M.E., 2021. Prion-Like Proteins in Phase Separation and Their Link to Disease. Biomolecules 11, 1014. https://doi.org/10.3390/biom11071014

Strasser, M.J., Mackenzie, N.C., Dumstrei, K., Nakkrasae, L.-I., Stebler, J., Raz, E., 2008. Control over the morphology and segregation of Zebrafish germ cell granules during embryonic development. BMC Dev Biol 8, 58. https://doi.org/10.1186/1471-213X-8-58

Strome, S., Wood, W.B., 1983. Generation of asymmetry and segregation of germ-line granules in early C. elegans embryos. Cell 35, 15–25. https://doi.org/10.1016/0092-8674(83)90203-9

Tam, P.P.L., Zhou, S.X., 1996. The Allocation of Epiblast Cells to Ectodermal and Germ-Line Lineages Is Influenced by the Position of the Cells in the Gastrulating Mouse Embryo. Developmental Biology 178, 124–132. https://doi.org/10.1006/dbio.1996.0203

Tsang, T.E., Khoo, P.-L., Jamieson, R.V., Zhou, S.X., Ang, S.-L., Behringer, R., Tam, P.P.L., n.d. The allocation and differentiation of mouse primordial germ cells.

Tzung, K.-W., Goto, R., Saju, J.M., Sreenivasan, R., Saito, T., Arai, K., Yamaha, E., Hossain, M.S., Calvert, M.E.K., Orbán, L., 2015. Early Depletion of Primordial Germ Cells in Zebrafish Promotes Testis Formation. Stem Cell Reports 4, 61–73. https://doi.org/10.1016/j.stemcr.2014.10.011

Vagin, V.V., Wohlschlegel, J., Qu, J., Jonsson, Z., Huang, X., Chuma, S., Girard, A., Sachidanandam, R., Hannon, G.J., Aravin, A.A., 2009. Proteomic analysis of murine Piwi proteins reveals a role for arginine methylation in specifying interaction with Tudor family members. Genes Dev. 23, 1749–1762. https://doi.org/10.1101/gad.1814809

Vastenhouw, N.L., Cao, W.X., Lipshitz, H.D., 2019. The maternal-to-zygotic transition revisited. Development 146, dev161471. https://doi.org/10.1242/dev.161471

Vernon, R.M., Chong, P.A., Tsang, B., Kim, T.H., Bah, A., Farber, P., Lin, H., Forman-Kay, J.D., 2018. Pi-Pi contacts are an overlooked protein feature relevant to phase separation. eLife 7, e31486. https://doi.org/10.7554/eLife.31486

von Wittich, W. H., 1845. Dissertatio Sistens Observationes Quaedam De Aranearum Ex Ovo Evolutione Halis Saxonum, Halle, Germany.

Vrettos, N., Maragkakis, M., Alexiou, P., Sgourdou, P., Ibrahim, F., Palmieri, D., Kirino, Y., Mourelatos, Z., 2021. Modulation of Aub–TDRD interactions elucidates piRNA amplification and germplasm formation. Life Sci. Alliance 4, e202000912. https://doi.org/10.26508/lsa.202000912

Wagner, R., 1837. Einige bemerkungen und fragen über das keimbläschen (vesicular germinativa). *Müller's Archiv Anat Physiol Wissenschaft Med* 268.1835 (1835): 373-7. Valentin, Gabriel. *Repertorium für anatomie und physiologie*.

Wang, J., Choi, J.-M., Holehouse, A.S., Lee, H.O., Zhang, X., Jahnel, M., Maharana, S., Lemaitre, R., Pozniakovsky, A., Drechsel, D., Poser, I., Pappu, R.V., Alberti, S., Hyman, A.A., 2018. A Molecular Grammar Governing the Driving Forces for Phase Separation of Prion-like RNA Binding Proteins. Cell. https://doi.org/10.1016/j.cell.2018.06.006

Wang, J., Saxe, J.P., Tanaka, T., Chuma, S., Lin, H., 2009. Mili Interacts with Tudor Domain-Containing Protein 1 in Regulating Spermatogenesis. Current Biology 19, 640–644. https://doi.org/10.1016/j.cub.2009.02.061

Wang, J.T., Seydoux, G., 2013. Germ Cell Specification, in: Schedl, T. (Ed.), Germ Cell Development in C. Elegans, Advances in Experimental Medicine and Biology. Springer New York, New York, NY, pp. 17–39. https://doi.org/10.1007/978-1-4614-4015-4_2

Weidinger, G., Stebler, J., Slanchev, K., Dumstrei, K., Wise, C., Lovell-Badge, R., Thisse, C., Thisse, B., Raz, E., 2003. dead end, a Novel Vertebrate Germ Plasm Component, Is Required for Zebrafish Primordial Germ Cell Migration and Survival. Current Biology 13, 1429–1434. https://doi.org/10.1016/S0960-9822(03)00537-2

Westerfield, M., 1995. The Zebrafish Book. A Guide for the Laboratory Use of Zebrafish (Danio rerio), Third Edition (University Oregon Press).

Westerich, K.J., Tarbashevich, K., Schick, J., Gupta, A., Zhu, M., Hull, K., Romo, D., Zeuschner, D., Goudarzi, M., Gross-Thebing, T., Raz, E., 2023. Spatial organization and function of RNA molecules within phase-separated condensates in zebrafish are controlled by Dnd1. Developmental Cell S1534580723003076. https://doi.org/10.1016/j.devcel.2023.06.009

Wienholds, E., Schulte-Merker, S., Walderich, B., Plasterk, R.H.A., 2002. Target-Selected Inactivation of the Zebrafish *rag1* Gene. Science 297, 99–102. https://doi.org/10.1126/science.1071762

Zhang, H., Liu, K., Izumi, N., Huang, H., Ding, D., Ni, Z., Sidhu, S.S., Chen, C., Tomari, Y., Min, J., 2017. Structural basis for arginine methylation-independent recognition of PIWIL1 by TDRD2. Proc. Natl. Acad. Sci. U.S.A. 114, 12483–12488. https://doi.org/10.1073/pnas.1711486114

Zhang, Y., Liu, W., Li, R., Gu, J., Wu, P., Peng, C., Ma, J., Wu, L., Yu, Y., Huang, Y., 2018. Structural insights into the sequence-specific recognition of Piwi by *Drosophila* Papi. Proc. Natl. Acad. Sci. U.S.A. 115, 3374–3379. https://doi.org/10.1073/pnas.1717116115